

UC San Diego

UC San Diego Electronic Theses and Dissertations

Title

Characterization of new marine secondary metabolites for the treatment of cancer and neglected tropical diseases

Permalink

<https://escholarship.org/uc/item/3kv8s54w>

Author

Simmons, Thomas Luke

Publication Date

2008

Peer reviewed|Thesis/dissertation

UNIVERSITY OF CALIFORNIA, SAN DIEGO

Characterization of New Marine Secondary Metabolites for the Treatment of Cancer
and Neglected Tropical Diseases

A Dissertation submitted in partial satisfaction of the requirement for the degree
Doctor of Philosophy

in

Oceanography

by

Thomas Luke Simmons

Committee in Charge:

Professor William H. Gerwick, Chair
Professor William H. Fenical, Co-chair
Professor Douglas H. Bartlett
Dr. Lena Gerwick
Professor Tadeusz F. Molinski
Professor Bradley S. Moore

2008

©

Thomas Luke Simmons, 2008

All rights reserved

The Dissertation of Thomas Luke Simmons is approved and it is
acceptable in quality and form for publication on microfilm

Chair

University of California, San Diego

2008

TABLE OF CONTENTS

Signature Page.....	iii
Table of Contents.....	iv
List of Figures.....	vii
List of Tables.....	xi
List of Abbreviations.....	xiii
Acknowledgments.....	xvi
Vita and Publications.....	xix
Abstract.....	xxi
I. Introduction.....	1
References.....	26
II. Belamide A, a new antimetabolic tetrapeptide from a Panamanian marine cyanobacterium.....	32
Abstract.....	33
Introduction.....	34
Results and Discussion.....	36
References.....	46
Acknowledgments.....	48

III. DMMC, a cyanobacterial depsipeptide with potent antitumor activity in the cyclic and linear forms.....	49
Abstract.....	50
Introduction.....	51
Results and Discussion.....	53
Experimental Section.....	66
References.....	73
Acknowledgments.....	75
IV. Viridamides A and B, lipodepsipeptides with anti-protozoan activity from the marine cyanobacterium <i>Oscillatoria nigro-viridis</i>	76
Abstract.....	77
Introduction.....	78
Results and Discussion.....	81
Experimental Section.....	91
References.....	100
Acknowledgments.....	104

V. Kaviol A, a halogenated phenolic inhibitor of histone deacetylase.....	105
Abstract.....	106
Introduction.....	107
Results and Discussion.....	108
Experimental.....	117
References.....	120
Acknowledgments.....	122
VI. Conclusion.....	123
Appendix.....	131

LIST OF FIGURES

Chapter I

- Figure I.1. The reported sources of 20 marine derived anticancer agents summarized in Table I.1.....8
- Figure I.2. The predicted sources (based on direct genetic evidence or biosynthetic rationale) of the 20 marine derived anticancer agents summarized in Table I.1.....8

Chapter II

- Figure II.1. Molecular structures of belamide A, dolastatin 15 and dolastatin 10.....35
- Figure II.2. HMBC and COSY correlations for the benzyl-methoxypyrrolinone residue in belamide A.....38
- Figure II.3. Tandem MS fragments of belamide A.....39
- Figure II.4. Untreated (negative control) rat intestinal A10 cells stained to show cytoskeletal microtubule network during mitotic cell division.....44

Figure II.5. Rat intestinal A10 cells treated with 20 μ M belamide A and stained to show microtubule depolymerization effects.....44

Figure II.6. Structural overlay of the lowest energy geometric conformations (Hartree-Fock, 6-31 basis set) for belamide A, dolastatin 15 and dolastatin 10..45

Chapter III

Figure III.1. Molecular structures of cyclic DMMC and its linear hydrolysis product.....56

Figure III.2. CID MS fragmentation pattern of DMMC.....57

Figure III.3. Cyclic depsipeptide skeleton and table with select molecules in this structure class.....58

Figure III.4. Effects of cyclic and linear DMMC on the actin cytoskeleton of A-10 cells.....61

Figure III.5. Clonogenic dose-response curve of H-116 human colon cancer cells exposed to DMMC.....62

Figure III.6. Therapeutic assessment of DMMC against HCT-116 human colon cancer growing subcutaneously in scid mice.....63

Figure III.7. Lowest energy conformations of DMMC and linear analog65

Chapter IV

Figure IV.1. The structure of the 5-methoxydec-9-ynoic acid moiety found in viridamides A and B.....83

Figure IV.2. Important fragmentations observed from FAB-MS and key HMBC connectivities used to sequence the series of residues in viridamide A.....84

Figure IV.3. The molecular structures of viridamides A and B.....84

Figure IV.4. The phylogenetic relationships of marine cyanobacteria of the order *Oscillatoriales* from 16S rRNA nucleotide sequences.....89

Chapter V

Figure V.1. Substructures of kaviol A showing HMBC and COSY derived partial structures.....110

Figure V.2. Key ROESY correlations used for the assignment of *Z*-olefin geometry of kaviol A.....111

Figure V.3. A Plausible Biosynthesis of kaviol A and other C₆-C₄-C₆ compounds..113

LIST OF TABLES

Chapter I

Table I.1. Relevant marine natural products and their current clinical status.....	6
--	---

Chapter II

Table II.1. NMR data for belamide A.....	43
--	----

Chapter III

Table III.1. ^1H and ^{13}C NMR Spectral data for DMMC.....	55
---	----

Table III.2. Cytotoxicity of DMMC and linear analog against a panel of cancer cell lines.....	59
--	----

Chapter IV

Table IV.1. Activity of viridamide A against a series of pathogen and cancer cell lines.....	86
Table IV.2. 1D and 2D NMR spectral data for viridamide A in CDCl ₃	98
Table IV.3. 1D and 2D NMR data for viridamide B in CDCl ₃	99

Chapter V

Table V.1. ¹ H and ¹³ C NMR data for kaviol A.....	112
Table V.2. Small-molecule pan inhibitors of HDAC and their respective IC ₅₀ values.....	115

LIST OF ABBREVIATIONS

ATP	adenosine triphosphate
BBS	bibenzyl synthase
CID	collision induced
CNS	central nervous system
DAIP	4',6-diamidino-phenylindole
DMMC	desmethoxymajusculamide C
Dmop	dimethyl-oxo-pentanoate
DNA	deoxyribonucleic acid
ESI	electrospray ionization
FAB	fast atom bombardment
FDAA	fluoro-dinitroalanine amide
FT-IR	Fourier transform infrared
gCOSY	gradient correlation spectroscopy
gHMBC	gradient heteronuclear multiple bond correlation
gHSQC	gradient heteronuclear single quantum coherence
GTP	guanosine triphosphate
HDAC	histone deacetylase
HMBA	hydroxymethyl-butanoic acid
HMPA	hydroxymethyl-pentanoic acid
HPLC	high-pressure liquid chromatography
HR	high resolution

ICBG	International Cooperative Biodiversity Group
IC ₅₀	50 % inhibitory concentration
LC/MS	liquid chromatography / mass spectrometry
MALDI	matrix-assisted laser desorption ionization
Mdyna	methoxydecynoic acid
MOA	mechanism of action
MHz	megahertz
MS	mass spectrometry
NCDDG	National Cooperative Drug Discovery Group
NOE	nuclear Overhauser effect
NMR	nuclear magnetic resonance
NP	normal phase
NRPS	non-ribosomal peptide synthetase
OPLS	optimization liquid simulation
PM3	parameterization model 3
PKC	protein kinase C
PKS	polyketide synthase
ROESY	rotating frame overhauser effect spectroscopy
RP	reversed-phase
SAM	S-adenosylmethionine
Si	silica
SPE	solid phase extraction
TEAP	triethylammonium phosphate

TOCSY	total correlation spectroscopy
TOF	time of flight
UV	ultraviolet
VLC	vacuum liquid chromatography

ACKNOWLEDGMENTS

This is a huge day for me and I am overjoyed to finally thank all the people who have helped and supported me during the course of my Ph.D. First and foremost I would like to express sincere appreciation to my advisor Professor William H. Gerwick. Bill has been a source of inspiration and enthusiasm through his excitement for science and wealth of creativity. I also thank Professors William Fenical, Bradley Moore, Tadeusz Molinski and Douglas Bartlett for their enthusiastic participation on my doctoral committee.

I owe a debt of gratitude to all the graduate students, post doctoral researchers and visiting scholars with whom I have shared lab space over the years. From them I have learned many things about science and myself. Particular thanks go to Drs. Kerry McPhail, Harald Gross and Alfonso Mangoni, without their guidance and friendship this thesis would not have been possible. My warmest thanks go to all the members of the Fenical and Moore groups who have enriched my experience here at SIO. Many thanks to all of the members of the Gerwick group (past and present) especially those who made the move from OSU with me; those experiences will stay with me forever. And thanks to Professors Phil Crews and David Sherman (and their groups) for making the dive expeditions in Papua New Guinea memories unforgettable.

I would like to express my deepest appreciation to Dr. David Newman and Thomas McCloud for opening my eyes to the potential of natural products research and encouraging me to pursue a Ph.D.

To my parents I offer endless thanks for your tireless support over the years. To my extended family and ‘old school’ friends, I can not thank each of you enough for your patience and support during the course of my PhD; may the ‘628’ live on in our hearts!

The text of II, in part, is published material as it appears in Simmons, T.L., McPhail, K.L., Ortega-Barría, Mooberry, S.L., Gerwick, W.H. Belamide A, a new antimitotic tetrapeptide from a Panamanian marine cyanobacterium. *Tetrahedron Letters* **2006**, *47*, 3387-3390.

The text of III, in full, is the manuscript draft to be submitted to an academic journal as it will appear: Simmons, T.L., Nogle, L.M.; Valeriote, F.A.; Mooberry, S.L.; Gerwick, W.H. DMMC, a Cyanobacterial Depsipeptide with Potent Cytotoxicity in Cyclic and Ring-opened Forms. The dissertation author was the primary author and directed and supervised the research, which forms the basis for this chapter.

The text of IV, in full, is the manuscript draft to be submitted to an academic journal as it will appear: Simmons, T.L., Engene, N., Gerwick, L., Gerwick, W.H. Viridamides A and B, lipodepsipeptides with anti-trypanosomal activity from the marine cyanobacterium *Oscillatoria nigro-viridis*. The dissertation author was the primary author and directed and supervised the research, which forms the basis for this chapter.

The text of V, in full, is the manuscript draft to be submitted to an academic journal as it will appear: Simmons, T.L., Wood, A., Fiorilla, C., Gerwick, W.H. Kaviol A, a Halogenated Phenolic Inhibitor of Histone Deacetylase from the marine

alga *Boodlea* sp. The dissertation author was the primary author and directed and supervised the research, which forms the basis for this chapter.

VITA

- 1997 B.S. Biology (minor in chemistry), University of Oregon.
- 1999-2002 Sr. Research Technician, NPSG, National Cancer Institute.
- 2008 Ph.D. Oceanography (marine natural products chemistry), Scripps Institution of Oceanography, University of California, San Diego.

PUBLICATIONS

- Simmons, T. L.; Nogle, L. M.; Media, J.; Valeriote, F. A.; Mooberry, S. L.; Gerwick, W. H. DMMC, a Cyanobacterial Depsipeptide with Potent Cytotoxicity in Cyclic and Ring-opened Forms. *J. Nat. Prod.* submitted.
- Simmons, T. L.; Engene, N.; Gerwick, L.; Gerwick, W. H. Viridamides A and B, lipodepsipeptides with anti-trypanosomal activity from the marine cyanobacterium *Oscillatoria nigro-viridis*. *J. Nat. Prod.* submitted.
- Simmons, T. L., Wood, A.; Fiorilla, C.; Gerwick, W. H. Kaviol A, a Halogenated Phenolic Inhibitor of Histone Deacetylase from the marine alga *Boodlea* sp. *J. Nat. Prod.* submitted.
- Simmons, T. L.; Coates, R. C.; Clark, B. R.; Engene, N.; Gonzalez, D.; Esquenazi, E.; Dorrestein, P. C.; Gerwick, W. H. Biosynthetic Origin of Natural Products Isolated from Marine Microorganism-Invertebrate Assemblages. *Proc. Nat. Acad. Sci. USA*. Accepted.
- Simmons, T. L.; Gerwick, W. H. In *Oceans and Human Health*, Walsh, P., Solo-Gabriele, H., Fleming, L.E., Smith, S.L., Gerwick, W.H. Eds.; Elsevier: New York, New York, **2008**; Ch. 22, Text in press.
- Simmons, T. L.; McPhail, K. L.; Ortega-Barría, E.; Mooberry, S. L.; Gerwick, W. H. Belamide A, a new antimitotic tetrapeptide from a Panamanian marine cyanobacterium. *Tetrahedron Letters* **2006**, *47*, 3387-3390.

- Ramaswamy, A. V.; Flatt, P. M.; Edwards, D. J.; Simmons, T. L.; Han, B.; Gerwick, W. H. The Secondary Metabolites and Biosynthetic Gene Clusters of Marine Cyanobacteria. Applications in Biotechnology. In *Frontiers in Marine Biotechnology*, Proksch, P., and Müller, W.E.G. Eds.; Horizon Bioscience: Norfolk, England, **2006**; pp 175-224.
- Simmons, T. L.; Andrianasolo, E.; McPhail, K. L.; Flatt, P.; Gerwick, W. H. Marine natural products as anticancer drugs. *Molecular Cancer Therapeutics* **2005**, *4*(2), 333-342.
- Simmons, T. L.; McCloud, T. G. Analysis of Stibonic Acids by Ion Exchange Chromatography with ESI-MS/Photodiode Array Detection. *Journal of Liquid Chromatography* **2003**, *26*(13), 2041-2051.

ABSTRACT OF THE DISSERTATION

Characterization of New Marine Secondary Metabolites for the Treatment of Cancer
and Neglected Tropical Diseases

by

Thomas Luke Simmons

Doctor of Philosophy in Oceanography

University of California, San Diego, 2008

Professor William H. Gerwick, Chair

Professor William H. Fenical, Co-chair

Small molecules from natural sources are vital to drug discovery by providing molecular diversity and novel chemical scaffolds for further pharmacological development. The emergence of multiple drug resistant pathogens and problems associated with natural product dereplication emphasize the continuing need for the discovery of new and relevant bioactive molecules for the treatment of human disease. This thesis describes the biological activity guided chemical investigation of several marine taxa with emphasis on the isolation and structure elucidation of new secondary metabolites with therapeutic efficacy against cancer and infectious disease.

Chapter I introduces the context, rationale and background which form the foundation of the thesis research. Chapter II describes the bioactivity guided discovery of a new cancer compound from a Panamanian marine cyanobacterium

Symploca sp. The linear tetrapeptide contains unusual and modified amino residues and exhibits sub-micromolar cancer toxicity with a classic antimitotic mechanism of action. Chapter III describes the discovery of DMMC a new cyclic depsipeptide isolated from a Fijian strain of *Lyngbya majuscula*. The antitumor effects displayed by this compound were very potent and selective for solid tumor cell lines. A linear analog of DMMC was generated during structure determination, this analog proved to maintain the exquisite and selective activity of the parent molecule. Chapter IV describes the discovery of the viridamides A and B from the cyanobacterium *Oscillatoria nigro-viridis*. Structure elucidation of these linear lipodepsipeptides revealed the presence of the novel 5-methoxydec-9-ynonic acid residue and subsequent biological evaluation indicated low micromolar efficacy against two species of disease causing protozoan pathogens. Chapter V describes the bioassay guided isolation and structure elucidation of kaviol A, a halogenated phenolic inhibitor of histone deacetylase (HDAC) from a Papua New Guinean strain of the green alga *Boodlea* sp. This unique C₆-C₄-C₆ structure contains multiple sites of halogenations and inhibits six isoforms of class II HDAC enzymes with very low micromolar IC₅₀ values. Chapter VI provides a conclusion of this thesis research.

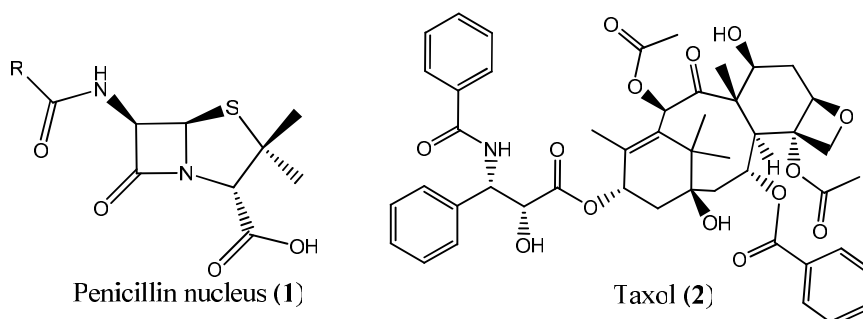
I

Introduction

I.1 General Introduction to Natural Products Chemistry

The exploitation of natural products for their bioactive properties has occurred since antiquity, with records of the recreational and therapeutic use of opiate alkaloids dating to Neolithic and ancient Egyptian times.^{1,2} More recently, small organic molecules from natural sources are of paramount importance to the discovery and development of new drugs. They provide both molecules with pharmaceutical potential and novel scaffolds for synthetic modification.^{3,4}

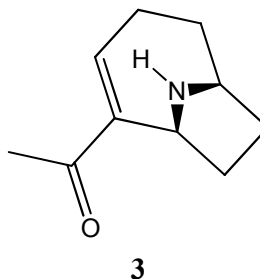
The ‘modern era’ of natural product chemical studies began in the 1800s and has aided the development of modern medicine with such discoveries as the penicillin antibiotics (**1**) by Alexander Fleming in the late 1920s and the anticancer agent taxol (**2**) in the following decades by Monroe Wall.^{5,6,7}

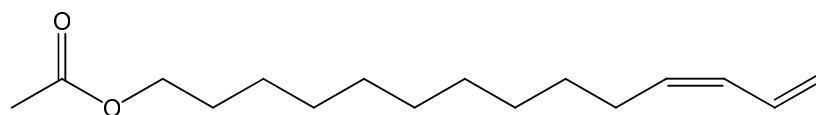


These pioneering efforts have paved the way for what has developed into the modern interdisciplinary fields of natural products chemistry and chemical biology. In recent decades researchers have begun exploring a molecular universe in ever finer detail and with recent advances in genomics, molecular biology, organic chemistry and computer science, the future looks exciting indeed.⁸

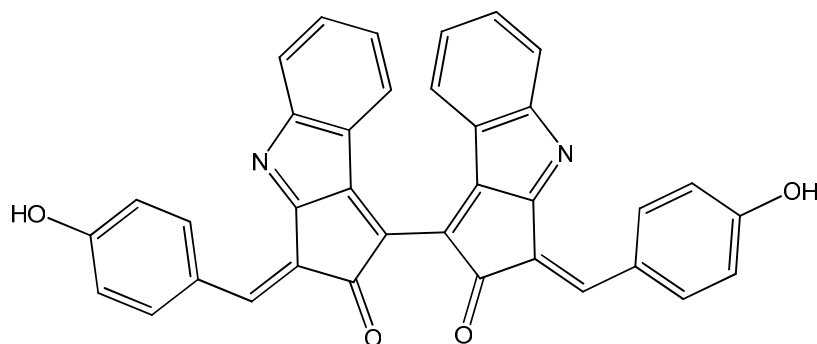
I.2 General Introduction to Thesis Research

Primary metabolic pathways and their products are essential for all life. Secondary metabolic pathways are not essential for the basic functioning of life, and ‘secondary metabolites’ are not necessarily produced under all conditions. While the precise function of these small molecules is not known in many cases, researchers in chemical biology and chemical ecology are beginning to assign roles for some and it appears that have diverse ecological and physiological roles. Some secondary metabolites are produced as toxic deterrents against predators. For example, anatoxin-A (**3**) a simple alkaloid toxin made by the cyanobacterium *Anabaena flos-aquae*, is an extremely potent neuro-toxic molecule thought to function as a predator deterrent. Other metabolites act as volatile attractants for members of the same or different species; in this case **4** is a sex pheromone of the South American Tortricid moth *Argyrotaenia spheropa*. Some secondary metabolites (for example scytonemin (**5**)) through their highly conjugated molecular structures serve as protection against harmful UV radiation from the sun, while others are vital to the well-being of host or symbiont species.^{9,10,11,12}





4



5

Regardless of the evolutionary ‘purpose’ of these molecules, many have proven to be pharmacologically active with efficacy against various forms of human disease, most prominently cancer.^{13,14,15,16}

Cancer is defined as a heterogeneous group of diseases characterized by aberrant cell growth and the metastatic invasion of healthy tissues and organs. Cancer is currently the second most common cause of death in the United States and will probably move to the number one spot in the near future.¹⁷ Despite the increasing occurrence of this lethal disease, success rates in cancer therapeutics are quite dismal.¹⁸ First generation anticancer drugs are primarily cytotoxic agents discovered by screening molecular libraries for compounds that kill tumor cells. Based on the concept that cancer cells are dividing and replicating their DNA more quickly than normal cells, researchers have developed discovery strategies focused on finding molecules that damage DNA, inhibit DNA synthesis (antimetabolites) or inhibit the ordered separation of DNA during mitotic of cell

division. Despite these efforts, the challenge of effectively treating cancer remains largely unmet. However recent advances in chemical biology and genomics are strengthening our approach and modern strategies now involve epigenetic regulation and the perturbation of signal transduction pathways involved in cellular proliferation.¹⁹

Marine natural products are increasingly prominent in cancer drug discovery for their capacity to kill tumor cells and modify gene expression in cancer cells.^{13,20} Why is this? And why are secondary metabolites produced by marine heterotrophic bacteria and cyanobacteria effective at killing cancer tumor cells? One theory holds that in the vastly competitive marine environment these secondary metabolites function as inhibitors of DNA-replication, DNA synthesis and the cell division of their microbial competitors. And as a consequence of their evolution as defensive agents these structurally diverse molecules also affect similar processes in tumor cells.

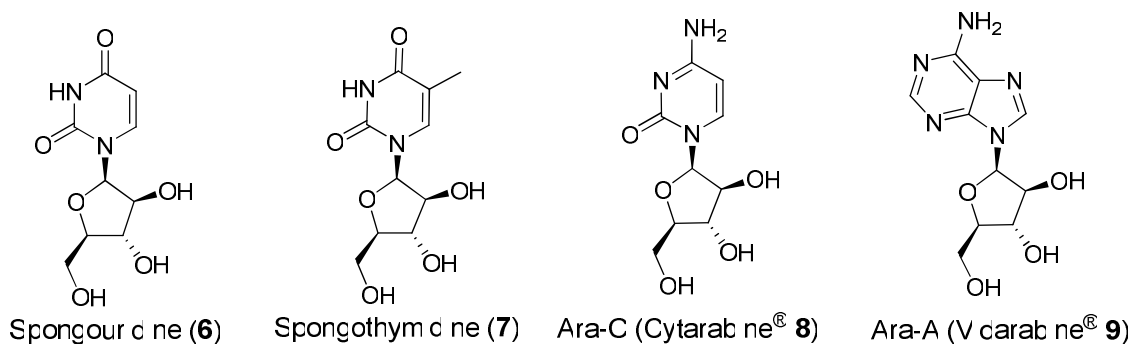
Table I.1 provides a summary of the important marine natural products, the organism from which they were originally isolated, their molecular targets and their current status in the clinical trial process.

Table I.1. Relevant marine natural products and their current clinical status.²⁰

Compound Name	Source Organism and Source of Material for Clinical Trial	Molecular target	Current Status
Ara-C (Cytarabine®; 9)	<i>Cryptotethya crypta</i> (sponge)	Nucleotide mimic	Clinically available; Phase I/II
Ecteinascidin 743 (10)	<i>Ecteinascidia turbinata</i> (tunicate)	Tubulin	Phase III (registered)
Å-941 (Neovastat®)	Shark cartilage	VEGF	Phase II/III (appears withdrawn Mar '07)
Bryostatin 1 (11)	<i>Bugula neritina</i> (bryozoan)	PKC	Phase I/II
Cemadotin (LU103793; Dolastatin 15 derivative)	<i>Dolabella auricularia</i> / <i>Symploca</i> sp. (mollusk/cyanobacterium; synthetic analog)	Tubulin	Phase I/II (Discontinued 2004)
Synthadotin (ILX651, Dolastatin 15 derivative)	<i>Dolabella auricularia</i> (synthetic analog)	Tubulin	Phase II
Kahalalide F (12)	<i>Elysia rufescens</i> / <i>Bryopsis</i> sp. (mollusk/green alga, synthetic)	Lysosomes / erbB pathway	Phase II
Squalamine	<i>Squalus acanthias</i> (shark)	Phospholipid bilayer	Phase II
Dehydrodidemnin B (13)	<i>Trididemnum solidum</i> (tunicate, synthetic)	Ornithine decarboxylase	Phase II
TZT-1027 (16)	<i>Dolabella auricularia</i> (synthetic analog)	Tubulin	Phase I/II
E7389 (18)	<i>Halichondria okadai</i> (sponge, synthetic)	Tubulin	Phase III
NVP-LAQ824 (19)	<i>Psammaphysilla</i> sp. (sponge, synthetic)	HDAC/DNMT	Phase I
Discodermolide (21)	<i>Discodermia dissoluta</i> (sponge)	Tubulin	Phase I (Discontinued 2005)
HTI-286 (23)	<i>Cymbastella</i> sp. (synthetic analog)	Tubulin	Phase I (Discontinued 2005)
LAF-389 (Bengamide B derivative)	<i>Jaspis digonoxea</i> (sponge, synthetic)	Methionine aminopeptidase	Phase I (Discontinued 2002)
KRN-7000 (25)	<i>Agelas mauritanus</i> (sponge, synthetic)	Vα24+NKT cell activation	Phase I
E7974 (24)	<i>Hemiasrella minor</i> (semi-synthetic analog)	Tubulin	Phase I
Zalypsis®	<i>Jorunna funebris</i> (mollusk; total synthesis)	DNA-binder	Phase I
Salinosporamide A (26)	<i>Salinospora</i> sp. (marine bacterium)	20S proteasome	Phase I
NPI-2358 (Halimide derivative)	<i>Aspergillus</i> sp. (fungus; semi-synthetic)	Tubulin	Phase I

The field of marine natural products drug discovery officially began in the 1950s with the discovery of spongouridine (**6**) and spongothymidine (**7**), nucleoside antimetabolites from the tropical marine sponge *Tethya crypta*.²¹ The subsequent

development of the synthetic analogs Ara-C (**8**) and Ara-A (**9**) produced two drugs now in clinical use for the treatment of non-Hodgkin lymphoma and viral infections, respectively.²²



The importance of these simple molecules came not only from their clinical application, but from the momentum they gave to the emerging field of marine natural products drug discovery. A recent analysis of the literature on the anticancer drugs used between 1940 and 2006 shows that 114 of 175 compounds are derived from natural products at some level.¹³ On the surface, drugs of marine origin appear to come from organisms belonging to a variety of taxonomic groups (Figure I.1).²⁰ However deeper investigations aided by advances in micro-chemical analysis, molecular genetics, mass spectrometry and cell sorting are showing that many of these molecules are actually the metabolic products of prokaryotes found in association with these marine invertebrates (Figure I.2).²⁰

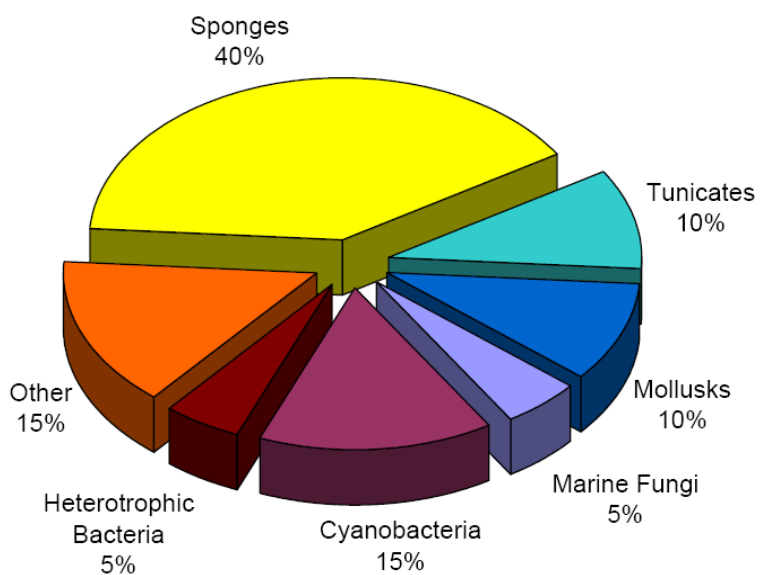


Figure I.1. The reported sources of 20 marine derived anticancer agents summarized in Table I.1.

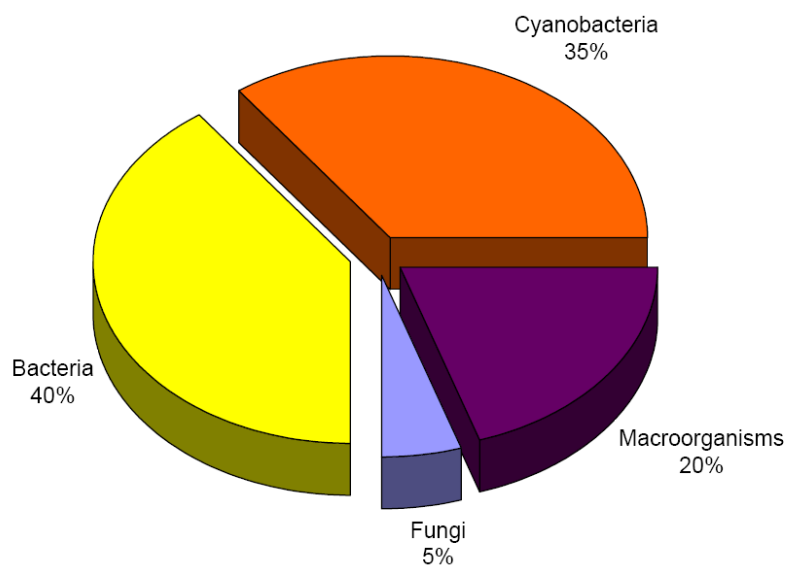
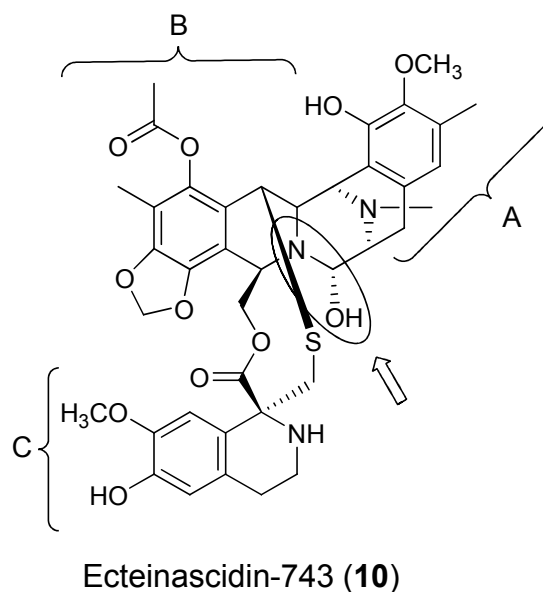


Figure I.2. The predicted sources of the 20 marine derived anticancer agents summarized in Table I.1 (based on direct genetic evidence or biosynthetic rationale).

I.3 Highlights of Marine Natural Product Drug Discovery

In the following sections I will discuss some of the more important anticancer marine natural products (and in some cases their synthetic descendants) with special attention to their discovery, biosynthesis, mechanism of action (MOA) and current drug development status.

As noted above, many bioactive molecules originally isolated from marine invertebrates are now thought to originate in prokaryotes. Ecteinascidin 743 (ET-743; **10**) provides a good example of this. In the late 1960s the organic extract of the tunicate *Ecteinascidia turbinata* was shown to display a variety of potent cytotoxic properties. And although it took more than 25 years to complete, the structure elucidation yielded several exciting and complex *tris*(tetrahydroisoquinoline) alkaloids, with the ecteinascidins as the active components.^{23,24,25} Early preclinical evaluation of these compounds initiated at the National Cancer Institute revealed good activity in various cancer models and has stimulated many further studies on their MOA, structure activity relationships (SAR) and biosynthesis.

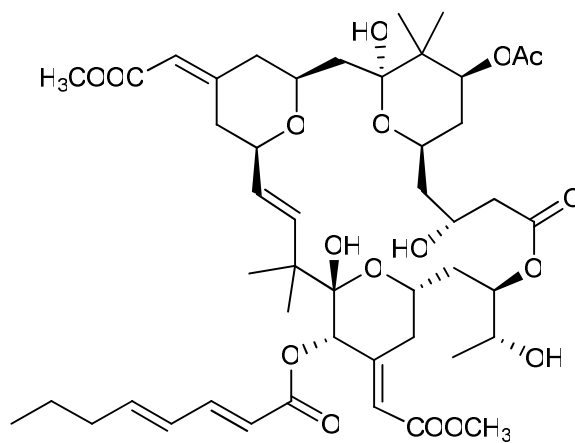


The strand-specific DNA binding properties of this structure class possessing the distinctive carbinolamine functionality (indicated by the arrow), have been studied extensively. Using advanced 2D NMR techniques researchers have shown that ET-743 (**10**) binds specifically at the N-2 position of guanine (in DNA minor groove), causing a distortion of tertiary structure which in turn interferes with gene transcription and induces apoptosis.²⁶ Phase II and III trials are currently ongoing for patients with advanced prostate and ovarian cancers.²⁷ Very recently **10** been accepted in Europe for the clinical treatment of advanced soft tissue sarcoma.²⁸

The biosynthesis of **10** and other 'gifted' molecules in this structure class is the result of a highly modified non-ribosomal peptide synthetase (NRPS) assembly which comprises three tetrahydroisoquinoline subunits (A-C). The diketopiperazine core (A and B subunits) is formed by condensation of two tyrosine-/Dopa-derived moieties with closure of the B ring occurring via (Pictet-Spengler) condensation with a serine-derived

aldehyde.²⁹ It is likely that *S*-adenosylmethionine (SAM) is the source for all pendant methyl groups in **10**.

While the chemical synthesis of ET-743 has been achieved several times, the low yield and high cost of these efforts have necessitated two ‘industrial scale’ approaches to supply **10** for clinical trials.^{30,31} Large scale production of ET-743 has been achieved in two ways; firstly, through aquaculture of the tunicate *Ecteinascidia turbinata*, and secondly, by the semi-synthesis of **10** from cyanosafrafin B, an alkaloid produced in large quantity by the bacterium *Pseudomonas fluorescens*. Although still quite laborious (21 step semi-synthesis), this second method is currently employed to supply ET-743 for clinical applications, as well as providing strong evidence for the microbial production of the ecteinascidins.³²



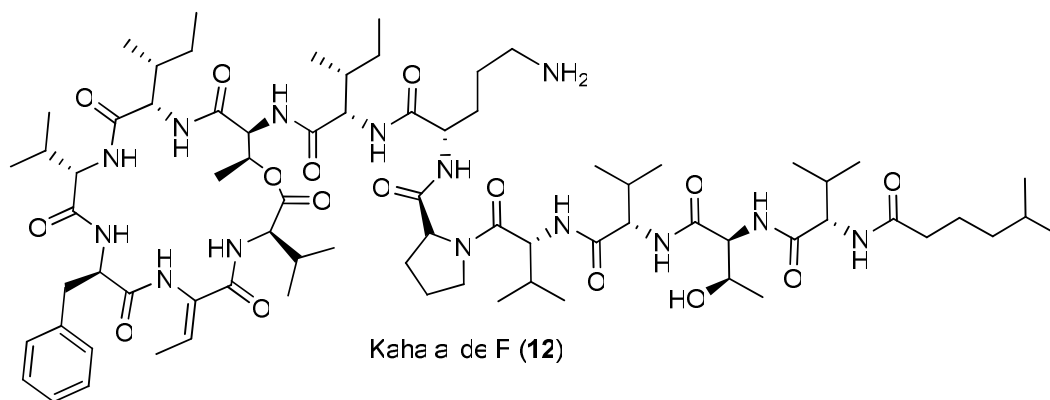
Bryostatin 1 (**11**)

The bryostatins are another family of complex molecules originally isolated from a marine invertebrate. After nearly 14 years of effort the structure of bryostatin 1 (**11**) was solved from extracts of the marine bryozoan *Bugula neritina*.³³ Bryostatin 1 is a

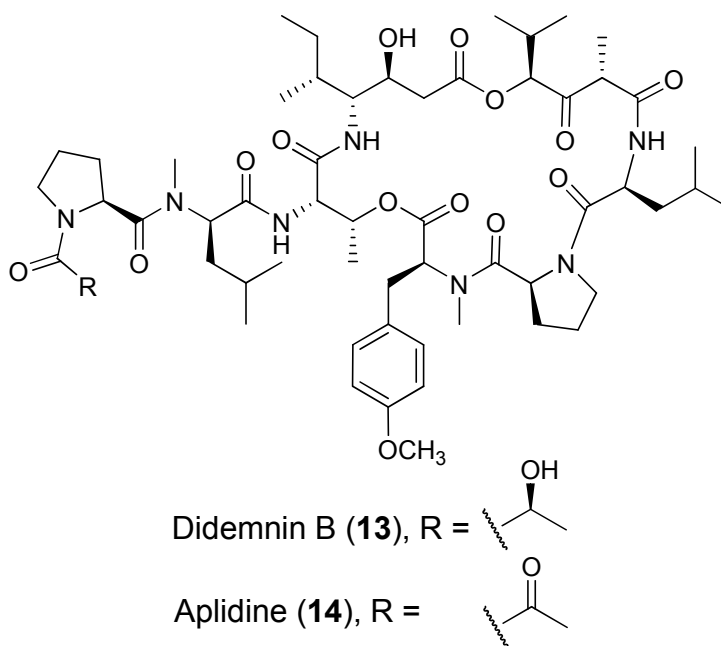
potent antineoplastic agent that induces cancer cell death through modulation of the protein kinase C (PKC) cell signaling pathway. While Phase II clinical trials have not shown much promise for bryostatin 1 when used as a single agent, there is evidence for its efficacy in combination drug therapies (e.g. with vincristine). The National Cancer Institute is currently recruiting patients for Phase I and Phase II clinical trials investigating **11** in combination therapies (www.clinicaltrials.gov).

A putative biosynthetic gene cluster for the bryostatins has been identified in two different strains of the newly characterized bacterium *Endobugula sertula*. This uncultured symbiotic γ -proteobacterial species was found in association with the free living larvae and mature colonies of *B. neritina*. Researchers have cloned a ~80 kbp polyketide synthase (PKS) gene cluster from *E. sertula* which encodes the biosynthetic proteins for a common precursor of all known bryostatins, thus revealing the origin of the bryostatin molecules.³⁴

There are other ways to obtain ‘defensive’ compounds; sacoglossan mollusks for example, have the ability to assimilate (and in some cases biotransform) metabolites from their diets for use as their own chemical deterrents.³⁵ These bioactive compounds are therefore often found in both the grazer and their respective fare. Kahalalide F (**12**) for example, is a cyclic depsipeptide first isolated from the marine mollusk *Elysia rufescens*, and then from the mollusks’ diet of the green alga *Bryopsis* sp. However, a recent report identifies a *Vibrio* bacterium living on the surface of the alga as the ultimate source of **12**.

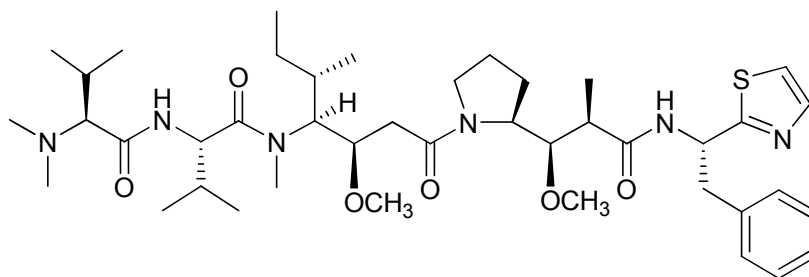
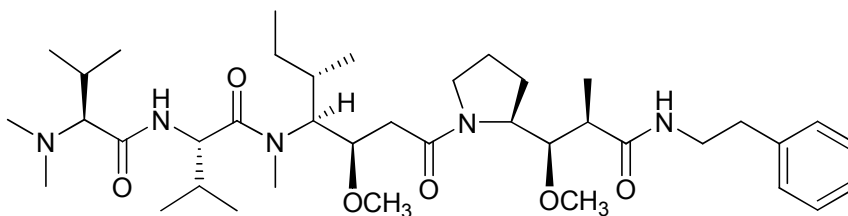


In 2005, kahalalide F entered phase I clinical trials for patients with advanced androgen refractory prostate cancer. Although the mechanism of action is not well understood, kahalalide F has been shown to induce cancer cell death via a necrosis-like process.³⁸ Currently, kahalalide F (**12**) is in phase II clinical trials for liver cancer, melanoma, and non-small cell lung cancer.³⁹

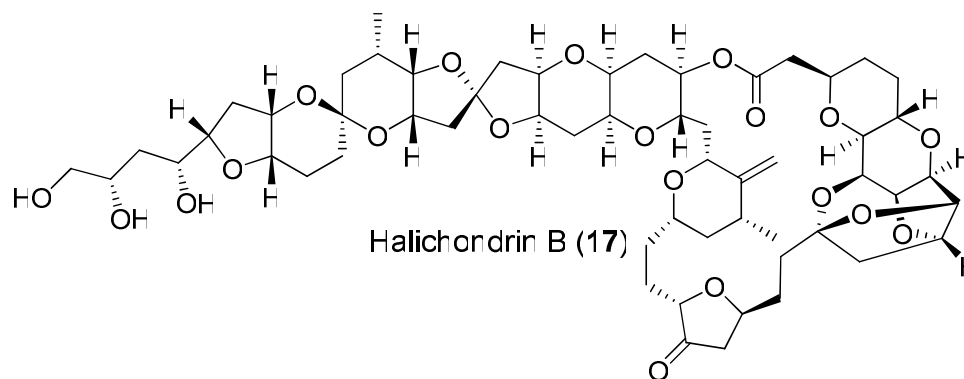


Didemnin B (**13**) is another medicinally relevant compound isolated from an ascidian (*Trididemnum solidum*). Reported in 1981 by the late Professor Ken Rinehart and colleagues, **13** displays high potency against L1210 leukemia cells with $LD_{50} = 0.0011 \mu\text{g/mL}$.⁴⁰ Didemnin B entered Phase I/II clinical trials in the late 1980s but was dropped due to its unpredictable toxicity in patients.

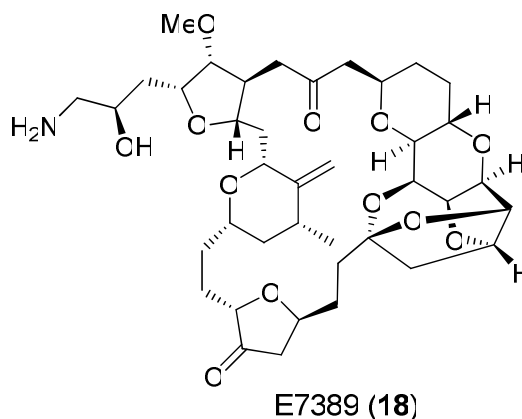
A close structural analog of **13**, aplidine (dehydrodidemnin B; **14**) continues to show promise for the clinical treatment of cancer. Also isolated from a tunicate (*Aplidium albicans*), **14** has been shown to inhibit DNA and protein synthesis, interfere with signal transduction events in proliferating cells, and block cell cycle progression at the G1 check point. Phase II clinical trials are underway with promising results in advanced melanoma and multiple myeloma patients previously treated with other anticancer agents.^{41,42} Although the genes encoding the biosynthesis of **13** or **14** have not been identified, the presence of a cyanobacterium (*Synechocystis trididemni*) within the tissues of the tunicate, and the peptide architecture of the compounds (likely the product of an NRPS assembly-line) is highly suggestive evidence for microbial secondary metabolism.⁴³

Dolastatin 10 (**15**)TZT-1027 (**16**)

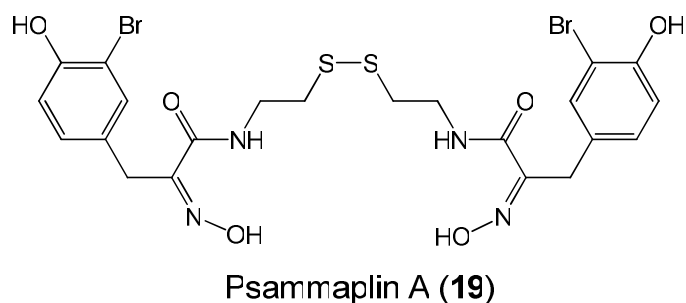
As for kahalalide F (**12**), dolastatin 10 (**15**) was first discovered in the organic extracts of a marine mollusk (*Dolabella auricularia*).⁴⁴ Subsequent studies have isolated **15** and several analogs directly from the favorite food of the nudibranch, filamentous marine cyanobacteria of the genus *Lyngbya*.⁴⁵ Based on their potent (in vivo) antimitotic properties these compounds have generated much excitement over the years. Although this natural product progressed into Phase II clinical trials, it was ultimately dropped as a single agent due to toxicity to peripheral tissues. Synthetic modifications of **15** to reduce toxicity resulted in the synthesis of TZT-1027 (Auristatin; Soblidotin; **16**), which recently completed a Phase II clinical trial in patients with advanced or metastatic soft-tissue sarcomas.⁴⁶ The authors of this latter study concluded that “TZT-1027 was found to be safe and well tolerated”.



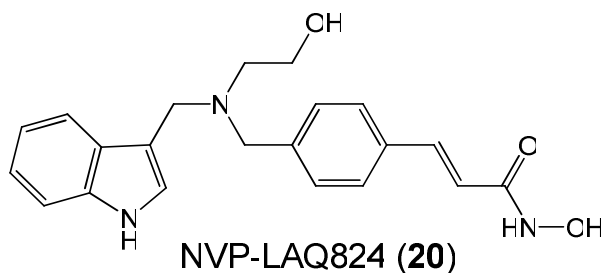
One of the most structurally complex and biologically potent marine natural products ever discovered is halichondrin B (**17**). This polyether macrolide is remarkably bioactive with IC_{50} values less than 100 $\mu\text{g/mL}$ against the B16 mouse melanoma in vitro.⁴⁷ Soon after its discovery, the National Cancer Institute (NCI) showed that the potent bioactivity of **17** was due (in whole or in part) to its ability to noncompetitively bind to β -tubulin.⁴⁸ Halichondrin B showed ‘across the board’ potent cancer cell toxicity when evaluated in the NCI’s 60 cell line panel with most IC_{50} values less than 100 μM .⁴⁹ Encouraged by these early results and to overcome the problem of very low natural abundance of **17** ($< 0.00001\%$ total weight of source sponge) a total synthesis of halichondrin B was completed in 1992. This work also led to synthesis of E7389 (**18**), a simplified and more effective antimitotic derivative of **17**.⁵⁰



E7389 (**18**), was recently tested in Phase II clinical trials for women with advanced breast cancer previously treated with other agents. Phase III trials are on-going to determine the efficacy of **18** in patients with locally recurrent or metastatic breast cancer. Polyether molecules like halichondrin B and the infamous okadaic acid (responsible for diarrhoeic shellfish poisoning worldwide) have been isolated from a variety of marine sponges and dinoflagellates. Biosynthetically these molecules originate as polyunsaturated fatty acids (PKS construction, suggesting microbial metabolism) which undergo epoxidation of the double bonds followed by a concerted epoxide opening/cyclization sequence leading to the extended polyether structure. Interestingly, a relatively non toxic compound (*GT4b*) is thought to be biosynthesized by the dinoflagellate *Gambierdiscus toxicus*. This precursor presumably passes through the food chain where it is eventually modified into the highly toxic ‘ciguatoxin’ by metabolic processes in the predatory organism.⁵¹

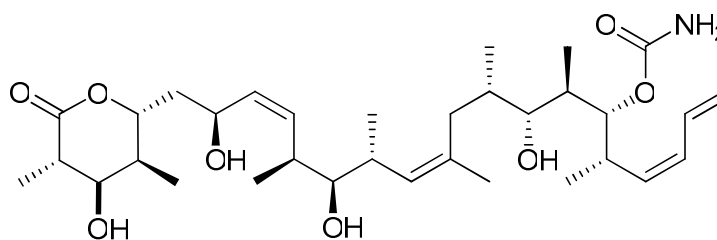


Psammaplin A (**19**) is a symmetrical oxime-containing bromotyrosine metabolite (isolated from the sponge *Psammaphysilla* sp.) which exhibits potent cytotoxicity against P388 cells ($IC_{50} = 0.3$ ng/mL).^{52,53,54}



This promising compound has stimulated a lot of interest both in terms of its wide spectrum of biological activity and as a target for total synthesis.⁵⁵ Interestingly, **19** is able to inhibit the function of several important enzymes in an array of prokaryotic and eukaryotic systems, including those involved in epigenetic gene regulation. Using a cell-based screen, scientists at Novartis have identified three natural products (trapoxin B, trichostatin A and **19**) that induce expression of the cyclin dependent kinase inhibitor p21^{waf1} (via inhibition of histone deacetylase (HDAC)). The three compounds were subsequently examined for their respective HDAC inhibitory pharmacophores. The

medicinal chemical studies that followed ultimately produced NVP-LAQ824 (**20**), a synthetic compound that combined the requisite features of all three molecules while displaying enhanced patient tolerability, efficacy and potency against HDAC.^{56,57,58} NVP-LAQ (**20**) is currently undergoing Phase I clinical trials for a variety of solid tumors and as a combination therapy against malignant melanoma.⁵⁹ While the metabolic origin of **19** remains uncertain, there are many examples of bromophenolic ethers and other halogenated (modified) amino acid derived structures being isolated directly from the *Oscillatoria spongelliae* a cyanobacterium typically found in association with sponges.⁶⁰

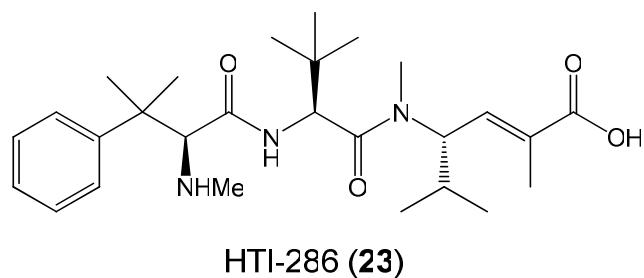
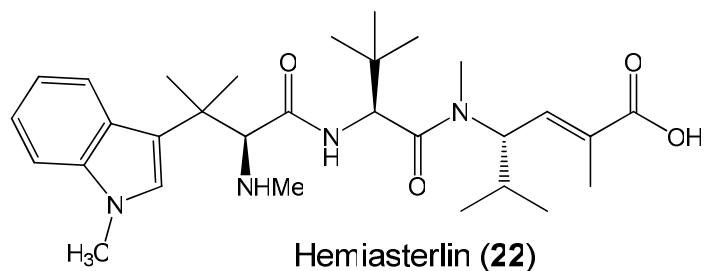


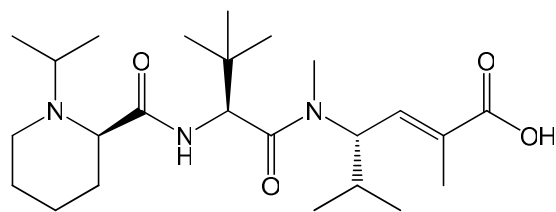
Discodermolide (**21**)

Not all marine natural products are found in shallow waters. Extracts of the deep water marine sponge *Discodermia dissoluta* for example, provide the potent antimetabolic polyhydroxylated lactone discodermolide (**21**) in low yield.⁶¹ Discodermolide displays activity in both anti-fungal and two-way mixed-lymphocyte culture assays. The mechanism of action for **21** has been studied in some detail, and like taxol, discodermolide binds β -tubulin and leads to microtubule stabilization. Discodermolide (**21**) has been taken into phase I clinical trials, but was withdrawn due to patient toxicity.

While the (presumably bacterial)⁶² gene cluster encoding the PKS modules responsible for the biosynthesis of **21** has not *yet* been obtained from the sponge, a synthetic gene approach has been attempted and intermediates along the route to discodermolide have been produced.⁶³

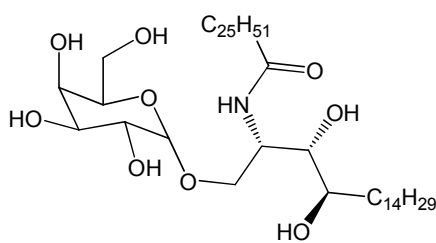
On occasion researchers discover organisms that either produce or contain numerous biologically active small molecules. The South African sponge *Hemiastrella minor* is a good example of this. In the mid 1990s *H. minor* yielded the previously described cyclic peptide jasplakinolide (jaspamide) as well as two new compounds, geodiamolide TA and hemiasterlin (**22**).⁶⁴ The latter molecule (**22**) has shown promising antimitotic efficacy against a variety of tumor types.



E-7974 (**24**)

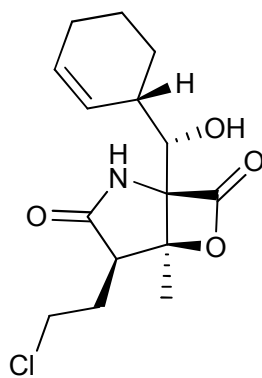
A synthetic analog was developed (HTI-286; **23**) which displays improved activity and pharmacologic properties.⁶⁵ In 2003, **23** entered Phase I clinical trials for the treatment of advanced malignant solid tumors where potent activity was demonstrated (in vitro) against several tumor types including both taxane-sensitive and taxane-resistant tumors.⁶⁶ Additional hemiasterlin analogs have been synthesized; for example E-7974 (**24**) is currently undergoing three Phase I clinical trials for patients with advanced solid malignancies.⁶⁷

Biomimetic small molecule natural products have also been studied for their inherent biological effects. For example, the α -galactosylceramide, KRN7000 (**25**), closely resembles monoglycosylated ceramides used by nearly all living cells for cellular regulation processes (e.g. neuronal regulation, protein kinase C activity, hormone receptor function and cell-cell recognition).

KRN7000 (**25**)

KRN7000 was first isolated from the marine sponge *Agelas mauritianus* as a novel immunomodulator with potent antitumor activity in B16 melanoma mouse models.⁶⁸ Recent clinical evaluations indicate that KRN7000 (**25**) activates human V α 24 natural killer T cells which then “show a strong antitumor activity against various malignant tumors”,⁶⁸ as well as activating other antitumor effector cells by enhanced production of cytokines such as IFN- γ and interleukin-4.⁶⁹

Increasingly, researchers are directly identifying marine prokaryotes that produce clinically relevant molecules. Moreover, advances in the cultivation of bacteria are allowing researchers to investigate how environmental conditions (i.e. induced microbial competition and variable media ingredients) affect the biosynthesis of secondary metabolites. These efforts have yielded some exciting new small molecules with antibacterial and anticancer properties.^{70,71} Salinosporamide A (**26**) for example, was discovered from a newly characterized marine actinomycete *Salinispora tropica*.⁷²



Salinosporamide A (**26**)

The absolute structure of this fused γ -lactam- β -lactone bicyclic compound (**26**) was solved by extensive NMR analysis and completed by a single-crystal X-ray

diffraction study. Evaluation of the biological activity of salinosporamide A against the HCT-116 human colon carcinoma cell line indicated cytotoxicity with an $IC_{50} = 11$ ng/mL, while mechanism-based and co-crystallization studies showed **26** to irreversibly bind in the yeast 20S proteasome core.⁷³ Salinosporamide A is currently undergoing Phase I clinical trials in relapsed and/or refractory multiple myeloma patients.⁷⁴

I.4. Rationale of Thesis

The examples presented above illustrate the incredible potential of marine natural products drug discovery, especially in the area of cancer therapeutics. Based on these examples I hypothesized that a systematic chemical investigation of prokaryotic and eukaryotic marine organisms with parallel cell toxicity and mechanism based disease assays would be an effective approach to the discovery of additional novel bioactive secondary metabolites. The objective of this dissertation research was to examine novel secondary metabolites from marine cyanobacterial and algal sources, and to isolate, purify and determine the structures of new bioactive compounds with potential for the treatment of human diseases.

I.5. Overview of Thesis Research

Chapter II describes the discovery of belamide A, a tetrapeptide from the marine cyanobacterium *Symploca* sp. which displays (in vitro) antimitotic activity with low micromolar IC_{50} s. Coauthors contributed the following, K.L. McPhail assisted with structure elucidation of belamide A, E. Ortega-Barria oversaw the initial bioassay for isolation and S.L. Mooberry performed the tubulin studies. The text of II, in part, is

published material as it appears in: Simmons, T.L., McPhail, K.L., Ortega-Barría, E., Mooberry, S.L., Gerwick, W.H. Belamide A, a new antimitotic tetrapeptide from a Panamanian marine cyanobacterium. *Tetrahedron Letters* **2006**, *47*, 3387-3390. The dissertation author was the primary author and directed and supervised the research which forms the basis for this chapter. A reprint of the published research article is provided in the appendix.

Chapter III describes the discovery of desmethoxymajusculamide C (DMMC) from the marine cyanobacterium *Lyngbya majuscula*. DMMC is a new cyclic depsipeptide which displays potent cancer cytotoxicity in its cyclic and linear forms. Coauthors contributed the following: L.M. Nogle assisted on the structure elucidation of DMMC, F.A. Valeriote performed the IC₅₀ and clonogenic studies for DMMC and S.L. Mooberry performed the microfilament studies. The text of III, in full, is the manuscript draft to be submitted to an academic journal as it will appear: Simmons, T.L., Nogle, L.M.; Valeriote, F.A.; Mooberry, S.L.; Gerwick, W.H. DMMC, a Cyanobacterial Depsipeptide with Potent Cytotoxicity in Cyclic and Ring-opened Forms. The dissertation author was the primary author and directed and supervised the research which forms the basis for this chapter.

Chapter IV describes the discovery of the viridamides A and B, linear lipodepsipeptides with anti-protozoan activity from the marine cyanobacterium *Oscillatoria nigro-viridis*. Coauthors contributed the following: N. Engene performed phylogenetic analysis of *O. nigro-viridis* and L. Gerwick assisted in the phylogenetic analysis of *O. nigro-viridis*. The text of IV, in full, is the manuscript draft to be submitted to an academic journal as it will appear: Simmons, T.L., Engene, N., Gerwick, L.,

Gerwick, W.H. Viridamides A and B, lipodepsipeptides with anti-trypanosomal activity from the marine cyanobacterium *Oscillatoria nigro-viridis*. The dissertation author was the primary author and directed and supervised the research which forms the basis for this chapter.

Chapter V describes the discovery of kaviol A, a novel secondary metabolite from the marine alga *Boodlea* sp. This unusual C₆-C₄-C₆ structure is highly halogenated and displays potent activity against six isoforms of the protein histone deacetylase. Coauthors contributed the following: A. Wood and C. Fiorilla were responsible for the HDAC inhibition assays. The text of V, in full, is the manuscript draft to be submitted to an academic journal as it will appear: Simmons, T.L., Wood, A., Fiorilla, C., Gerwick, W.H. Kaviol A, a Halogenated Phenolic Inhibitor of Histone Deacetylase from the marine alga *Boodlea* sp. The dissertation author was the primary author and directed and supervised the research which forms the basis for this chapter.

Chapter VI summarizes my work, briefly discusses potential directions of the field and provides conclusions based upon the thesis research.

The appendix provides supplemental information for each of the research chapters.

References

- (1) Cohen, M.M. *Tex. Med.* **1969**, *65*, 76-85.
- (2) Mann, J., *Murder Magic and Medicine*. Oxford University Press: New York, 1992, pp 1-17.
- (3) Clardy, J., Walsh, C. *Nature* **2004**, *432*, 829-837.
- (4) Koehn, F.E., Carter, G.T. *Nat. Rev. Drug Disc.* **2005**, *4*, 206-220.
- (5) Sondheimer, J.B., Simeone, E. *Chemical Ecology*. Academic Press, New York, 1970.
- (6) Fleming, A. *Br. J. Exp. Pathol.* **1929**, *10*, 226-236.
- (7) Wall, M. *Med. Res. Rev.* **1998**, *18*, 299-314.
- (8) (a) Faulkner, D.J. *Nat. Prod. Rep.* **2000**, *17*, 1-6; (b) Faulkner, D.J. *Nat. Prod. Rep.* **2002**, *1*, 1-49; (c) Blunt, J.W., Copp, B.R., Hu, W-P., Munro, M.H.G., Northcote, P.T., Prinsep, M.R. *Nat. Prod. Rep.* **2007**, *24*, 31-86.
- (9) Gerwick, W.H., Tan, L., Sitachitta, N. *The Alkaloids*; Academic Press: San Diego, 2001; Vol. 57, pp. 75-184.
- (10) Paul, V.J., Puglisi, M.P., Ritson-Williams, R. *Nat. Prod. Rep.* **2006**, *23*, 153-180.
- (11) Pawlik, J.R. *Chem. Rev.* **1993**, *93*, 1911-1922.
- (12) Faulkner, D.J., Ghiselin, M.T. *Mar. Ecol. Prog. Ser.* **1983**, *13*, 295-301.
- (13) Simmons, T.L., Andrianasolo, E., McPhail, K., Flatt, P. Gerwick, W.H. *Mol. Cancer Thera.* **2005**, *4*, 333-342.

- (14) Newman, D.J., Cragg, G.M. *Curr. Drug Targets* **2006**, *7*, 279-304.
- (15) Newman, D.J., Cragg, G.M. *J. Nat. Prod.* **2007**, *70*, 461-477.
- (16) Mayer, A.M.S., Gustafson, K.R. *Eur. J. Cancer* **2006**, *42*, 2241-2270.
- (17) Varmus, H. *Science* **2006**, *312*, 1162-1165.
- (18) Kamb, A.; Wee, S.; Lengauer, C. *Nat. Rev. Drug Disc.* **2007**, *6*, 115-120.
- (19) Collins, I.; Workman, P. *Nat. Chem. Biol.* **2006**, *2*, 689-700.
- (20) Simmons, T.L., Gerwick, W.H. In *Oceans and Human Health*, Walsh, P., Solo-Gabriele, H., Fleming, L.E., Smith, S.L., Gerwick, W.H. Eds.; Elsevier: New York, New York, **2008**; Ch. 22, Text in press.
- (21) Bergmann, W., Feeney, R.J. *J. Org. Chem.* **1951**, *16*, 981-987.
- (22) Bodey, G.P., Freirich, E.J., Monto, R.W., Hewlett, J.S. *Cancer Chemother.* **1969**, *53*, 59-66.
- (23) Sigel, M.M., Wellham, L.L., Lichter, W., Dudeck, L.E., Gargus, J.L. Lucas, L.H. 1970. In food-drugs from the sea, Proceedings, 1969; Youngken, H.W., (Ed.), Marine Technology Society: Washington DC., pp 281-295.
- (24) Rinehart, K.L., Holt, T.G., Fregeau, N.L., Stroh, J.G., Keifer, P.A., Sun, F., Li, H.L., Martin, D.G. *J. Org. Chem.* **1990**, *55*, 4512-4515.
- (25) Wright, A.E., Forleo, D.A., Gunawardana, G.P., Gunasekera, S.P., Koehn, F.E., McConnell, O.J. *J. Org. Chem.* **1990**, *55*, 4508-4512.

(26) (a) Moore, B.M. II, Seaman, F.C., Wheelhouse, R.T., Hurley, L.H. *J. Am. Chem. Soc.* **1998**, *120*, 2490-2491; (b) Seaman, F.C., Hurley, L.H. *J. Am. Chem. Soc.* **1998**, *120*, 13028-13041.

(27) (a) www.clinicaltrials.gov; (b) Beumer, J.H. Buckle, T., Ouwehand, M., et al. *Invest. New Drugs* **2006**, *25*, 1-7.

(28) <http://www.emea.europa.eu/humandocs/Humans/EPAR/yondelis/yondelis.htm>

29) (a) Sakai, R., Jares-Erijiman, E.A., Manzanares, I., Elipe, M.V.S., Rinehart, K.L. *J. Am. Chem. Soc.* **1996**, *118*, 9017-9023; (b) Kerr, R.G., Miranda, N.F. *J. Nat. Prod.* **1995**, *58*, 1618-1621.

(30) Martinez, E.J., Owa, T., Schreiber, S.L., Corey, E.J. *Proc. Natl. Acad. Sci.* **1999**, *96*, 3496-3501.

(31) Chen, X., Chen, J., Zhu, J. *Synthesis* **2006**, *23*, 4081-4086.

(32) Cuevas, C., Perez, M., Martin, M.J., et al. *Org. Lett.* **2000**, *2*, 2545-2548.

(33) Pettit, G.R., Day, J.F., Hartwell, J.L., Wood, H.B. *Nature* **1970**, *227*, 962-963.

(34) Sudek, S., Lopanik, N.B., Waggoner, L.E., Hildebrand, M., Anderson, C., Liu, H., Patel, A., Sherman, D.H., Haygood, M.G. *J. Nat. Prod.* **2007**, *70*, 67-74.

(35) (a) Gerwick, W.H., Whatley, G. *J. Chem. Ecol.* **1989**, *15*, 677-683; (b) Stallard, M.O., Faulkner, D.J. *Comp. Biochem. Physiol.* **1974**, *48b*, 25-35.

(36) Hamann, M.T., Scheuer, P.J. *J. Am. Chem. Soc.* **1993**, *115*, 5825-5826.

(37) Hill, R.T., Hamann, M.T., Enticknap, J., Rao, K.V. PCT Int. Appl. **2005**, WO 2005042720

- (38) Janmaat, M.L., Rodriguez, J.A., Jimeno, J., Kruyt, F.A.E., Giaccone, G. *Mol. Pharmacol.* **2005**, *68*, 502-510.
- (39) http://www.pharmamar.com/en/press/news_release.cfm?newsReleaseID=148&year=2006
- (40) Rinehart, K.L., Gloer, J.B., Cook, J.C. *J. Am. Chem. Soc.* **1981**, *103*, 1857-1859.
- (41) Maroun, J.A., Belanger, K., Seymour, L., et al. *Ann. Oncol.* **2006**, *17*, 1371-1378.
- (42) Straight, A.M., Oakley, K., Moores, R., et al. *Cancer Chemother. Pharmacol.* **2006**, *57*, 7-14.
- (43) Sings, H.L., Rinehart, K.L. *J. Ind. Microbiol.* **1996**, *17*, 385-396.
- (44) Pettit, G.R., Kamano, Y., Herald, C.L., Tuinman, A.A., Boettner, F.E., Kizu, H., Schmidt, J.M., Baczynskyj, L., Tomer, K.B., Bontems, R.J. *J. Am. Chem. Soc.* **1987**, *109*, 6883-6885.
- (45) (a) Harrigan, G. G., Luesch, H., Yoshida, W. Y., Moore, R. E., Nagle, D. G., Paul, V. J., Mooberry, S. L., Corbett, T. H., Valeriote, F. A. *J. Nat. Prod.* **1998**, *61*, 1075-1077;
(b) Luesch, H., Moore, R. E., Paul, V. J., Mooberry, S. L., Corbett, T. H. *J. Nat. Prod.* **2001**, *64*, 907-910.
- (46) Patel, S., Keohan, M.L., Saif, M.W., et al. *Cancer* **2006**, *107*, 2881-2887.
- (47) Hirata, Y., Uemura, D. *Pure Appl. Chem.* **1986**, *58*, 701-710.
- (48) Bai, R., Paull, K.D., Herald, C.L., Malspeis, L., Pettit, G.R., Hamel, E. *J. Biol. Chem.* **1991**, *266*, 15882-15889.
- (49) Fodstad, O., Bristol, K., Pettit, G.R., Shoemaker, R.H., Boyd, M.R. *J. Exp. Ther. Oncol.* **1996**, *1*, 119-125.

(50) (a) Aicher, T.D., Buszek, K.R., Fang, F.G., Forsyth, C.J., Jung, S.H., Kishi, Y., Matelich, M.C., Scola, P.M., Spero, D.M., Yoon, S.K. *J. Am. Chem. Soc.* **1992**, *114*, 3162-3164; (b) http://dtp.nci.nih.gov/timeline/noflash/success_stories/S4_halichondrinB.htm

(51) Murata, M., Legrand, A.M., Ishibashi, Y., Fukui, M., Yasumoto, T. *J. Am. Chem. Soc.* **1990**, *112*, 4380-4386.

(52) Quiñoá, E., Crews, P. *Tetrahedron Lett.* **1987**, *28*, 3229-3232.

(53) Arabshahi, L., Schmitz, F.J. *J. Org. Chem.* **1987**, *52*, 3584-3586.

(54) Rodriguez, A.D., Akee, R.K., Scheuer, P.J. *Tetrahedron Lett.* **1987**, *42*, 4989-4992.

(55) Godert, A.M., Angelino, N., Woloszynska-Read, A., S.R., James, S.R., Karpf, A.R., Sufrin, J.R. *Bioorg. Med. Chem. Lett.* **2006**, *16*, 3330-3333.

(56) Remiszewski, S.W. *Curr. Med. Chem.* **2003**, *10*, 2392-2402.

(57) Catley, L., Weisberg, E., Tai, Y-T., et al. *Br. J. Cancer* **2006**, *95*, 961-965.

(58) Kim, D.H., Shin, J., Kwon, H.J. *Exp. Mol. Med.* **2007**, *39*, 47-55.

(59) Kato, Y., Salumbides, B.C., Wang, X-F., et al. *Mol. Cancer Ther.* **2007**, *6*, 70-81.

(60) (a) Unson, M.D., Faulkner, D.J. *Experientia* **1993**, *49*, 349-353; (b) Unson, M.D., Holland, N.D., Faulkner, D.J. *Mar. Biol.* **1994**, *119*, 1-8; (c) Flowers, A.E., Garson, M.J., Webb, R.I., Dumbel, E.J., Charan, R.D. *Cell Tissue Res.* **1998**, *292*, 597-603.

(61) Gunasekera, S.P., Gunasekera, M., Longley, R.E., Schulte, G.K. *J. Org. Chem.* **1990**, *55*, 4912-4915.

(62) Piel, J. *Curr. Med. Chem.* **2006**, *13*, 39-50.

- (63) Burlingame, M.A., Mendoza, E., Ashley, G.W., Myles, D.C. *Tetrahedron Lett.* **2006**, *47*, 1209-1211.
- (64) Talpir, R., Benayahu, Y., Kashman, Y., Pannell, L., Schleyer, M. *Tetrahedron Lett.* **1994**, *35*, 4453-4456.
- (65) Nieman, J.A., Coleman, J.E., Wallace, D.J., et al. *J. Nat. Prod.* **2003**, *66*, 183-199.
- (66) Ratain, M.J., Undevia, S., Janisch, L., et al. *Proc. Am. Soc. Clin. Oncol.* **2003**, *22*, 129.
- (67) Campagna, S., Pop, M.M. (Eisai Co., Ltd., Japan) *PCT Int. Appl.* **2006**, WO 2006121857 A2 20061116
- (68) Kobayashi, E., Motoki, K., Takeshi, U., Fukushima, H., Koezuka, Y. *Oncol. Res.* **1995**, *7*, 529-534.
- (69) Motohashi, S., Ishikawa, A., Ishikawa, E., et al. *Clin. Cancer Res.* **2006**, *12*, 6079-6086
- (70) Fenical, W., Jensen, P.R. *Nature Chem. Biol.* **2006**, *2*, 666-673.
- (71) Mincer, T.J., Jensen, P.R., Kauffman, C.A., Fenical, W. *Appl. Environ. Microbiol.* **2002**, *68*, 5005-5011.
- (72) Feling, R.H., Buchanan, G.O., Mincer, T.J., Kauffman, C.A., Jensen, P.R., Fenical, W. *Angew. Chem. Int. Ed.* **2003**, *42*, 355-357.
- (73) Groll, M., Huber, R., Potts, B.C.M. *J. Am. Chem. Soc.* **2006**, *128*, 5136-5141.
- (74) Chauhan, D., Hideshima, T., Anderson, K.C. *Br. J. Cancer* **2006**, *95*, 961-965.

II

Belamide A, a new antimitotic tetrapeptide from a Panamanian marine cyanobacterium

Abstract

The isolation and structure elucidation of belamide A from the marine cyanobacterium *Symploca* sp. is described. Belamide A is a highly methylated linear tetrapeptide with structural analogy to the important linear peptides dolastatins 10 and 15. Disruption of A-10 microtubule network was observed at 20 μM and displayed classic tubulin destabilizing antimitotic characteristics. Additionally, the moderate cytotoxicity (IC_{50} 0.74 μM vs. HCT-116 colon cancer line) of belamide A gives additional insight into structure-activity relationships for this drug class.

Introduction

Marine cyanobacteria synthesize a myriad of structurally complex and biologically active secondary metabolites.¹ Of specific importance to human health is a diverse family of peptides and depsipeptides known as the dolastatins. Originally isolated from the sea hare *Dolabella auricularia*, dolastatins 10 and 15 display extraordinary cytotoxicity to cancer cells (IC₅₀ values 0.059 and 2.9 nM, respectively).² Although neither of these two compounds is still undergoing clinical evaluation, they have stimulated extensive synthetic efforts resulting in several drug leads currently in clinical trials.³ These synthetic efforts have generated considerable structure-activity knowledge in this compound family.³ Here we report a novel structural analog of dolastatin 10 and 15, belamide A (**1**), as a major metabolite of the marine cyanobacterium *Symploca* sp.

Belamide A, a highly methylated tetrapeptide, contains two characteristic residues of dolastatin 15 (figure II.1), the N-terminal N,N-dimethylvaline and C-terminal benzyl-methoxypyrrolinone moieties. This work expands on the repertoire of linear peptides from marine cyanobacteria and contributes to our knowledge of SAR features for this important class of lead anticancer compounds.

The organic oil (CH₂Cl₂: MeOH, 360 mg) of a Panamanian cyanobacterium *Symploca* sp.⁴ was initially found to be highly cytotoxic to the MCF-7 breast cancer cell line (IC₅₀ = 8 ng/mL), and was thus fractionated using a silica gel solid phase extraction column and elution solvents of increasing polarity. The resultant four fractions (A-D)⁵ were profiled by ¹H NMR and fraction D exhibited interesting signals typical for a

modified peptide. Thus, it was subjected to exhaustive RPHPLC⁶ to yield 3.6 mg of pure belamide A (**1**) (figure II.1).

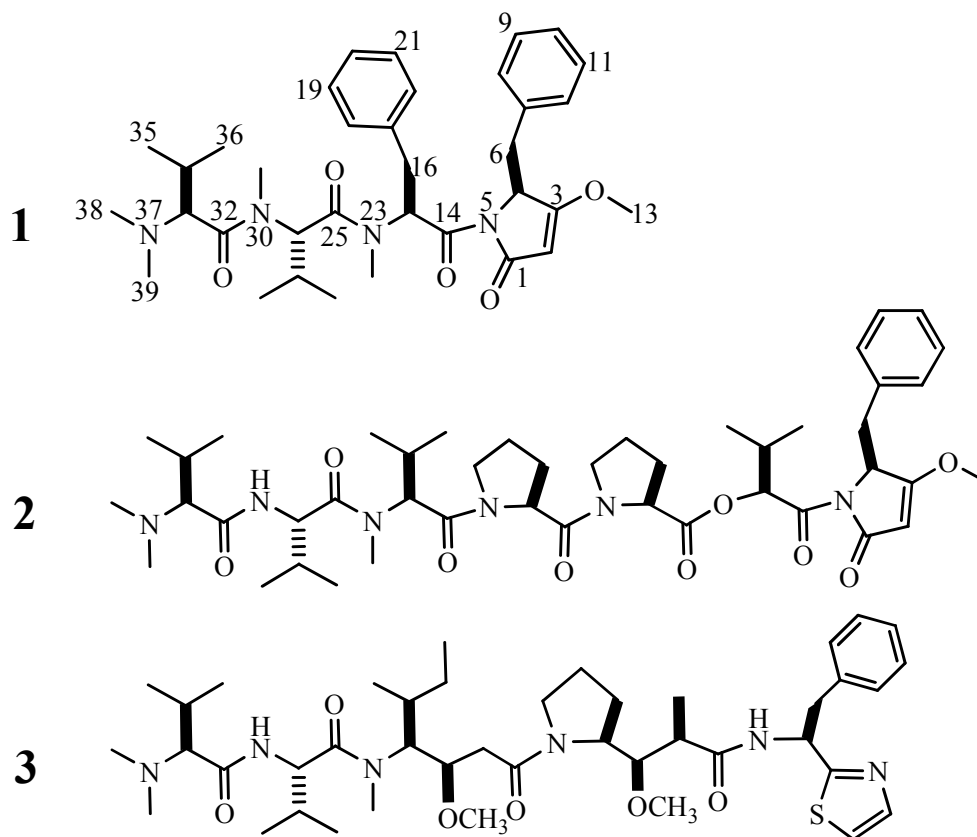


Figure II.1. Molecular structures of belamide A (**1**), dolastatin 15 (**2**), and dolastatin 10 (**3**).

Results and Discussion

HR TOF MS (ES+) measurement indicated a molecular formula of $C_{35}H_{48}N_4O_5$ (M+H obs. m/z 605.3643; calc. 605.3624), and was in agreement with the observed physical data.⁷ Although **1** readily dissolved in $CDCl_3$, some isochronous proton chemical shifts were observed; these were resolved in C_6D_6 which was used in the remainder of this study (Table II.1).

1D NMR (Table II.1) spectra were well dispersed in C_6D_6 , and indicated the presence of *N*- and *O*-methyl functionalities. Three *N*-methylated amino acid substructures were deduced from 2D NMR data (1H - 1H COSY, multiplicity edited 1H - ^{13}C HSQC, and 1H - ^{13}C HMBC) as well as tandem MS data (Figure II.3), including *N*-Me-Phe (C-14 to C-23); *N*-Me-Val (C-25 to C-32) and *N,N*-diMe-Val (C-33 to C-39; see Table II.1).

The interesting chemical shifts recorded for a methine carbon (C-2, δ_C 95.0; δ_H 4.28) adjacent to the quaternary carbon at δ_C 177.7 (C-3) suggested oxygenation at the latter position. Additionally, HMBC correlations between H-2 (δ 4.28) and C-1 (δ 169) and C-4 (δ 59.9); H-4 (δ 4.57) and C-2 (δ 95.0); H-5 (δ 2.91) and C-3 (δ 177.7) were observed, and defined a substituted pyrrolinone ring (see figure II.2). By additional HMBC correlations from the C-6 methylene protons to C-7 and C-8/12, one substituent was revealed as a benzyl moiety. A second substituent was a methoxy group (3H at δ 3.38) located at C-3 by a long range 1H - ^{13}C correlation between the methoxy proton resonance (H₃-12) and C-3. These data were reinforced by MS/MS fragments (see figure II.3)

which further supported a benzyl-methoxypyrrolinone moiety was present at the C-terminus of **1**.

It was readily apparent that the N,N-diMe-Val residue formed the N-terminus and the benzyl-methoxypyrrolinone moiety formed the C-terminus of belamide A. Sequencing of the remaining residues was accomplished by HMBC (Table II.1) and Tandem MS (Figure II.3). Correlations between H-26 (δ 5.65) and C-31 (δ 30.3) as well as H₃-31 (δ 2.57) and C-32 (δ 171.7) linked the N-Me-Val and N,N-diMe-Val residues. Finally, correlations between H-15 (δ 2.77) and C-25 (δ 173.0) and H-26 (δ 5.65) and C-25 linked the N-Me-Val and N-Me-Phe residues. Tandem electrospray ionization (ESI) mass spectral fragmentation patterns were straightforward and allowed facile residue sequencing for the planar structure of belamide A (**1**).

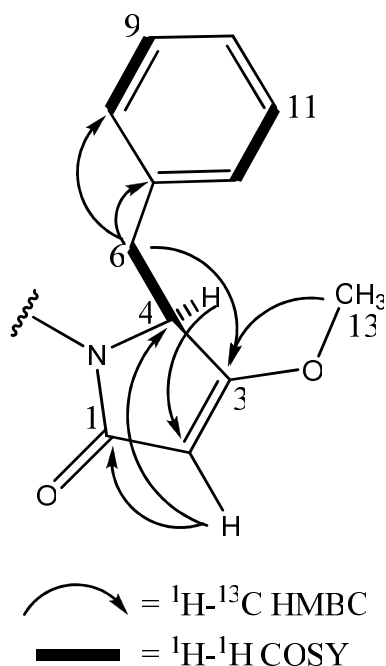


Figure II.2. HMBC and COSY correlations for the benzyl-methoxypyrrolinone (“dolapyrrolidone”) residue in belamide A (**1**).

The absolute configuration of **1** was based on chiral HPLC analysis.⁸ Retention times of the 6N HCl hydrolysate components of **1** were compared to commercially available amino acid standards, and indicated *L*-configurations for the N-Me-Phe and N-Me-Val units. In the case of N,N-diMe-Val, analytical standards were synthesized from *S*- and *R*-valine using literature methods,⁹ and compared with the hydrolysate of **1** by chiral HPLC; this residue was also of *L*-configuration. Determination of C-4 required ozonolysis of **1** followed by acid hydrolysis which yielded free phenylalanine; this was also determined to be *L* by chiral HPLC.⁸

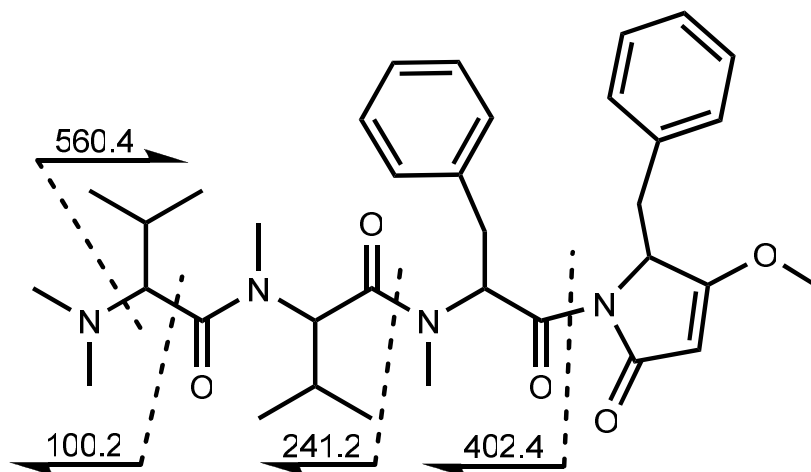


Figure II.3. Tandem MS fragments of belamide A (**1**).

Pure belamide A (**1**) assayed against the MCF7 breast cancer cell line, displayed an $IC_{50} = 1.6 \mu\text{M}$, while to the HCT-116 colon cancer cell line it was somewhat more potent giving an $IC_{50} = 0.74 \mu\text{M}$.

Bai et al. have shown that β -tubulin binding for this class of linear peptides (there now exist many synthetic analogs) is mainly influenced by the N-terminal residue sequence and configuration at key stereogenic centers.¹⁰ Mitra and Sept have developed an alternative model based on the in silico binding behavior of known tubulin binding compounds (viz. dolastatin 10, cryptophycin 52, and others), in conjunction with multiple X-ray crystal structures of bovine β -tubulin.¹¹ These models support a single high affinity binding pocket at the ‘plus’ end of the β -tubulin monomer adjacent to the exchangeable GTP site; however, there is some discussion regarding which residues of dolastatin 10 and 15 are critical for this interaction.¹⁰⁻¹³ Interestingly, structural features

of both of these two drugs are found in belamide A, and appear to be consistent with the SAR developed from extensive analog work evaluated both *in vitro*¹² and *in vivo*.¹³

The N-terminus of belamide A is formed by an N,N-dimethylvaline residue, a feature found in both dolastatin 10 and 15, and which is reported to be one of the more critical residues for potent biological activity. However, the naturally occurring analog symplostatatin 1 possesses an N,N-dimethylisoleucine residue and is nearly as potent as dolastatin 10,¹⁴ and synthetic analogs possessing a N,N-dimethylglycine terminus were only modestly diminished in potency.¹³ The second residue is also a valyl derivative (as in both 2 and 3); however, in belamide A this residue is N-methylated. No reported analogs in the dolastatin 10 or 15 series possess N-methylation at this position, and this may explain the lower potency of compound **1**. In the dolastatin 15 series, the third residue is N-methyl valine; synthetic studies have shown that slight variations in side chain structure result in analogs with only modest variations in potency. In fact, in the dolastatin 10 series, residues with a bulkier side chain at residue-3 (i.e. isoleucyl derivative) have greater *in vivo* potency vs. the smaller valine analog.¹⁵ Therefore, the larger N-methyl Phe residue of belamide A should not necessarily diminish activity of **1**.

Residue-3 of both dolastatin 10 and 15 is N-methylated, as it is in belamide A; this is a required feature for high potency as demonstrated by synthetic analogs.¹³

The final residue of belamide A is precisely as found for the C-terminal residue of dolastatin 15, benzyl-methoxypyrrolinone. Numerous analogs of the carboxy terminus in both the dolastatin 10 and 15 series have been examined, and in general, this residue is highly tolerant of change, although the required structural feature appears to be a benzyl

group. In the case of a terminating benzyl-methoxypyrrolinone residue, the S-stereoconfiguration as found in belamide A has been shown to be critical.¹⁶ Truncated tri- and tetra-peptides have been synthesized and examined for their properties as well. Analogs composed of the N-terminal first three residues or C-terminal four residues of dolastatin 10 were active in inhibiting tubulin assembly, but only weakly cytotoxic.¹⁷

Given the structural similarity of belamide A to the dolastatins 10 and 15, we were interested to further understand the reduced bioactivity of belamide A. From molecular mechanics calculations of the energy minimized structures of belamide A (**1**) and dolastatin 15 (**2**) and aligning of their C-termini, only a weak overlap correlation was observed (Figure II.6).¹⁸ However alignment of the N-terminal regions of these two linear peptides resulted in a reasonably good fit for the first three residues of both compounds. However, the two adjacent proline residues in **2** results in back-to-back β -turns, thereby 'swinging' the C-terminal pyrrolinone moiety out of conformational overlap with belamide A. Similar analysis was performed with dolastatin 10 (**3**); in this case, alignment of the N-termini of **1** and **3** resulted in a very poor conformational overlap. The dolaproine unit of dolastatin 10 causes the peptide to adopt an overall 'sickle' shape whereas belamide A retains a more linear conformation (Figure II.6).

In the absence of definitive crystal structures of **2** or **3** bound to tubulin, there remains debate regarding the critical pharmacophore for this family of anticancer agents. Our results for belamide A are intermediate between the pharmacophore hypotheses put forth by Bai et al.¹⁰ (dolavaline-valine-dolaisoleuine) and that of Mitra and Sept.¹¹ (valine-dolaisoleuine-dolaproine). Belamide A displays classic microtubule

depolymerizing effects including concentration dependent interphase microtubule loss, micronucleation and abnormal mitotic spindle formation at 20 μM (Figures II.4 and II.5). Belamide A also possesses moderately potent cytotoxicity (IC_{50} 0.74 μM , vs. HCT-116 cells), these moderately potent biological effects may be attributed to the N-terminal residue sequence and its hydrophobic binding interaction within the peptide-groove of β -tubulin. Conversely, if belamide A does bind to this peptide-groove, it does so with relatively low affinity, possibly due to one or a combination of missing structural features or steric hindrance, as discussed above. Further biological evaluation of belamide A is needed to fully appreciate the biomedical potential of this compound.

Table II.1.) NMR data for belamide A (600 MHz for ^1H ; 75 MHz for ^{13}C).

Unit	C/H no.	δ_{H} , mult, (J in Hz)	δ_{C} (75MHz, mult.)	^1H - ^1H COSY	^1H - ^{13}C HMBC*	
Bn-O-Me-pyrrolinone	1		169.0 (C)			
	2	4.28 (s)	95.0 (CH)		C1, C4	
	3		177.7 (C)			
	4	4.57 (dd, 3.3, 3.6)	59.9 (CH)	H-6	C2	
	N-5					
	6	2.91 (dd, 3.0, 2.8) 3.68 (dd, 4.4, 4.5)	35.10 (CH ₂)	H-4	C3, C7, C8/12	
	7		138.1 (C)			
	8/12	7.27 (m)	130.1 (CH)	H-9/11		
	9/11	7.28 (m)	128.6 (CH)	H-8/12		
	10	7.00 (m)	126.8 (CH)			
	13	3.38 (s, 3H)	58.9 (CH ₃)		C3	
	N-Me-Phe	14		172.6 (C)		
		15	2.77 (m)	57.3 (CH)	H-16	C14, C17, C24, C25
16		2.82 (dd, 3.7, 2.6) 3.52 (dd, 3.4, 3.2)	34.1 (CH ₂)	H-15	C18/22	
17			134.9 (C)			
18/22		7.43 (m)	129.2 (CH)	H-19/21		
19/21		7.09 (m)	128.7 (CH)	H-18/22		
20		7.08 (m)	127.4 (CH)			
N-23						
24		2.75 (s)	32.8 (CH ₃)			
N-Me-Val		25		173.0 (C)		
	26	5.65 (d, 10.4)	58.3 (CH)	H-27	C25, C31	
	27	2.53 (m)	27.7 (CH)	H-26,28,29		
	28	0.90 (d, 6.7)	19.2 (CH ₃)	H-27	C26, C27, C29	
	29	1.11 (d, 6.4)	20.1 (CH ₃)	H-27	C26, C27, C28	
	N-30					
N,N-diMe-Val	31	2.57 (s)	30.3 (CH ₃)		C32	
	32		171.7 (C)			
	33	2.85 (d, 10.3)	68.9 (CH)	H-34	C32, C38, C39	
	34	2.33 (m)	28.8 (CH)	H-33,35,36		
	35	1.03 (d, 6.6)	20.3 (CH ₃)	H-34	C33	
	36	0.57 (d, 6.7)	20.5 (CH ₃)	H-34	C33	
	N-37					
	38	2.36 (s)	41.4 (CH ₃)		C33	
	39	2.36 (s)	41.4 (CH ₃)		C33	

* Includes data from 1D ^1H - ^{13}C HMBC with a delay time for the evolution of long-range heteronuclear coupling optimized for 4 Hz (125 ms).

NMR chemical shifts were assigned by ^1H - ^1H COSY, ^1H - ^{13}C HSQC, and modified 1D ^1H - ^{13}C HMBC experiments (C_6D_6 ; 128.02/7.16 ppm).

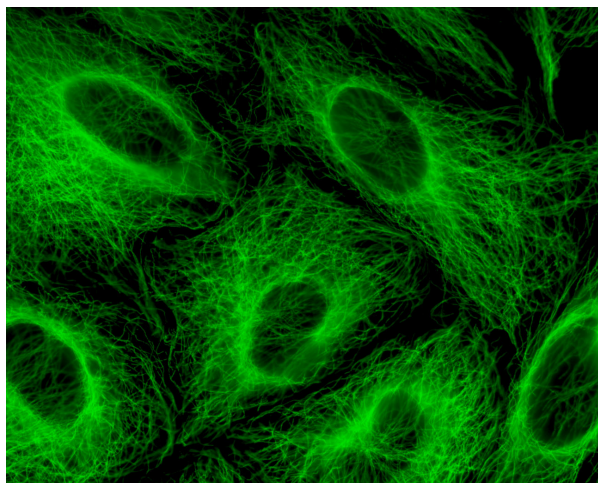


Figure II.4. Untreated (negative control) rat intestinal A10 cells stained to show cytoskeletal microtubule network during mitotic cell division.

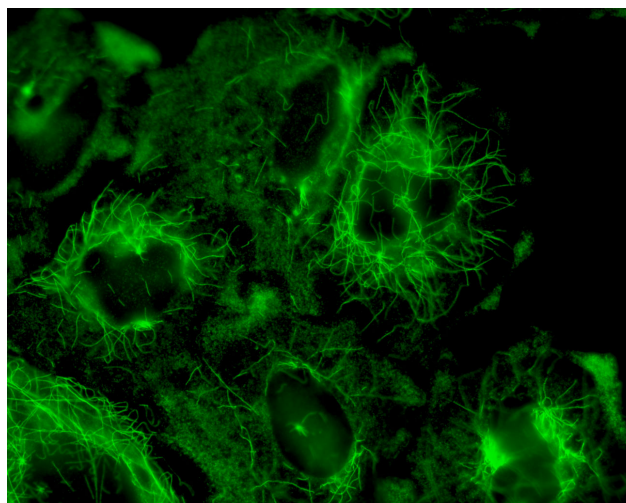


Figure II.5. Rat intestinal A10 cells treated with 20 μM belamide A (**1**) and stained to show microtubule depolymerization effects. This illustrates the effects of a classic antimitotic agent with concentration dependent interphase microtubule loss, micronucleation and abnormal mitotic spindle formation.

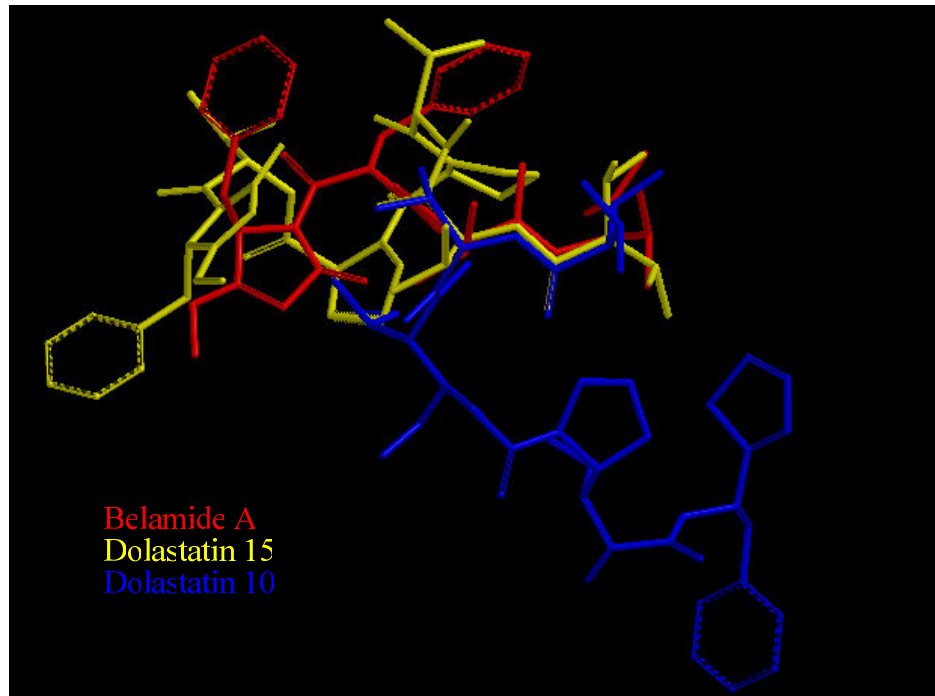


Figure II.6. Structural overlay of the lowest energy geometric conformations (Hartree-Fock, 6-31 basis set) for belamide A (red), dolastatin 15 (yellow) and dolastatin 10 (blue). This figure illustrates the conformational divergence and adds insight to the variable biological activity observed for these compounds.

References and Notes

- (1) Gerwick, W.H.; Tan, L.T.; Sitachitta, N. "Nitrogen-containing metabolites from marine cyanobacteria" In "The Alkaloids" G. Cordell, ed., Academic Press, San Diego, **2001**, Vol. 57; pp 75-184.
- (2) a) Pettit, G.R.; Kamano, Y.; Herald, C.L.; Tuinman, A.A.; Boettner, F.E.; Kizu, H.; Schmidt, J.M.; Baczynskyj, L.; Tomer, K.B.; Bontems, R.J. *J. Am. Chem. Soc.* **1987**, *109*, 6883-6885; b) Pettit, G.R.; Kamano, Y.; Dufresne, C.; Cerny, R.L.; Herald, C.L.; Schmidt, J.M. *J. Org. Chem.* **1989**, *54*, 6005-6006.
- (3) a) Newman, D.J. and Cragg, G.M. *J. Nat. Prod.* **2004**, *67*, 1216-1238; b) Simmons, T.L.; Andrianasolo, E.; McPhail, K.; Flatt, P.; Gerwick, W.H. *Mol. Cancer Ther.* **2005**, *4*, 333-342.
- (4) Live algal sample collected on 11/3/03 at Salmedina Reef, Portobelo, Panama; N 09°33.799' x W 79°41.642'; in shallow water by Drs. Kerry L. McPhail and William H. Gerwick.
- (5) Phenomenex Strata (Si-1; 55µm particle) NP solid phase extraction column eluted with 100 mL of each the following solvent compositions, fraction: A [8:2] hexanes:EtOAc; B [1:1] hexanes:EtOAc; C 100% EtOAc; D 100% MeOH.
- (6) Phenomenex Synergi 4µ Fusion-RP 250x10mm column; isocratic [8:2] MeOH:H₂O, then [7:3] MeOH:H₂O
- (7) Belamide A (1) was isolated as a yellow glassy oil, $[\alpha]_D^{25} + 16^\circ$ (c 0.002; CDCl₃); UV (CHCl₃) λ_{\max} 240 nm; IR ν_{\max} (KBr) 2960, 2926, 2853, 2790, 1997, 1722, 1697, 1630 cm⁻¹.
- (8) All chiral HPLC analysis was performed using a Phenomenex Chirex 3126 D column with a 2mM CuSO₄/CH₃CN mobile phase except the N,N-diMe-Val which required 100% 2mM CuSO₄ buffer.
- (9) Pettit, G.R., inventor; Arizona Board of Regents, assignee. Synthesis of Dolastatin 10. United States patent US 4978744. 1990 Dec 18.

(10) Bai, R.; Roach, M.C.; Jayaram, S.K.; Barkoczy, J.; Pettit, G.R.; Ludueña, R.F.; Hamel, E. *Biochem. Pharmacol.* **1993**, *45*, 1503-1515.

(11) Mitra, A. and Sept, D. *Biochemistry* **2004**, *43*, 13955-13962.

(12) Pettit, G.R.; Srirangam, J.K.; Barkoczy, J.; et al. *Anti-Cancer Drug Design* **1998**, *13*, 243-277.

(13) Miyakaki, K.; Kobayashi, M.; Natsume, T.; Gondo, M.; Mikami, T.; Sakakibara, K.; Tsukagoshi, S. *Chem. Pharm. Bull.* **1995**, *43*, 1706-1718.

(14) Luesch, H.; Moore, R.E.; Paul, V.J.; Mooberry, S.L.; Corbett, T.H. *J. Nat. Prod.* **2001**, *64*, 907-910.

(15) Bai, R.; Pettit, G.R.; Hamel, E. *Biochem. Pharmacol.* **1990**, *40*, 1859-1864.

(16) Poncet, J.; Busquet, M.; Roux, F.; Pierré, A.; Atassi, G.; Jouin, P. *J. Med. Chem.* **1998**, *41*, 1524-1530.

(17) a) Hamel, E. *Biopolymers (Pept Sci)* **2002**, *66*, 142-160; b) Hamel, E. and Covell, D.G. *Curr. Med. Chem.: Anti-Cancer Agents* **2002**, *2*, 19-53.

(18) Spartan '04, Wavefunction, Inc., Irvine, CA.

Acknowledgments

The text of II, in part, is published material as it appears in Simmons, T.L., McPhail, K.L., Ortega-Barría, E., Mooberry, S.L., Gerwick, W.H. Belamide A, a new antimitotic tetrapeptide from a Panamanian marine cyanobacterium. *Tetrahedron Letters* **2006**, *47*, 3387-3390. A reprint of the published research article is provided in appendix A. The dissertation author was the primary author and directed and supervised the research, which forms the basis for this chapter.

III

DMMC, a Cyanobacterial Depsipeptide with Potent Cytotoxicity in Cyclic and Ring-opened Forms

Abstract

A cytotoxicity assay guided fractionation of the organic extract of a Fijian *Lyngbya majuscula* led to desmethoxymajusculamide C (DMMC) as the bioactive metabolite. Spectroscopic analysis including 1D and 2D NMR, MS/MS, as well as chemical degradation and derivatization were used to assign the planar structure and configuration of this new cyclic depsipeptide. Biological evaluation of DMMC demonstrated potent and selective anti-solid tumor activity with an $IC_{50} = 19$ nM against the HCT-116 human colon carcinoma cell line in vitro via disruption of cellular microfilament networks. A linear form of DMMC was generated by base hydrolysis to facilitate mass spectroscopic analysis and allow confirmation of the proposed amino acid sequence. The linear DMMC was subsequently evaluated and shown to maintain potent actin depolymerization characteristics while displaying equivalent solid tumor selectivity in the disk diffusion assay. A clonogenic assay assessing cytotoxicity to HCT-116 cells as a function of exposure duration showed that greater than 24 h of constant exposure was required to yield significant cell killing. Therapeutic studies on HCT-116 bearing scid mice demonstrated efficacy at the highest dose used: 0.625 mg/kg daily for 5 days.

Introduction

Actin is among the most ubiquitous and highly conserved proteins known, existing in either globular (G-actin monomer) or filamentous (F-actin polymer) forms. Actin microfilaments are in a tightly controlled dynamic equilibrium with actin monomers which is crucial for cell growth and division, motility, signaling and tertiary cellular structure.¹ Transformed cancer cells are known to undergo distinct changes in actin cytoskeletal organization and protein regulation which contribute to the abnormal growth characteristics of tumor cells. As a consequence of altered microfilament dynamics, the cancer cell has enhanced capacity for tissue adhesion, tumorigenesis and an increased ability to metastasize.^{2,3} Metastatic tissue invasion involves a form of cellular motility usually termed ‘amoeboid motility’, a process driven by cycles of actin polymerization, cell adhesion, and acto-myosin contraction.⁴ These cellular processes, therefore, offer logical starting points for the development of anticancer drug discovery screens.

A large number of small organic secondary metabolites have been isolated from marine invertebrates and microorganisms which show promising anticancer activities.^{5,6} Of these, several have been shown to selectively modulate the actin polymerization cycle. Jasplakinolide,⁷ hectochlorin⁸ and dolicolide,⁹ for example are known to stimulate actin polymerization, while latrunculin¹⁰ and various trisoxazole containing macrolides display actin depolymerization properties.¹¹ The mechanism of action had been studied in some detail for jasplakinolide and dolicolide, with both causing cell cycle arrest at the G₂/M phase by inducing the hyperpolymerization of purified actin and aggregation of the

resultant F-actin. In addition, both compounds were able to competitively displace a fluorescent phalloidin derivative from the actin polymer.⁷ Interestingly, hectochlorin displayed many of the same effects on actin polymerization but was unable to displace fluorescent phalloidin from the polymerized protein.⁸ The cyclic depsipeptides majusculamide C, dolastatins 11 and 12 have also shown very promising cytotoxic activity by arresting cells at cytokinesis by stimulating a rapid reorganization (hyperpolymerization) of the cellular microfilament network in a dose- and time-dependent manner.^{12,13} Conversely, the polyketide derived latrunculin and non-ribosomal peptide derived trisoxazole class of compounds stimulate F-actin depolymerization. Latrunculin and the trisoxazole macrolides alter actin-monomer interactions, inhibiting polymerization and nucleotide (ATP) exchange, respectively, ultimately causing microfilament depolymerization and cancer cell death.^{9,10}

Here we report the discovery of desmethoxymajusculamide C (DMMC; **1**), a new cyclic depsipeptide with potent actin depolymerization properties in both the native cyclic (**1**) and ring-opened linear forms (**2**). In initial screening strong cytotoxicity was observed in the organic extract of the cyanobacterium *Lyngbya majuscula* collected from the Kauriti Reef, Fiji. Bioassay-directed isolation led to DMMC (**1**) as the active constituent. Extensive chemical and spectroscopic structure elucidation revealed **1** to be a close structural analog to a well known class of bioactive depsipeptides (Figure III.3). DMMC, like its structural relatives, displays potent activity against a variety of cancer cell lines by the disruption of cytoskeletal actin microfilament networks. Perhaps of greater significance, we have demonstrated that the ring-opened linear form of DMMC maintains equivalent efficacy and solid tumor selectivity as the cyclic molecule. These

findings raise significant questions regarding the active form of the many biologically active cyclic (depsi)peptides reported in the literature to date.

Results and Discussion

Structure Determination of 1. Desmethoxymajusculamide C (DMMC; **1**) was isolated as a light yellow glassy oil with a molecular formula of $C_{49}H_{78}N_8O_{11}$ as determined by HR FAB MS (obsd m/z $[M + H]^+$ 955.5867; calcd for m/z 955.5868). This molecular formula combined with the observed IR absorption bands at 1739 and 1641 cm^{-1} for ester and amide functionalities, respectively, indicated a molecule of peptide origin. The 1H and ^{13}C NMR spectra for **1** were well dispersed in $CDCl_3$ (Table 1 and supporting information) and allowed the construction of nine partial structures by 2D NMR (COSY, HMBC) and accounted for all atoms in the molecular formula for **1**. Six standard amino acids were deduced as alanine (Ala), *N*-methyl-valine (*N*-MeVal), *N*-methyl-phenylalanine (*N*-MePhe), *N*-methyl-isoleucine (*N*-MeIle) and two glycine (Gly) units. Two additional residues were assembled to form the α -hydroxy acid, 2-hydroxy-3-methylpentanoate (Hmpa) and the β -amino acid, 3-amino-2-methylpentanoate (Map). The ninth and final moiety, deduced mainly from HMBC, was constructed as 4-amino-2,2-dimethyl-3-oxo-pentanoate (Dmop).

Amino and hydroxy acid sequencing was accomplished by HMBC connectivities (Table 1) and was supported by CID MS fragmentation of the base hydrolysis product of **1** (Figure III.2). The configuration of the stereogenic centers found in **1** was determined by chiral HPLC and Marfey's analysis. Fortunately, the doubling and broadening of

specific ^1H - and ^{13}C NMR signals, as were observed for dolastatin 12, lyngbyastatin 1 and others, did not occur in our analysis, thus suggesting the presence of a single C-15 epimer.¹²

Table III.1. ^1H and ^{13}C NMR Spectral data for DMMC (**1**) recorded in CDCl_3 at 400 and 75 MHz, respectively.

Residue	#	δ_{C}	δ_{H} (mult.)	HMBC ^a
Map	1	172.8		
	2	42.7	2.76, qd (7.0, 1.6)	1, 3
	3	51.4	4.52, m	
	4 (NH)		7.07, d (10.1)	3, 8
	5	10.0	1.10, d (7.0)	1, 2, 3
	6	26.3	1.56, 1.48	2, 3, 7
	7	11.2	0.93, t (7.4)	3, 6
	8	173.0		
Ala	9	48.5	4.45	8, 11
	10 (NH)		7.76, d (7.9)	9, 11, 12
	11	15.7	1.07, d (7.9)	8, 9
	12	172.3		
Dmop	13	55.1		
	14	210.3		
	15	52.0	4.92	14, 19
	16 (NH)		7.32, d (6.4)	14, 15, 20
	17	22.5	1.53, s	12, 13, 14, 18
	18	21.7	1.48, s	12, 13, 14, 17
	19	19.3	1.16, d (6.8)	14, 15
	20	168.0		
N-Me Phe	21	61.0	5.23	20, 23, 24, 30
	22 (N)			
	23	35.7	3.31, dd (14.0, 6.3) 2.89, dd (14.0, 8.2)	20, 21, 24, 25/29
	24	137.0		
	25/29	129.7	7.25	23, 24, 26/28, 27
	26/28	129.0	7.28	24, 25/29
	27	127.2	7.20, t (6.9)	25/29
	30	29.5	2.99, s	21, 31
N-MeVal	31	170.4		
	32	58.3	4.79, d (10.6)	31, 34, 35, 36, 37, 38
	33 (N)			
	34	27.3	2.22, m	32, 35, 36
	35	18.7	0.33, d (6.4)	32, 34, 36
	36	18.6	0.74, d (6.5)	32, 34, 35
	37	29.5	2.97, s	32, 38
	38	169.5		
Gly	39	40.8	4.62, dd (17.6, 7.9) 3.47, d (17.6) 7.58 d (7.9)	38, 41
	40 (NH)			41
	41	171.3		
	42	61.4	4.91	41, 44, 45, 47, 48, 49
N-Melle	43 (N)			
	44	33.0	2.11	
	45	25.2	1.46, 1.11	44
	46	10.3	0.89	44, 45
	47	15.8	1.03, d (7.3)	42, 44, 45
	48	30.6	3.22, s	42, 49
	49	170.2		
Gly	50	41.0	4.44	49, 52
			3.57, dd (15.9, 4.6) 7.36, t (5.5)	
	51 (NH)			49, 50
Hmpa	52	170.7		
	53	78.6	5.21	1, 52, 54, 55, 57
	54	37.6	2.07	
	55	24.0	1.47, 1.24	53, 54, 56
	56	11.9	0.90	54, 55
	57	15.36	0.90	53, 54

^a Proton showing correlation to indicated carbon resonance.

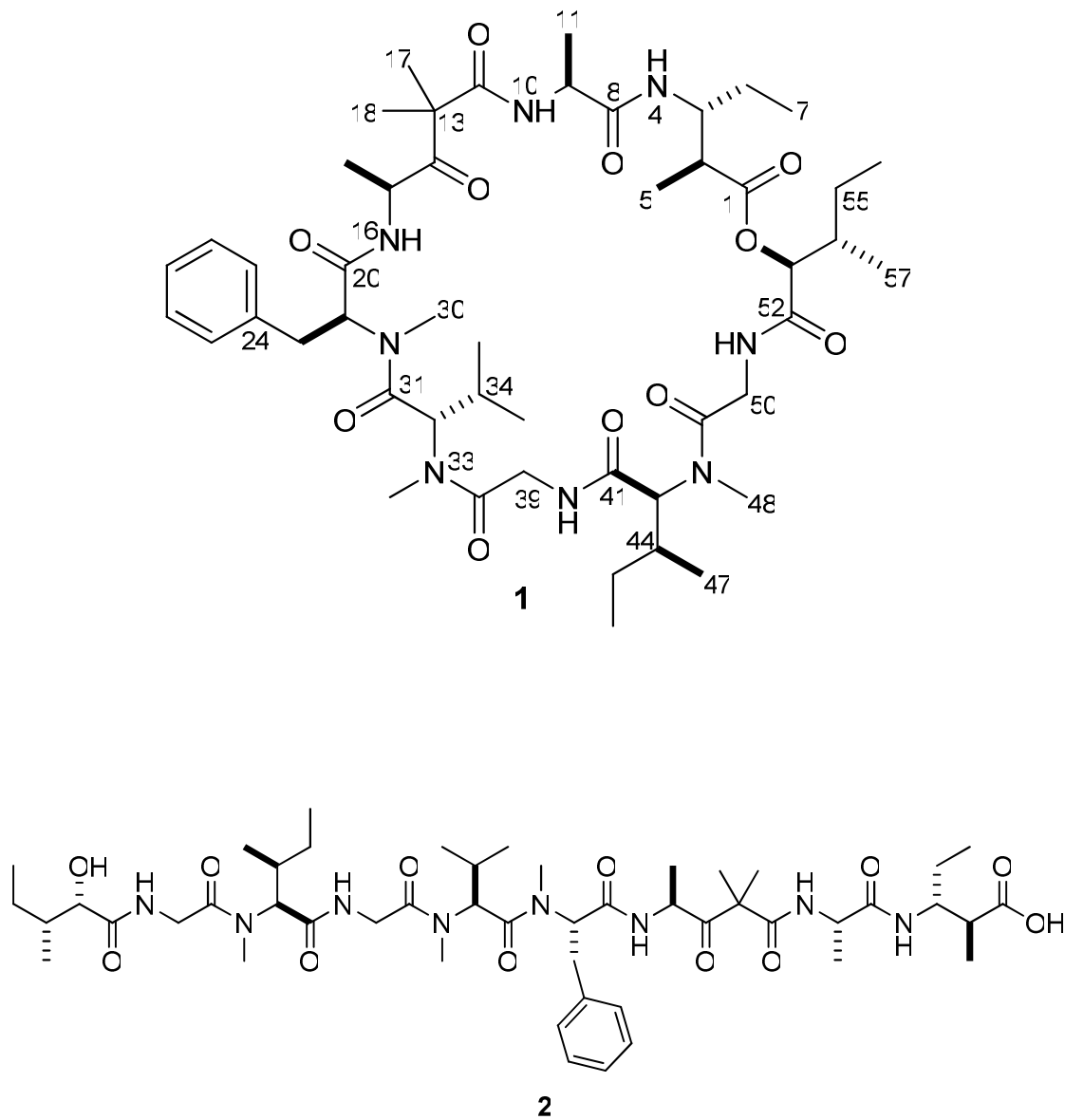


Figure III.1. Molecular structures of cyclic DMMC (**1**) and its linear hydrolysis product (**2**).

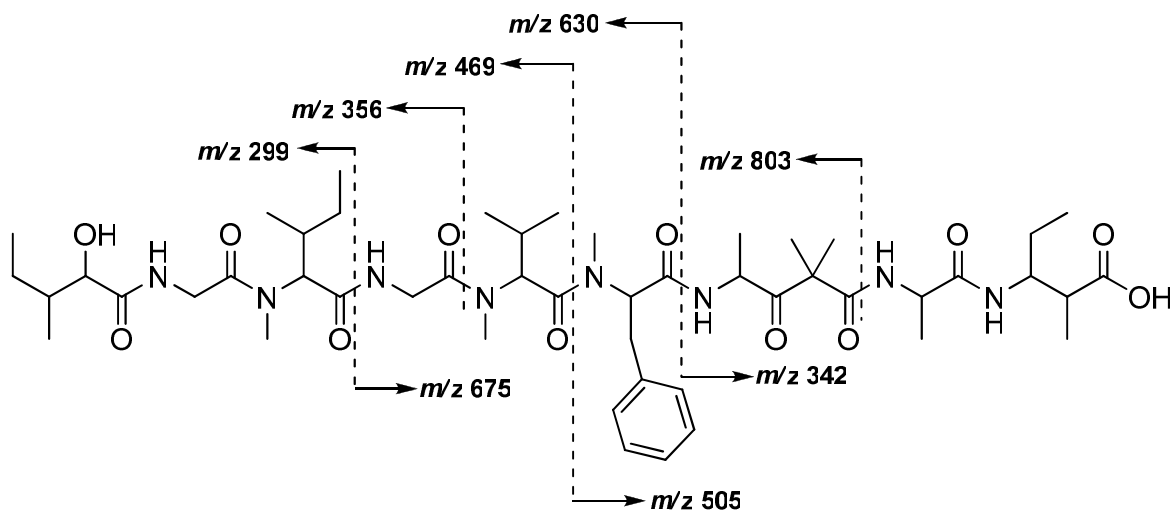
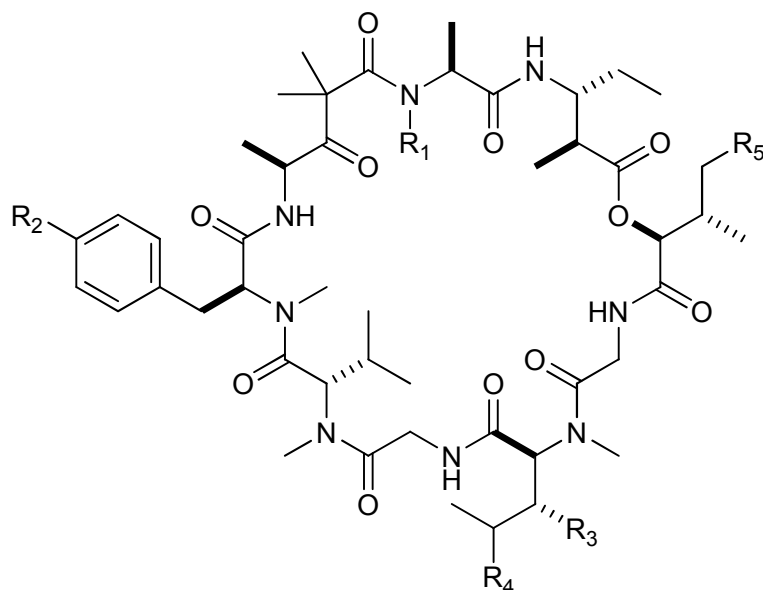


Figure III.2. CID MS fragmentation pattern of 2.



Compound	R ₁	R ₂	R ₃	R ₄	R ₅
Desmethoxymajusculamide C (1)	H	H	CH ₃	H	CH ₃
Majusculamide C ¹⁴	H	OCH ₃	CH ₃	H	CH ₃
Dolastatin 11 ¹⁵	H	OCH ₃	H	CH ₃	CH ₃
Dolastatin 12 ¹⁶	CH ₃	H	H	CH ₃	CH ₃
57-Normajusculamide C ¹⁶	H	OCH ₃	CH ₃	H	H
Lyngbyastatin 1 ¹²	CH ₃	OCH ₃	H	CH ₃	CH ₃

Figure III.3. Cyclic depsipeptide skeleton and table with select molecules in this structure class.

Cytotoxicity of cyclic (1) and linear DMMC (2). The original extract (Gerwick-1338) was identified as solid tumor selective and very potent. The zone differential between the three human tumor cell lines HCT-116 human colon cancer, H125 human lung cancer, MCF-7 human breast cancer and the CCRF-CEM human leukemia was 500 zone units when 2.3 μ g of extract was applied to the filter disk. Bioassay directed

fractionation yielded DMMC (**1**). The same zone value for HCT-116 and H125 achieved with the 2.3 μg of crude extract was obtained with 117 ng of **1** and 35 ng of **2** indicating a 20-fold purification from crude extract to obtain DMMC.

IC_{50} determinations were carried out for both **1** and **2** against 4 cells lines as shown in Table III.2. HCT-116 was the most sensitive cell lines with IC_{50} values of 19 ng/ml and 15 ng/ml, respectively. H460 was about 5-fold less sensitive, MDA-MB-435 over 10-fold less sensitive; and, Neuro-2A resistant to both compounds.

Table III.2. Cytotoxicity of **1** and **2** against a panel of cancer and neuronal cell lines.

	<u>Cyclic (1)</u> IC_{50} ($\mu\text{g}/\text{mL}$)	<u>Linear (2)</u> IC_{50} ($\mu\text{g}/\text{mL}$)
<u>HCT-116</u> human colon carcinoma	0.019	0.015
<u>H460</u> human large cell lung carcinoma	0.06	0.09
<u>MDA-MB-435</u> human carcinoma	0.21	0.22
<u>Neuro-2A</u> murine neuroblastoma	> 1.0	> 1.0

To understand the mechanism of action for **1** and **2**, actin microfilament disruption assays were conducted. Cyclic (**1**) and linear (**2**) DMMC at 52 nM caused the complete loss of filamentous (F)-actin coincident with dramatic changes in cell morphology when tested against A-10 cells (Figure III.4). The effects were specific for microfilaments as there was no evidence of microtubule loss at these concentrations. Binuclear cells were present, consistent with inhibition of the actin-dependent process of

cytokinesis. Evidence of apoptosis and the breakdown of nuclei into apoptotic bodies were prevalent at 52 nM, and altered cellular morphology accompanied total disruption of the microfilament network at this concentration.

Next, a clonogenic concentration-survival study was conducted for **1** both to define the effect of exposure duration on cytotoxicity and to provide input to determine the most effective dose schedule for the subsequent therapeutic assessment.¹⁷ As shown in Figure III.5, clonogenic survival of HCT-116 cells was determined at three different exposure durations: 2 h, 24 h and continuous (168 h or 7 day), as a function of drug concentration. The concentration for an exposure duration that yields a surviving fraction of 10% (tS_{10}) was determined: ${}_2S_{10} > 10 \mu\text{g/ml}$; ${}_{24}S_{10} > 10 \mu\text{g/ml}$; ${}_{168}S_{10} = 2 \text{ ng/ml}$. These results indicate that for a therapeutic effect, the concentration of **1** exposed to tumor HCT-116 cells in vivo would have to be $>10 \mu\text{g/ml}$ for either 2 h or 24 h if a single, bolus dose was administered; or continuously $>2 \text{ ng/ml}$ if a chronic (7 day) dosing was given.

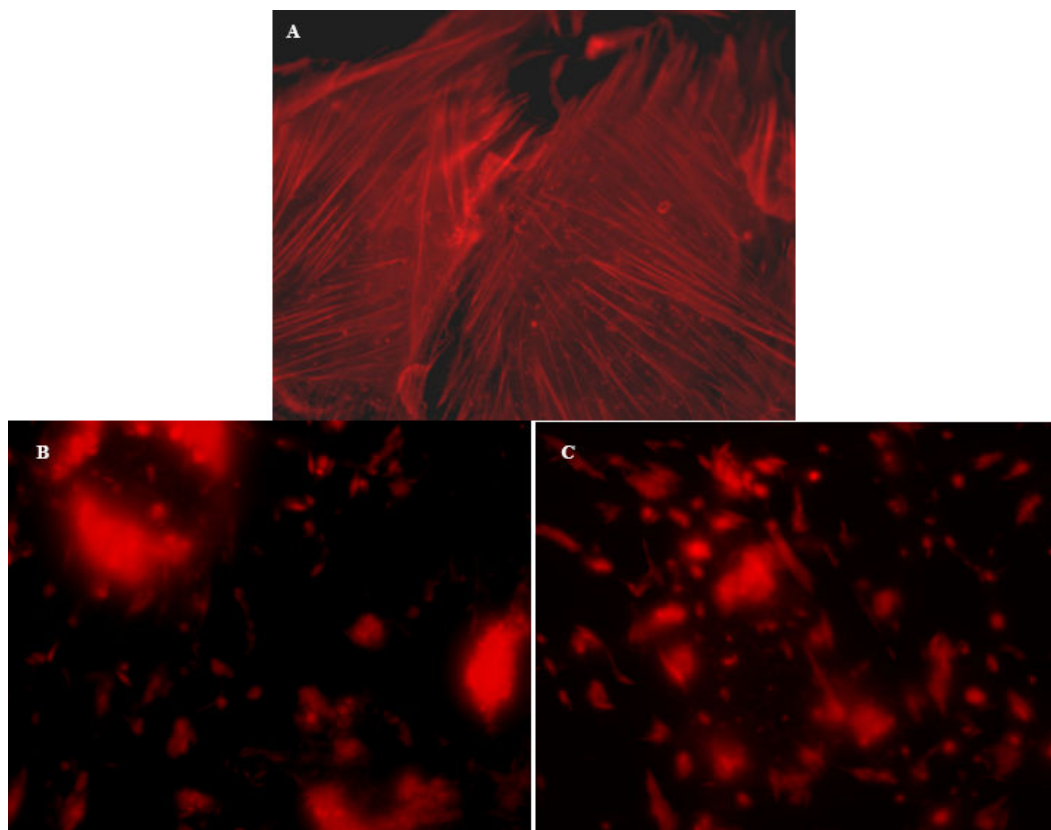


Figure III.4. Effects of cyclic (**1**) and linear (**2**) DMMC on the actin cytoskeleton of A-10 cells. The compounds were added, and after 24 h cells were fixed, permeabilized and exposed to the microfilament-staining reagent TRITC-phalloidin (visualized as red). The control was treated with vehicle. (A) Control cells. (B) Treatment of cells with DMMC (**1**) at 52 nM caused complete loss of the cellular microfilament network and generated binucleated cells (not shown). (C) Treatment of cells with linear DMMC (**2**) at 52 nM also induced the complete disruption of cellular microfilament networks and generated binucleated cells (not shown).

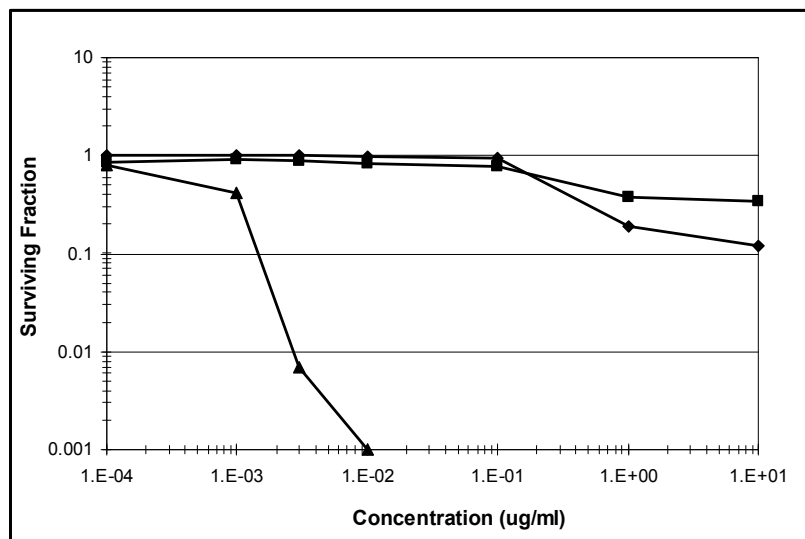


Figure III.5. Clonogenic dose-response curve of H-116 human colon cancer cells exposed to DMMC (**1**) for 2 h (square), 24 h (diamond), and 168 h (triangle) in vitro.

The clonogenic results were sufficiently encouraging to design a therapeutic efficacy trial of DMMC (**1**) using HCT-116 tumor cells in scid mice. We first determine the maximum tolerated dose to be approximately 2.5 mg/kg for scid mice. Unfortunately, we did not have sufficient drug to carry out a 5-day therapeutic trial at 2.5 mg/kg/day. Since we needed two doses of drug to carry out the trial, given the limitation of drug, we chose 0.62 and 0.31 mg/kg/day. The results are presented in Figure III.6 and shows that the tumor growth rate for the lower dose schedule was identical to the untreated control. However, the higher dose yielded a %T/C value of 60% at 17 days. These results indicate the therapeutic potential for DMMC (**1**) administered in a chronic schedule as efficacy was found at about one-fourth of the maximum tolerated dose. A further 30 mg of DMMC (**1**) would need to be prepared or synthesized for an adequate trial against

HCT-116; which, if effective would need to be repeated in both a multiple treatment schedule and against other tumor types.

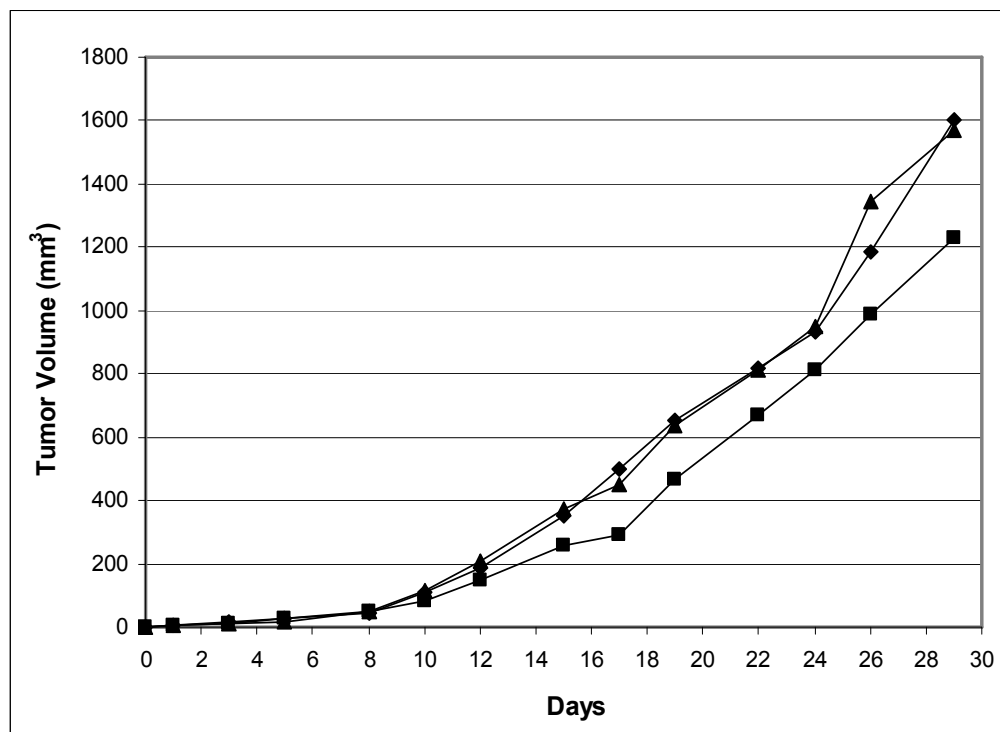


Figure III.6. Therapeutic assessment of DMMC (1) against HCT-116 human colon cancer growing subcutaneously in scid mice. Drug was administered daily for 5 days intravenously: Untreated control (circle), 0.31 mg/kg/day (triangle), 0.62 mg/kg/day (square).

Conclusions

The discovery of DMMC (**1**) was guided by the potent cancer cell cytotoxicity observed throughout the isolation process and extends our knowledge base of this class of bioactive marine natural products. Here, we demonstrate that DMMC displays a mechanism of activity and levels of both potency and selectivity that are consistent with the most active members in this structure class. Unexpectedly, we have also observed a high level of cytotoxic activity in the ring-opened linear form of this compound with IC_{50} values equivalent to those of the parent structure. In vitro cellular and limited in vivo therapeutic studies indicate the potential for DMMC (and possibly its linear form) in cancer treatment. Molecular optimization of **1** and **2** with models representing aqueous cellular conditions and hydrophobic cell membrane bilayers show the two molecules behave differently under these conditions. Using the semi-empirical optimized potentials for liquid simulations (OPLS) modeled at pH 7.2, the linear **2** takes on a ‘double hair-pin like’ conformation, where as the cyclic **1** maintains a similar conformation under both conditions. **2** ‘unwinds’ to a nearly linear conformation in the hexadecane parameterized model 3 (PM3) calculations (Figure III.7).¹⁸

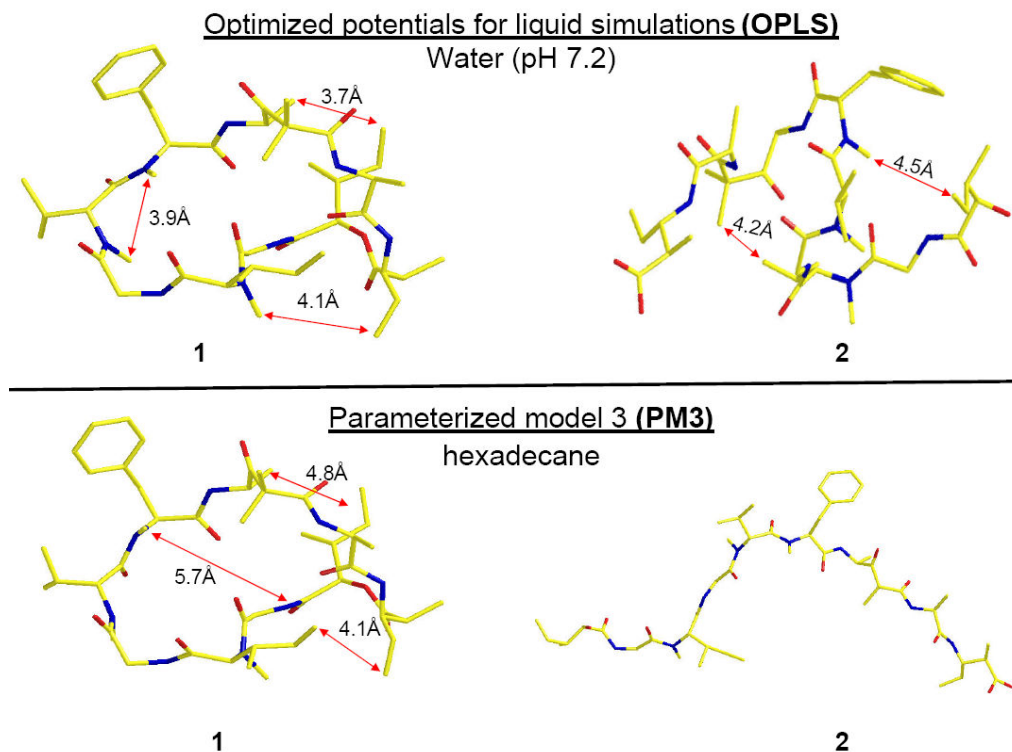


Figure III.7. Lowest energy conformations of **1** and **2**. Top, structures optimized under physiological conditions; bottom, structures optimized for cell wall conditions.

The differences in the lowest energy conformations of **1** and **2** (for the given solvent parameters), suggest that the cyclic compound may be acting as a pro-drug whereby the more hydrophobic cyclic molecule crosses the cell membrane and is cleaved (to yield the linear form) by any number of esterases found in the cytosol.

This structure class displays interesting structural features from a biosynthetic perspective. The first and most obvious is the variable degree of methylation on the mixed PKS/NRPS backbone. As illustrated in Figure III.3, there are five sites of variable *C*-, *N*- and *O*-methylation which give rise to the diversity found in this structural class. While some of the variability can be attributed to promiscuity of amino acid

incorporation during NRPS chain extension (e.g. Tyr/Phe, Ile/Leu, Map/Ampa), additional variability derives from variable methylation of the tyrosine oxygen, as well as the amide nitrogen of several amino acid residues. Whether it's a case of variable adenylation or active methylation, this secondary metabolic pathway seems to be flexible and is generating an expanding family of bioactive cyclic depsipeptide analogs which may provide important SAR information for future drug development studies.

Experimental Section. The optical rotation was measured on a Perkin-Elmer 243 polarimeter, UV was recorded on a Waters Millipore Lambda-Max model 480 LC spectrophotometer and the IR spectrum was recorded on a Nicolet 510 Fourier transform IR spectrophotometer. All NMR spectral data were recorded on a Bruker AM400 spectrometer, with the solvent CDCl_3 used as an internal standard (δ_{C} 77.0, δ_{H} 7.26). Chemical shifts are reported in ppm and coupling constants (J) are reported in Hz. The FAB mass spectrum and CID mass spectrum were recorded on Kratos MS50TC and Perkin Elmer Sciex API3 mass spectrometers, respectively. HPLC isolation of **1** was performed using Waters 515 HPLC pumps.

Cyanobacterial Collection and Identification. The marine cyanobacterium *Lyngbya majuscula* was collected by B. Marquez and T. Okino from the Kauviti Reef of Yanuca Island, Fiji on February 16, 2000. The specimen was identified morphologically by WHG (voucher specimen available as collection number VKR-16/Feb/00-05). The material was stored in 2-propanol at reduced temperature until extraction.

Isolation of DMMC (1). Approximately 300 grams dry weight of the cyanobacterium was repetitively extracted with 2:1 CH₂Cl₂/CH₃OH to yield 5.5 g of crude extract. A portion of the extract (5.3 g) was fractionated by vacuum liquid chromatography (VLC) over silica gel. The fraction eluting with 100% EtOAc was further chromatographed by C₁₈ SPE (7:3 CH₃OH/H₂O) followed by RP HPLC (Phenomenex Spherclone 5 μ m ODS column, 17:3 CH₃OH/H₂O) to yield 27.5 mg of pure **1**.

Desmethoxymajusculamide C (1). Glassy oil; $[\alpha]_D^{22}$ -104.1 (*c* 1.86, CH₂Cl₂); IR (neat) 3315, 2966, 2934, 2877, 1739, 1641, 1519, 1460, 1410, 1286 cm⁻¹; ¹H and ¹³C NMR data, see Table III.1; HR FAB MS *m/z* [M + H]⁺ 955.5867 (calculated for C₄₉H₇₉N₈O₁₁, 955.5868).

Base Hydrolysis of 1. Approximately 6 mg of **1** was suspended in 2 mL of a 1:1 CH₃OH/0.5 M NaOH solution and allowed to stand overnight at room temperature. The CH₃OH was removed by evaporating under N₂, and the mixture was neutralized with HCl and extracted with EtOAc. The organic layer was dried under N₂ and purified using HPLC (85% CH₃OH in H₂O) to give the base hydrolysis product **2** at > 98% yield. Hydrolysate of **1**: FAB MS (3-nitrobenzylalcohol) *m/z* 973 (35), 803 (25), 675 (41), 630 (52), 505 (30), 469 (100), 356 (66), 342 (54), 299 (82), 244 (31).

Absolute Configuration of the Standard Amino Acid Residues in 1. Approximately 1.0 mg of **1** was hydrolyzed with 6N HCl (Ace high pressure tube,

microwave, 1.0 min), and the hydrolysate was evaporated to dryness and resuspended in H₂O (50 μ L). A 0.1% 1-fluoro-2,4-dinitrophenyl-5-L-alaninamide (Marfey's reagent) solution in acetone (50 μ L) and 20 μ L of 1N NaHCO₃ were added, and the mixture was heated at 40°C for 1 h. The solution was cooled to room temperature, neutralized with 10 μ L of 2N HCl and evaporated to dryness. The residue was resuspended in H₂O (50 μ L) and analyzed by reversed-phase HPLC (LiChrospher 100 C₁₈, 5 UV detection at 340 nm) using a linear gradient of 9:1 50 mM triethylammonium phosphate (TEAP) buffer (pH 3.1)/CH₃CN to 1:1 TEAP/CH₃CN over 60 min. The retention times (t_R , min) of the derivatized residues in the hydrolysate of **1** matched L-Ala (22.1; D-Ala, 26.9), *N*-Me-L-Val (36.5; *N*-Me-D-Val, 39.7), and *N*-Me-L-Phe (38.5; *N*-Me-D-Phe, 39.2). Given that only *N*-Me-L-Ile and *N*-Me-L-*allo*-Ile were commercially available, the D-Marfey's reagent was used to make the *N*-Me-D-Ile and *N*-Me-D-*allo*-Ile chromatographic equivalents. The retention time of the hydrolysate Ile derivative matched that of *N*-Me-L-Ile (40.7 min; *N*-Me-L-*allo*-Ile, 41.2 min; *N*-Me-D-Ile, 44.2min; *N*-Me-D-*allo*-Ile, 44.7 min).

Absolute configuration of the non-standard amino- and hydroxy-acid residues in 1. Determination of the absolute configuration for the 3-amino-2-methylpentanoic (Map), 2-hydroxy-3-methylpentanoic (Hmpa), and 4-amino-2,2-dimethyl-3-oxopentanoic acid (Ibu) residues was accomplished using both Marfey's method and chiral HPLC. Authentic chromatographic standards for the Map and Ibu residues were obtained as gifts from the laboratory of R.E. Moore, Department of Chemistry, University of Hawaii. In both cases, approximately 1.0 mg of **1** was

hydrolyzed with 6N HCl (Ace high pressure tube, microwave, 1.0 min), and the hydrolysate was evaporated to dryness and resuspended in H₂O (50 μL). A 0.1% 1-fluoro-2,4-dinitrophenyl-5-L-alaninamide (Marfey's reagent) solution in acetone (50 μL) and 20 μL of 1N NaHCO₃ were added, and the mixture was heated at 40°C for 1 h. The solution was cooled to room temperature, neutralized with 10 μL of 2N HCl and evaporated to dryness. The residue was resuspended in H₂O (50 μL) and analyzed by reversed-phase HPLC (LiChrospher 100 C₁₈, 5μm, UV detection at 340 nm) using a linear gradient of 9:1 50 mM triethylammonium phosphate (TEAP) buffer (pH 3.1)/CH₃CN to 4:6 TEAP/CH₃CN over 60 min. Retention times, under these conditions, for the hydrolysate of **1** indicated 2*S*,3*R*-Map (47.0 min; 2*R*,3*S*-Map, 36.5 min; 2*S*,3*S*-Map, 37.0 min; 2*R*,3*R*-Map, 28.9 min; 4*S*-Dmop (34.2 min; 4*R*-Dmop, 32.8 min, respectively).

Preparation and chiral analysis of HMPA. L-Ile (100 mg, 0.75 mmol) was dissolved in 50 mL 0.2 N perchloric acid (0°C). To this was added a cold (0°C) solution of Na₂SO₃ (1.4 g, 20 mmol) in 20 mL H₂O with rapid stirring. With continued stirring the reaction mixture was allowed to reach room temperature until evolution of N₂ subsided (~ 30 min). The solution is then brought to boil for 3 min., cooled to room temperature, and saturated with NaCl. The mixture was then extracted with Et₂O and dried under vacuum. The three other stereoisomers (2*R*, 3*R*)-HMPA, (2*R*, 3*S*)-HMPA, and (2*S*, 3*R*)-HMPA were synthesized in a similar manner from D-Ile, D-*allo*-Ile, and L-*allo*-Ile, respectively.¹⁹ A portion of the resultant oil was dissolved in aq 2 mM CuSO₄ buffer for HPLC. The retention time [Chirex-D, isocratic system (85:15) 2 mM CuSO₄: MeCN] of

the natural product hydrolysate matched that for 2*S*,3*S*-HMPA (17.1 min; 2*R*,3*S*-HMPA, 11.8 min; 2*S*,3*R*-HMPA, 9.2 min and 2*R*,3*R*-HMPA, 21.2 min, respectively).

Determination of IC₅₀ values for 1 and 2 against HCT-116 cells.

Concentration-cell number studies (IC₅₀ assay) were carried out against HCT-116 cells. These cells are grown in 5 ml culture medium (RPMI-1640 + 15% FBS containing 1% penicillin-streptomycin, and 1% Glutamine) at 37°C and 5% CO₂ at a starting concentration of 5x10⁴ cells/T25 flask. On day 3, cells are exposed to different concentrations of the drug. Flasks are incubated for 120 h (5 d) in a 5% CO₂ incubator at 37°C and the cells harvested with trypsin, washed once with HBSS and resuspended in HBSS and counted using a hemocytometer. The results are normalized to an untreated control. The IC₅₀ value is determined using Prism 4.0.

DMMC (1) Clonogenic Dose-Response Analysis against HCT-116 Cells.

Concentration- and time-survival studies were carried out with HCT-116 cells seeded at 200 or 20,000 cells in 60 mm dishes. DMMC (1) was added to the medium (RPMI + 10% FBS) to a final concentration of 10 µg/mL and 10-fold dilutions thereof. At either 2 or 24 h, the drug containing medium was removed and fresh medium without drug was added. For continuous exposure to drug, the media containing the compounds remained in contact with the cells for the entire incubation period (168 h). The dishes were incubated for 7 days, the medium was removed, and the colonies were stained with methylene blue. Colonies containing 50 cells or more were counted. The results were normalized to an untreated control. Plating efficiency for the untreated cells was about 90%.

Therapeutic Assessment of 1 and 2. The in vivo therapeutic assessment trial was carried out using the HCT-116 human colon tumor model as previously described.²⁰ Individual mouse body weights for each experiment were within 5 g, and all mice were over 17 g at the start of therapy. The mice were supplied food and water ad libidum. SCID mice were pooled, implanted subcutaneously with 10^6 tissue derived tumor cells, and pooled again before distribution to treatment and control groups (5 mice per group). Treatment with **1** started 1 day after tumor inoculation. Mice were sacrificed after 30 days had elapsed from tumor inoculation. Tumor weights were estimated using two-dimensional caliper measurements done three times per week using the following formula: tumor weight (mg) $(a \times b^2)/2$, where a and b are the tumor length and width, respectively, in mm. The median tumor weight was calculated as an indication of antitumor effectiveness. The parameter, %T/C, was determined after each measurement and the minimum value reported as therapeutic efficacy. Compounds **1** was prepared as a stock solution in DMSO, diluted 1:1 (v/v) with Cremophor-propylene glycol (40:60 v/v) and further diluted at least 10-fold with saline before injection. Drug was prepared at 10, 5, and 2 mg/mL for intravenous administration in 0.25 mL volumes via the tail vein. Drug was prepared at 0.05 and 0.025 mg/mL for intravenous administration as a bolus injection daily for 5 days in 0.25 mL volumes via the tail vein (0.62 and 0.31 mg/kg/day, respectively).

Microfilament Disrupting Activity of 1 and 2. Cyclic (**1**) and linear (**2**) DMMC were tested for microfilament-disrupting activity using rhodamine-phalloidin dye

visualization. A-10 cells were grown on glass cover slips in Basal Medium Eagle (BME) containing 10% fetal calf serum. The cells were incubated with the test compounds for 24 h and then fixed with 3% paraformaldehyde for 20 min, permeabilized with 0.2% Triton X-100 for 2 min, and chemically reduced with sodium borohydride (1 mg/mL in PBS) three times for 5 min each. Following a 45 min incubation with 100 nM TRITC-phalloidin in phosphate buffered saline, the cover slips were washed, stained with 4,6-diamidino-2-phenylindole (DAPI), mounted on microscope slides, and examined using a Nikon Eclipse ES800 fluorescence microscope with a digital camera .

References and Notes

- (1) Papakonstanti, E.A.; Stournaras, C. *Methods Enzymol.* **2007**, *428*, 227-240.
- (2) Janmey, P.A.; Chaponnier, C. *Curr. Opin. Cell Biol.* **1995**, *7*, 111-117.
- (3) Jordan, M.A.; Wilson, L. *Curr. Opin. Cell Biol.* **1998**, *10*, 123-130.
- (4) Sahai, E. *Nat. Rev. Cancer* **2007**, *7*, 737-749.
- (5) Simmons, T.L.; Andrianasolo, E.; McPhail, K.L.; Flatt, P.; Gerwick, W.H. *Mol. Cancer Ther.* **2005**, *4*, 333-342.
- (6) Simmons, T.L.; Gerwick, W.H. *Oceans and Human Health*, Elsevier: New York, New York, 2008; Ch. 22, Text in press.
- (7) Bubb, M.R.; Senderowicz, A.M.J.; Sausville, E.A.; Duncan, K.L.K.; Korn, E.D. *J. Biol. Chem.* **1994**, *269*, 14869-14871.
- (8) Marquez, B.L.; Watts, K.S.; Yokochi, A.; Roberts, M.A.; Verdier-Pinard, P.; Jimenez, J.I.; Hamel, E.; Scheuer, P.J.; Gerwick, W.H. *J. Nat. Prod.* **2002**, *65*, 866-871.
- (9) Bai, R.; Covell, D.G.; Liu, C.; Ghosh, A.K.; Hamel, E. *J. Chem. Biol.* **2002**, *277*, 32165-32171.
- (10) Morton, W.M.; Ayscough, K.R.; McLaughlin, P.J. *Nat. Cell Biol.* **2000**, *2*, 376-378.
- (11) Klehchin, V.A.; Allingham, J.S.; King, R.; Tanaka, J.; Marriott, G.; Rayment, I. *Nat. Struct. Biol.* **2003**, *10*, 1058-1063.

- (12) Harrigan, G.G.; Yoshida, W.Y.; Moore, R.E.; Nagle, D.G.; Park, P.U.; Biggs, J.; Paul, V.J.; Mooberry, S.L.; Corbett, T.H.; Valeriote, F.A. *J. Nat. Prod.* **1998**, *61*, 1221-1225.
- (13) Bia, R.; Verdier-Panard, P.; Gangwar, S.; Stessman, C.C.; McClure, K.J.; Sausville, E.A.; Pettit, G.R.; Bates, R.B.; Hamel, E. *Mol. Pharmacol.* **2001**, *59*, 462-469.
- (14) Carter, D. C.; Moore, R. E.; Mynderse, J. S.; Niemczura, W. P.; Todd, J. S. *J. Org. Chem.* **1984**, *49*, 236-241.
- (15) Pettit, G.R.; Kamano, Y.; Kizu, H., et al. *Heterocycles* **1989**, *28*, 553-558.
- (16) Mynderse, J.S.; Hunt, A.H.; Moore, R.E. *J. Nat. Prod.* **1988**, *51*, 1299-1301.
- (17) Subramanian, B.N.; Tenney, K.; Crews, P.; Gunatilaka, L.; Valeriote, F.A. *J. Exp. Ther. Oncol.* **2006**, *5*, 195-204.
- (18) Spartan '02 (Linux), Wavefunction Inc., Irvine, CA, 92612.
- (19) Mamer, O.A. *Meth. Enzymol.* **2000**, *324*, 3-10.
- (20) Corbett, T.; Valeriote, F.; LoRosso, P.; et al. *J. Pharmacog.* **1995**, *S33*, 102-122.

Acknowledgments

The text of III, in full, is the manuscript draft to be submitted to an academic journal as it will appear: Simmons, T.L., Nogle, L.M.; Valeriote, F.A.; Mooberry, S.L.; Gerwick, W.H. DMMC, a Cyanobacterial Depsipeptide with Potent Cytotoxicity in its Cyclic and Ring-opened Forms. The dissertation author was the primary author and directed and supervised the research which forms the basis for this chapter.

IV

Viridamides A and B, lipodepsipeptides with anti-protozoan activity from the marine cyanobacterium *Oscillatoria nigro-viridis*

Abstract

Parallel chemical and phylogenetic investigation of a marine cyanobacterium from Panama led to the isolation of two new PKS-NRPS derived compounds, viridamides A (1) and B (2). The structures of these metabolites were determined by NMR and mass spectroscopic methods, and the absolute configuration was assigned by Marfey's method and chiral HPLC analysis. In addition to six standard, *N*-methylated amino and hydroxy acids, these metabolites contained the structurally novel 5-methoxydec-9-ynoic acid and an unusual proline methyl ester terminus. Morphologically, this cyanobacterium was identified as *Oscillatoria nigro-viridis*, and its 16S rDNA sequence is reported here for the first time. Phylogenetic analysis of these sequence data has identified *O. nigro-viridis* strain OSC3L to be closely related to two other marine cyanobacterial genera, *Trichodesmium* and *Blennothrix*. Viridamide A showed anti-trypanosomal activity with an IC_{50} = 1.1 μ M and anti-leishmania activity with an IC_{50} = 1.5 μ M.

Introduction

The World Health Organization (WHO) estimates that over 1 billion people suffer from one or more neglected tropical diseases (NTDs) such as malaria, leishmaniasis, trypanosomiasis, schistosomiasis, cholera and others.¹ On a global scale NTDs account for greater than 10% of global disease burden yet only 16 of the 1393 new drugs marketed between 1975 and 1999 were developed for their treatment.² A major cause for this extraordinarily unimpressive number is the fact that those people most burdened by these diseases are amongst the World's most impoverished.³

Trypanosomiasis (Chagas, sleeping sickness) and leishmaniasis are caused by infection by parasitic members of the protozoan order *Trypanosomatida* which enter the blood stream via insect vectors or transfusion of infected blood.⁴ Symptoms of Chagas occur in two phases: an acute stage characterized by a constellation of symptoms known as 'Romaña's sign', and a chronic stage which may develop over a decade or more. Chronic stage infection, if left untreated results in protozoan infestation of all major organs, leading to neurological disorders, intestinal damage and fatal cardiomyopathy. Leishmaniasis is caused by 20 different species and can affect humans as three forms: visceral (VL; 'kala azar'), cutaneous and mucocutaneous. The pan-tropical phlebotomine sand fly is the known vector of leishmaniasis, with VL being the most severe disease form. If untreated visceral leishmaniasis can be 100 % lethal within two years.⁵ The WHO estimates that greater than 200 million people are at risk of leishmaniasis or trypanosomiasis worldwide^{6,7} Several drugs are currently available and used to treat trypanosomal infections; however, these all suffer from one or more

shortcomings. Suramin, a polysulfonated naphthylurea is effective against early stage trypanosomal infection although due to issues concerning the blood-brain barrier is unlikely to treat second or central nervous system (CNS) stage of the disease.⁸ Melarsoprol, an arsenic-containing toxin, was developed over 50 years ago and is known to kill up to 12% of the patients 'treated'. Eflornithine (α -difluoromethylornithine) is a suicide inhibitor of ornithine decarboxylase that is quite effective in treating the disease, including the rescue of comatose patients in late stage disease.⁹ However, drug resistance is emerging and threatens the future utility of this agent.¹⁰ In 2000 Aventis donated supplies of eflornithine to Doctors without Borders for distribution throughout impoverished tropical nations. However, this voluntary donation program was slated only through 2006 and no long term supplier of the drug has been identified.

There are also several drugs currently used to treat leishmaniasis and extensive eradication programs ongoing, particularly in tropical India. However resistance is commonplace and it is estimated that there are 500,000 new cases each year on the Indian subcontinent alone.⁶ Despite the pressing and obvious global need for new and more effective anti-protozoan medicines, no new drugs are currently being developed for the treatment of these pan-tropical diseases.¹¹ While drug discovery programs are making progress against these pathogens, with synthetic phospholipids, the going is slow, treatments are expensive and often cause undesirable side effects.¹²

As part of a Panama-based International Cooperative Biodiversity Group (ICBG) project, we have been evaluating the extracts of tropical marine plants, endophytic fungi, and marine algae and cyanobacteria for activity against several tropical parasitic diseases including malaria, leishmaniasis, and Chagas' disease.¹³ Marine cyanobacteria are

extremely rich in diverse lipopeptide natural products, many of which have very potent biological activities.¹⁴ In the process of adapting a collection of the marine cyanobacterium *Lyngbya majuscula* to laboratory culture, collected from near the island of Curaçao, a second epiphytic cyanobacterium was also isolated. This was cultured in scaled-up quantities and its extract examined for unusual secondary metabolites by LCMS and NMR screening. Subsequently, these efforts were rewarded by the discovery of two novel lipopeptides, termed viridamide A (**1**) and B (**2**). Evaluation of these in our suite of tropical disease assays in Panama identified the major component, viridamide A, to be nearly equipotent at inhibiting the leishmania and Chagas' disease causing parasites ($IC_{50} = 1.1$ and $1.5 \mu M$, respectively).

An additional dimension of this study involved a detailed investigation into the taxonomic identity of the viridamide-producing strain of cyanobacterium. We reasoned that this strain was dissimilar to those we had previously worked with and that this presented an opportunity to broaden our base of natural product-rich cyanobacteria genera for future studies. Hence, we engaged in a two-pronged investigation using both traditional morphological characters and 16S rDNA sequence information. However, in the course of these studies, we realized a number of problems in the phylogenetic approach, mainly due to a) the level of sequence conservation of the 16S rRNA gene is too high for precise species differentiation, and b) the general unavailability of 16S rDNA sequence data for many of the morphologically-defined species of cyanobacteria. In response to the first point above, we used the present study as an opportunity to explore additional genes in cyanobacteria that could improve the phylogenetic analysis. In response to the second issue, we and others are actively engaged in expanding the

availability of 16S rRNA gene sequences which are well correlated to morphologically described species.¹⁵ This two pronged approach has allowed us to identify the source of the viridamides as the marine cyanobacterium *Oscillatoria nigro-viridis*, and to describe its phylogenetic relationship to other genera and species of marine cyanobacteria.

Results and Discussion

Isolation and structure elucidation of the viridamides

The dark green and very small cyanobacterial filaments of strain OSC3L (10 μm wide by > 1 cm long) were isolated as a contaminating (epiphytic) species from a partially purified culture of *Lyngbya majuscula* 3L (GenBank acc. No. AY599501) collected at the CARMABI Research Station in Curacao, Netherlands Antilles in 1993. The filaments of OSC3L were isolated on solid agar plates using standard isolation techniques and then cultured in enriched seawater medium under cool white fluorescent lights for 21 days. Harvest of filaments was achieved by filtration through paper filters, and extraction and initial fractionation was performed using our standard protocols.¹⁶ Screening of fractions by LCMS and NMR showed two mid-polar fractions to contain interesting metabolites, and two compounds, named viridamide A (**1**) and B (**2**), were subsequently isolated by repetitive reversed-phased HPLC in 1.9% (30 mg) and 0.2% (3.6 mg) yield, respectively.¹⁷

Viridamide A (**1**) was isolated as a colorless glassy oil with a molecular formula of $C_{46}H_{79}N_5O_{10}$ as determined by HR ESI TOF MS (obsd $[M+H]^+$ at m/z 862.5847; calcd $[M+H]^+$ 862.5827). This formula agreed with deductions from the 1H and ^{13}C NMR data (Table IV.2), and corresponded to 10 degrees of unsaturation. FT-IR absorption peaks at 1640 and 1750 cm^{-1} indicated the presence of amide and ester functionalities, respectively. The 1H NMR spectrum of **1** was well dispersed in $CDCl_3$ and displayed a pattern of chemical shifts typical for peptides (two NH doublets at δ_H 6.21 and 6.45 and a series of α -amino and α -hydroxy protons at δ_H 4.37-5.0). Two 3H singlets at δ_H 3.01 and 3.07 indicated the presence of two *N*-methylated amides whereas two sharp methyl singlets at δ_H 3.29 and 3.64 were consistent with two methoxy groups. The ^{13}C NMR spectrum of **1** displayed all 46 carbon resonances, and seven of the ten double bond equivalents were attributable to seven ester/amide carbonyl resonances between 160 and 175 ppm. Carbon resonances at δ_C 68.4 and 84.3, in combination with gHMBC data, were determined to comprise a terminal acetylenic group, and thus accounted for an additional two degrees of unsaturation. These data suggested viridamide A contained a single ring.

Interpretation of two dimensional NMR spectra (gCOSY, gHSQC, and gHMBC) defined partial structures for an *N*-methyl isoleucine, two valine residues, an *N*-methyl valine, a 2-hydroxy-3-methylpentanoic acid residue, and a terminal proline methylester (Table IV.2). These structural fragments accounted for 680 Da, leaving $C_{11}H_{17}O_2$ still to be determined. Further analysis of the 2D-gHSQC-TOCSY NMR data revealed seven continuously coupled proton bands beginning with one at δ_H 2.20 (δ_C 36.6) and correlated to δ_H 1.67 (δ_C 21.5), δ_H 1.48 (δ_C 32.8), δ_H 3.15 (δ_C 80.1), δ_H 1.56 (δ_C 32.3), δ_H 1.55 (δ_C

24.1), and δ_{H} 2.18 (δ_{C} 18.5). Combining these TOCSY data with gCOSY and gHMBC interpretations allowed development of a structurally-novel methoxylated fatty acid, 5-methoxydec-9-ynoic acid (Figure IV.1). These seven partial structures accounted for all atoms present in the molecular formula of viridamide A (**1**).

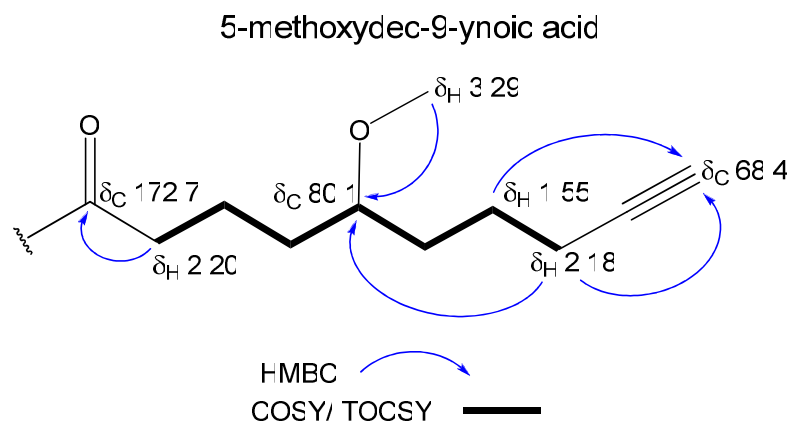


Figure IV.1. The structure of the 5-methoxydec-9-ynoic acid moiety found in viridamides A (**1**) and B (**2**).

The linear sequence of the partial structures assigned above was determined by combined 1D-HMBC and FAB-MS/MS fragmentation patterns. Interpretation of the HMBC correlations from the α -amino and α -hydroxy proton resonances (4-5 ppm) to the adjacent carbonyl carbons, and from the two amide protons to their adjacent carbonyl carbons, allowed the assembly of a linear sequence for most of viridamide A (**1**). A 1D HMBC experiment was used to observe correlation from H-5 through the oxygen atom to the adjacent C-12 ester carbonyl resonance. Interpretation of the FAB MS/MS

fragmentation pattern fully supported the linear sequence proposed from the HMBC analysis.

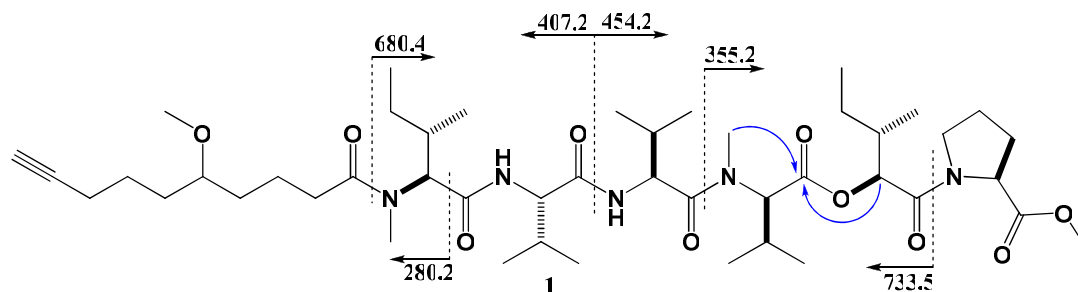


Figure IV.2. Important fragmentations observed from FAB-MS and key HMBC connectivities used to sequence the series of residues in viridamide A (1).

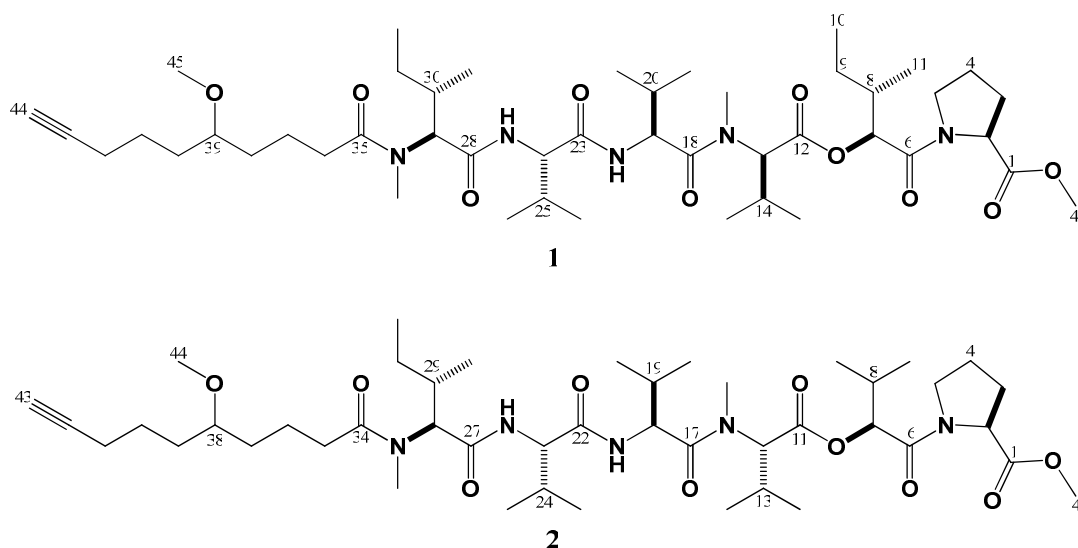


Figure IV.3. The molecular structures of viridamides A (1) and B (2).

The absolute configurations of the α -amino and α -hydroxy acid residues in viridamides A and B were determined by combined chiral HPLC (for Val, *N*-Me-Val,

Pro, and HMPA) and application of the advanced Marfey's method (*N*-Me-Ile).^{18,19} Chiral HPLC was achieved using a dioctyl-(D)-penicillamine (Chirex 3126; Phenomenex) column with aqueous 2.0 mM CuSO₄ in CH₃CN. Comparison of retention times for the acid hydrolysate of **1** (6 N HCl at 110° for 18 hours) with authentic standards indicated an L-configuration for the Val, *N*-Me-Val, Pro and HMPA residues. Configurational assignment of the *N*-Me-Ile required division of a portion of the acid hydrolysate and derivatization of each with either L- or D-FDAA (1-fluoro-2,4-dinitrophenyl-5-alanine amide) to produce the chromatographic equivalents of D-*N*-Me-Ile and L-*N*-Me-Ile. Reverse-phase HPLC of the FDAA derivatives indicated an L-(2*S*, 3*S*)-configuration for this residue.

Viridamide B (**2**) was isolated as a colorless oil with a molecular formula of C₄₅H₇₇N₅O₁₀ as determined by HR-TOF-MS (obsd [M+H]⁺ at *m/z* 848.5661; calcd [M+H]⁺ 848.5670), and this molecular formula was also supported by the ¹H and ¹³C NMR data (Table IV.3). The ¹H and ¹³C NMR spectra of **2** closely resembled those recorded for viridamide A (**1**); however, there was a notable absence of a high field methyl carbon resonance in the 10-11 ppm range, assigned to the C-10 methyl of the HMPA residue in **1**, and this appeared to explain the 14 Da mass reduction found between the two compounds. Careful analysis of the 2D gHSQC and gHMBC NMR spectra of **2** revealed that viridamide B contained a 2-hydroxy-3-methylbutanoic acid (HMBA) residue versus the 2-hydroxy-3-methylpentanoic acid residue found in viridamide A. The remaining structural features were identical between the two metabolites as determined by detailed NMR and MS analysis. Because viridamide B was isolated in much smaller yield than viridamide A, its absolute stereoconfiguration was not

studied experimentally; however, based on its co-occurrence with A and nearly identical structural and NMR features, we predict it possesses the same configuration at comparable centers.

Biological Evaluation of viridamide A

Inspired by the bioactivity of other recently discovered linear peptides of cyanobacterial origin,^{13, 20} viridamide A (**1**) was test against a series of relevant tropical pathogens and cancer cell lines. Interestingly, **1** displayed significant activity against the three parasitic protozoa *T. cruzi*, *L. mexacana* and *P. falciparum* with little toxicity to the cancer cell lines treated. The assay results are summarized below in Table IV.1.

Table IV.1. Activity of viridamide A (**1**) against a series of pathogen and cancer cell lines.

Compound	<i>T. Cruzi</i> IC ₅₀ (μM)	<i>L. mexacana</i> IC ₅₀ (μM)	<i>P. falciparum</i> IC ₅₀ (μM)	HCT-116* zone (mm)	H-125* zone (mm)
1	1.1	1.5	5.8	250	200

*indicates disk diffusion zone of inhibition

The variable toxicity between pathogen and human derived cell lines is encouraging and may suggest therapeutic value for these new compounds, studies are ongoing to more fully understand these results.

Characterization of the viridamide producing cyanobacterium

The culture sample of strain OSC3L was observed as a blackish-green, mat-forming, filamentous cyanobacterium. Microscopically, it possessed cylindrical trichomes that were straight or slightly waved that measured 9-10 μm wide. The trichomes were covered with a thin, barely visible sheath and there were slight constrictions at the cross walls between cells. The cells were disk-shaped with a cell length (2-3 μm) to width (9-10 μm) ratio of approximately 0.25, and were granulated near the crosswalls. The terminal cells were capitated and the trichomes slightly attenuated towards their tips. On the basis of these morphological features, strain OSC3L was identified as *Oscillatoria nigro-viridis* Thwaites in Harvey.²¹

To gain further insight into the phylogenetic relationship of this collection of *O. nigro-viridis* to other species and genera of cyanobacteria, a detailed molecular genetic analysis was conducted of strain OSC3L by amplifying its nearly full length 16S rRNA gene sequence using cyanobacterial specific primers (1378 bp, 93% of 16S gene; GC content 54.79%; GenBank accession number EU244875). Unfortunately, because characterization of the species *O. nigro-viridis* is based entirely on a morphological description, a 16S rRNA gene sequence was not available for comparison with our data (e.g. this is the first report of the 16S rRNA gene sequence for this species). However, BLAST analysis revealed this gene sequence to be 99.3% identical to that of a filamentous cyanobacterium (strain PAB-21) we recently collected from the Caribbean coast of Panama (GenBank accession number EU253967). This latter collection was also characterized as an *Oscillatoria* sp. based on its morphological features. In addition, BLAST analysis showed that strain OSC3L was phylogenetically closely related to

several other *Oscillatoria* and *Trichodesmium* strains, including *Trichodesmium erythraeum* IMS101 (97.4%; GenBank accession CP000393) and *Oscillatoria sancta* PCC 7515 (97.2%; GenBank accession AF132933).

Phylogenetic trees were constructed from the 16S rRNA gene sequence obtained for strain OSC3L and related sequences recovered from Genbank following the BLAST analysis. Three commonly employed algorithms for constructing phylogenetic trees were used in this analysis (parsimony, distance, and maximum likelihood; see Methods and Supporting Information), and all gave very similar topologies. However, the maximum-likelihood method (ML) provided the most robust boot-strap values and thus was used to construct the phylogenetic tree shown in Figure IV.4. As predicted from the BLAST analysis, strain OSC3L clusters in a distinct and well boot-strap supported monophyletic clade that contains various strains of *Oscillatoria* and *Trichodesmium*.

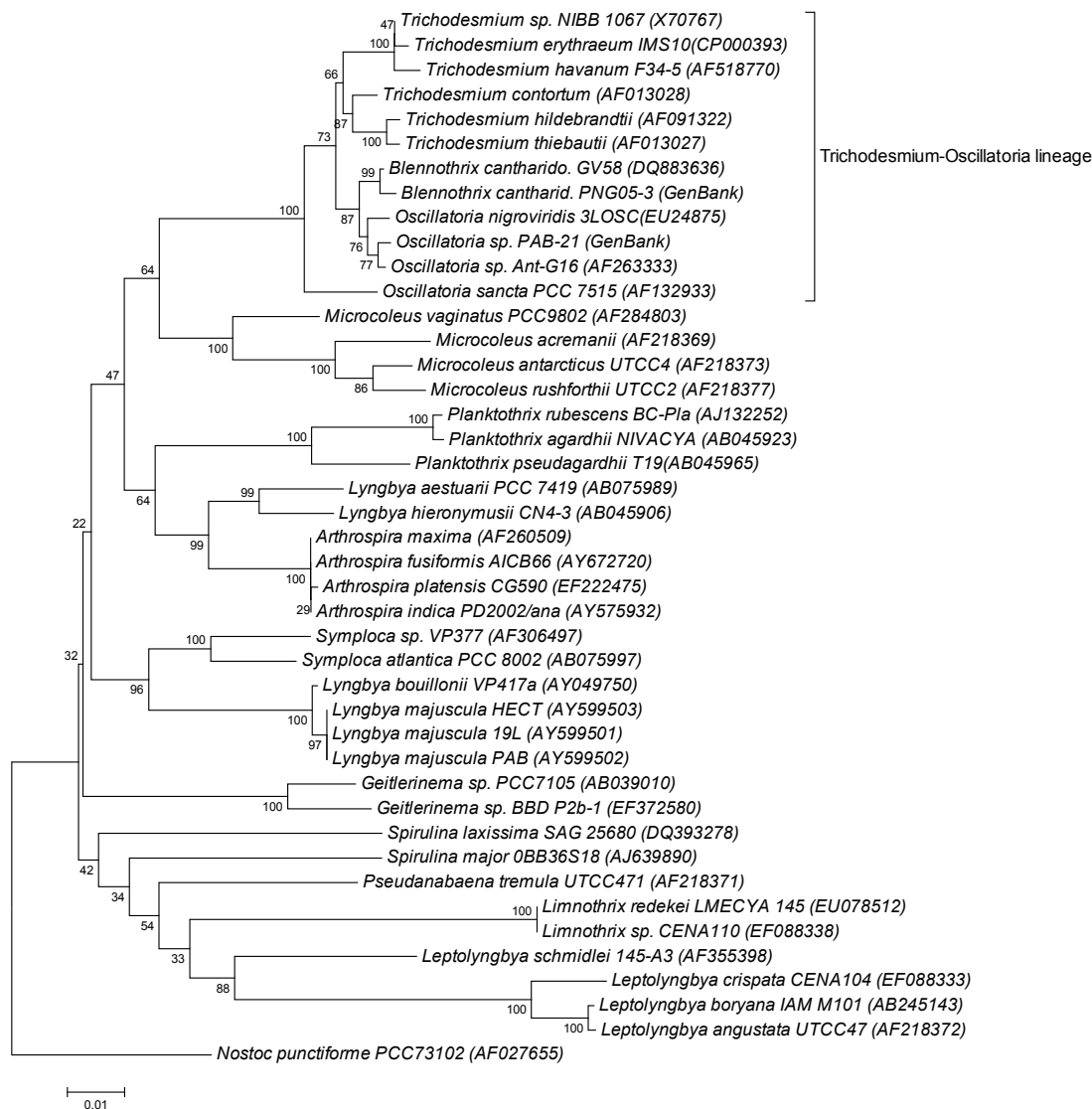


Figure IV.4. The phylogenetic relationships of marine cyanobacteria of the order *Oscillatoriales* from 16S rRNA nucleotide sequences (ML).

O. nigro-viridis OSC3L groups closely with other strains of *Trichodesmium* and *Oscillatoria*. This clade is described in Bergey's manual as the *Trichodesmium-Oscillatoria* lineage.^{22 13} Recently, it was shown that the genus *Blennothrix* (former *Hydrocoleum* sensu Komárek & Anagnostidis, 2005; *B. cantharidosmum* GenBank

accession EU253967) also clades within the *Trichodesmium-Oscillatoria* lineage and this has led to a proposal that these genera derive from a common evolutionary origin.²³ While several strains of *Oscillatoria*, *Trichodesmium*, and recently *Blennothrix*, have been associated with the production of biological active secondary metabolites,^{15,24} the genus *Oscillatoria* is clearly the richest in this regard.²⁵ *O. nigro-viridis* contributes to Harmful Alga Blooms (HABs) by causing dermatitis and inflammation in humans,²⁶ and is reported to have fish anti-feedant properties.²⁷ Chemical analyses of Pacific strains of *O. nigro-viridis* have yielded several bioactive compounds, including debromoaplysiatoxin, oscillatoxin A, 21-bromooscillatoxin A, 19,21-dibromooscillatoxin A, and 19-bromoaplysiatoxin, a suite of metabolites which likely explains the toxic effects of this species in humans.²⁸ Whether these reports truly reflect a greater ability of *Oscillatoria* to produce natural products versus *Trichodesmium* and *Blennothrix*, or rather, identifies that benthic cyanobacteria have been better studied than those with a mainly planktonic habit, is uncertain at present. Ongoing studies which partner detailed culture, chemical, pharmacologic and phylogenetic investigations should give valuable insights into this important question.

Here we report an expansion of the bioactive marine natural product and cyanobacterial taxonomy knowledgebases. This was achieved through the discovery of the new anti-protozoan viridamides A and B (**1** and **2**) and the molecular characterization of the cyanobacterium that produces them. The unique molecular structures of **1** and **2** belong to a class of acetylnic lipopeptides (e.g. carmabins²⁹, jamaicamides³⁰, apramides³¹) that exhibit a broad spectrum of bioactivities. Further we have combined morphological and molecular phylogenetic approaches to fully characterize *O. nigro-*

viridis and show its taxonomic relationships to other cyanobacterial species. The ability to study the complete secondary metabolome and molecular phylogeny of prokaryotic organisms such as marine cyanobacteria has great scientific potential on many fronts. This type of analysis allows a deeper understanding of the biosynthetic capacity of a given organism with respect to that organism's taxonomic lineage. Moreover, as the details of molecular genetics come into focus researchers are increasingly able to compare and contrast the evolutionary and metabolic trends of these diverse and chemically rich organisms.

Experimental Section

General Experimental Procedures. Optical rotations were measured using a Perkin-Elmer 241 polarimeter with a 10 cm cell. UV was recorded on a Waters model 996 LC photodiode array detector and IR spectra were acquired on a ThermoElectron Nicolet IR100 FT-IP spectrometer. ^1H and 2D NMR spectral data were obtained on a Varian Inova spectrometer operating at 500 MHz. ^{13}C NMR spectra were acquired on a Varian Inova spectrometer operating at 75 MHz. CDCl_3 residual solvent peaks were used as internal references (δ_{H} 7.26; δ_{C} 77.0 ppm). Low resolution LC/MS and MS/MS data were acquired on a Thermo Finnigan LCQ Advantage Max spectrometer with ESI source and Surveyor Series LC. The FAB mass spectrum was recorded on Kratos MS50TC mass spectrometer. High resolution mass spectra were collected on a high accuracy Agilent ESI-TOF at the Scripps Research Institute, La Jolla, CA.

Collection, Isolation and Culture of *Oscillatoria nigro-viridis* strain OSC3L.

Strain OSC3L was isolated from an assemblage of *Lyngbya majuscula* collected at the CARMABI Research Station in Curaçao, Netherlands Antilles in 1993. The OSC3L filaments were isolated on solid agar plates using standard isolation techniques, as previously described.³² The isolated OSC3L filaments were cultured in BG-11 medium at 28°C with 33 g/L Instant Ocean salt (Aquarium Systems, Mentor). The cultures were kept in a 16 h/8 h light/dark cycle with a light intensity of *ca.* 500 LUX provided by 40W cool white fluorescent lights. Scaled-up cultures for organic extraction or DNA extraction were produced using 75 ml Erlenmeyer flasks, 3 L Fernbach flasks and 15 L pans, with the medium changed every 21 days. Total culture time varied from 21 to 30 days.

Isolation of Viridamides A (1) and B (2). The crude extract (1.56 g) was fractionated by normal phase vacuum liquid chromatography (VLC) on Si gel resulting in nine fractions of increasing polarity (A, 100% hexanes; B, 10% EtOAc in hexanes; C, 20% EtOAc in hexanes; D, 40% EtOAc in hexanes; E, 60% EtOAc in hexanes; F, 80% EtOAc in hexanes; G, 100% EtOAc; H, 25% CH₃OH in EtOAc; I, 100% CH₃OH). These nine fractions and the crude extract were then simultaneously screened by NMR and LC MS and evaluated for cancer cell cytotoxicity. The parallel screening of fractions G and H indicated the presence of unknown compounds and showed cytotoxicity in the initial screen.¹⁰ These fractions were subjected to RP C₁₈ HPLC (Phenomenex RP-Fusion semi preparative column 10 x 250 mm) monitored at 254 nm; 45 min gradient elution 80% aq CH₃OH to 100% CH₃OH at 3.0 mL/min flow rate). Viridamides A and B (30 and 3.6

mg, respectively) were further purified from the fractions eluting at 19.5 and 17.5 min, respectively, by repeated isocratic HPLC (Phenomenex RP-Fusion semi preparative column 10 x 250 mm; CH₃CN: H₂O (7:3) at 3.0 mL/min.

Viridamide A (1): colorless oil; $[\alpha]_D$ -107.4 (*c* 0.05, CDCl₃); UV (CH₃CN) λ_{\max} (log ϵ) 210 (2.9); IR (neat) ν_{\max} 3500, 3313, 2962, 2971, 2873, 1737, 1643, 1533, 1461, 1442, 1192, 1100, 1011 cm⁻¹; ¹H NMR (500 MHz, CDCl₃) and ¹³C NMR (75 MHz, CDCl₃), see table IV.2; FAB MS *m/z*; 735.51 (C₄₀H₆₉N₄O₈), 608.45 (C₃₅H₆₂N₅O₈), 454.29 (C₂₃H₄₀N₃O₆), 407.29 (C₂₃H₃₉N₂O₄), 355.22 (C₁₈H₃₁N₂O₅), 280.22 (C₁₇H₃₀NO₂); HR ESI TOF MS (obsd [M+H]⁺ at *m/z* 862.5847; calcd [M+H]⁺ 862.5827).

Viridamide B (2): colorless oil; $[\alpha]_D$ -98 (*c* 0.10, CDCl₃); UV (CH₃CN) λ_{\max} (log ϵ) 210 (3.1); IR (neat) ν_{\max} 3500, 3313, 2962, 2971, 2873, 1737, 1643, 1533, 1461, 1442, 1192, 1100, 1011 cm⁻¹; ¹H NMR (500 MHz, CDCl₃) and ¹³C NMR (75 MHz, CDCl₃), see table IV.3; HR TOF MS (obsd [M+H]⁺ at *m/z* 848.5661; calcd [M+H]⁺ 848.5670)

Acid Hydrolysis, Chiral HPLC, and Advanced Marfey's Analysis. Viridamide A (1 mg) was hydrolyzed in 0.5 mL of 6N HCl at 110°C for 18 h. Excess aq HCl was removed under vacuum. The dry material was resuspended in 0.5 mL of H₂O. Retention time comparisons of the commercially available L- and D- free amino acids by chiral HPLC (Chirex 3126, UV detection at 245 nm), indicated an L-configuration for all residues. L-Ile with 85:15 2 mM CuSO₄/CH₃OH (15.4 min; L-*allo*-Ile, 12.9 min; D-Ile, 24.3 min; D-*allo*-Ile 20.0 min), L-Val with 2 mM CuSO₄ (23.0 min; D-Val, 36.1 min), N-

Me- L-Val with 2 mM CuSO₄ (15.5 min; *N*-Me- D-Val, 24.8 min), L-Pro with 2 mM CuSO₄ (18.2 min; D-Pro, 32.3 min).

For determination of the configuration of the *N*-Me-Ile residue, the hydrolysate of **1** was divided into two portions and dissolved in 1N NaHCO₃ (100 μL) followed by the separate addition of 50 μL of 3 mg/mL (acetone) L-FDAA and D-FDAA, respectively. The reaction mixture was incubated at 80°C for 3 min. The reaction mixture was quenched by neutralization with 50 μL of 2N HCl. Next, 300 μL of 50% aq CH₃CN was added to the solution and the products were analyzed by reversed-phase HPLC (LiChrosphere 100 C₁₈, UV detection at 340 nm) using a linear gradient of 9:1 50 mM triethylammonium phosphate (TEAP) buffer (pH 3)/CH₃CN to 1:1 TEAP/CH₃CN over 60 min. Because only *N*-Me-L-Ile and *N*-Me-L-*allo*-Ile were commercially available, the D-Marfey's reagent was used to make the *N*-Me-D-Ile and *N*-Me-D-*allo*-Ile chromatographic equivalents. The retention times (*t*_R, min.) of the Ile derivative from the hydrolysate of **1** matched that of *N*-Me-L-Ile, (40.7 min ; *N*-Me-L-*allo*-Ile, 41.2 min; *N*-Me-D-Ile, 44.2 min; *N*-Me-D-*allo*-Ile, 44.7 min).

Preparation and chiral analysis of HMPA. L-Ile (100 mg, 0.75 mmol) was dissolved in 50 mL 0.2 N HClO₄ at 0°C. To this was added a cold (0°C) solution of NaNO₃ (1.4 g, 20 mmol) in 20 mL H₂O with rapid stirring. With continued stirring the reaction mixture was allowed to reach room temperature at which time evolution of N₂ subsided (*ca.* 30 min). The solution was then boiled for 3 min, cooled to room temperature, and then saturated with NaCl. This mixture was extracted with Et₂O and

dried under vacuum. The three other stereoisomers (2*R*, 3*R*)-HMPA, (2*R*, 3*S*)-HMPA, and (2*S*, 3*R*)-HMPA were synthesized in a similar manner from D-Ile, D-*allo*-Ile, and L-*allo*-Ile, respectively. A portion of the resultant oil was dissolved in aq 2 mM CuSO₄ buffer for HPLC. The retention time (Chirex-D, linear gradient 100:0 2 mM CuSO₄: CH₃CN to 95:5 over 20 min) of the natural product hydrolysate matched that for 2*S*,3*S*-HMPA (18.7 min; 2*R*,3*S*-HMPA, 15.2 min; 2*S*,3*R*-HMPA and 2*R*,3*R*-HMPA, 23.2 min).

Intracellular *T. cruzi* Assay. The anti-trypanosomal activity was determined using a recombinant Tulahuen clone C4 of *T. cruzi* that expresses β -galactosidase as a reporter enzyme.³³ The method is based on the growth inhibition effect of test samples on trypomastigote, the intracellular form of the parasite, infecting Vero cells, as previously described.³⁴

Antileishmanial Bioassay. Leishmaniasis bioassays were performed using a method based on parasite (*Leishmania mexicana*) DNA fluorescence, as previously described.³⁵

Morphological Analysis of strain OSC3L. The morphological characterization of OSC3L was performed using an Olympus BH-2 light microscope. The following parameters were selected to describe its morphology: length, width and length/width ratios of vegetative cells, presence/absence of specialized cells such as heterocysts, akinetes or calyptra, the size and shape of trichomes, granulation, constrictions at cross-walls, morphology of terminal cells, and thallus growth characteristics and coloration.

Morphological identification was made in accordance with traditional phycological²⁰ and bacteriological systems.¹⁸

DNA extraction, 16S rRNA gene PCR-amplification and Cloning. Genomic DNA was extracted from 40 mg of cleaned algal tissue using the Wizard[®] Genomic DNA Purification Kit (Cat. A1120) following the manufacturer's specifications (Promega, Madison, WI). The isolated genomic DNA was further purified using a Genomic-tip 20/G kit from Qiagen[®] (Cat. 10223). The 16S rRNA gene was amplified from isolated DNA using the cyanobacterial-specific primers, 106F and 1509R, as previously described.²¹ The reaction volume was 25 μ L containing 0.5 μ L of DNA (50 ng), 2.5 μ L of 10 x PfuUltra IV reaction buffer, 0.5 μ L of dNTP mix (25 mM each of dATP, dTTP, dGTP, and dCTP), 0.5 μ L of each primer (10 μ M), 0.5 μ L of PfuUltra IV fusion HS DNA polymerase (Cat. 600760) and 20.25 μ L dH₂O. The PCR reaction was performed in an Eppendorf[®] Mastercycler[®] gradient as follows: initial denaturation for 2 min at 95°C, 30 cycles of amplification: 20 sec at 95°C, 20 sec at 50°C and 1.5 min at 72°C, and final elongation for 3 min at 72°C. PCR products were subcloned using the Zero Blunt[®] TOPO[®] PCR Cloning Kit (Cat. K2800-20SC) from Invitrogen, into the pCR[®]-Blunt IV TOPO[®] vector, and then transformed into TOPO[®] cells and cultured on LB-kanamycin plates. Plasmid DNA was isolated using the QIAprep[®] Spin Miniprep Kit (Cat. 27106) from Qiagen and sequenced with pCR[®]-Blunt IV TOPO[®] vector specific primers M13F/M13R and internal middle primers 359F and 781R as previously described.²¹

Phylogenetic Analysis of Strain OSC3L. The bi-directional 16S rRNA gene sequences of OSC3L were combined and the resulting consensus sequence was inspected both visually and by secondary structure analysis using the CLC DNA Workbench 3. The GC content was determined using the MCBF Oligo Calculator from the Dana-Farber Cancer Institute, Molecular Biology Core Facilities (<http://mbcf.dfci.harvard.edu/docs/oligocalc.html>). The 16S rRNA gene was aligned together with related cyanobacterial strains representing 13 major genera of the order *Oscillatoriales* (subsection III) obtained from GenBank (<http://www.ncbi.nlm.nih.gov>) and the Ribosomal Database Project IV (<http://rdp8.cme.msu.edu/html/>). The multiple sequence alignments were performed using ClustalX in MEGA 4³⁶ with standard gap opening and extension penalties without gaps. The aligned 16S rRNA gene sequences were used to generate phylogenetic trees in MEGA 4. The phylogenetic relation of the cyanobacterial 16S rDNA genes were compared by (1) the distance method by Neighbor-Joining (NJ), (2) Maximum Parsimony (MP), and (3) the Maximum-Likelihood (ML) method. The evolutionarily distant cyanobacterium *Nostoc punctiforme* PCC73102 (GenBank Accession AF027655), from the order Nostocales, was used as an outgroup. Selection of the phylogenetic method used for the tree appearing in Figure IV.4 was based on tree topology and boot-strap values.

Table IV.2. 1D and 2D NMR spectral data for viridamide A (**1**) in CDCl₃ (¹H NMR at 500 MHz; ¹³C NMR at 75 MHz).

Residue	#	δ _C	δ _H (mult.)	gHMBC	gCOSY/TOCSY
Mdyna	44	68.4 (CH)			
	43	84.3 (C)			
	42	18.5 (CH ₂)	2.18 (dd; 6.1, 6.3)	44, 41, 39	41
	41	24.1 (CH ₂)	1.55 (m)	44	40, 42
	40	32.3 (CH ₂)	1.56 (m)		39, 41
	39	80.1 (CH)	3.15 (m)		38, 40
	38	32.8 (CH ₂)	1.48 (m)	36	37, 39
	37	21.5 (CH ₂)	1.67 (m)		36, 38
	36	36.6 (CH ₂)	2.20 (m)	37, 35	37
	35	172.7 (C)			
45	56.4 (CH ₃)	3.29 (s)	39		
N-Melle	34	31.7 (CH ₃)	3.07 (s)	35, 29	
	29	60.7 (CH)	5.00 (d; 10.2)	28	30
	30	33.4 (CH)	1.96 (m)		29
	33	15.6 (CH ₃)	0.96 (d; 6.8)	29	
	31	24.8 (CH ₂)	1.01/1.33 (m)		
	32	10.77 (CH ₃)	0.85 (dd; 6.5, 6.8)		
	28	172.9 (C)			
Val 1	NH		6.21	28	
	24	53.6 (CH)	4.81 (d; 6.3)	28	25
	25	31.2 (CH)	1.99 (td; 6.3, 6.5)		24
	26	17.4 (CH ₃)	0.89 (d; 6.3)		
	27	19.6 (CH ₃)	0.96 (d; 6.3)		
	23	169.5 (C)			
Val 2	NH		6.45	23	
	19	55.5 (CH)	4.58 (d; 6.8)	23	20
	20	30.8 (CH)	1.99 (td; 6.3, 6.8)		19
	21	19.7 (CH ₃)	0.95 (d; 6.3)		
	22	17.7 (CH ₃)	0.87 (d; 6.3)		
	18	170.3 (C)			
N-MeVal	17	30.3 (CH ₃)	3.01 (s)	18, 13	
	13	62.1 (CH)	4.72 (d; 10.7)	12	14
	14	25.9 (CH)	2.27 (td; 6.5, 10.7)		13
	16	18.1 (CH ₃)	0.78 (d; 6.5)		
	15	14.8 (CH ₃)	0.88 (d; 6.5)		
	12	170.5 (C)			
Hmpa	7	74.9 (CH)	4.98 (d; 7.0)	9	8
	8	35.7 (CH)	2.01 (m)	7	7
	11	19.5 (CH ₃)	0.95 (d; 6.3)		
	9	24.4 (CH ₂)	1.19/1.61 (td; 6.3, 7.0)		
	10	10.8 (CH ₃)	0.87 (t; 7.0)		
	6	170.0 (C)			
MePro	5	47.1 (CH ₂)	3.52/3.92 (m)		
	4	24.5 (CH ₂)	1.98/1.33 (m)		
	3	29.2 (CH ₂)	1.97/2.14 (m)	2	
	2	58.6 (CH)	4.37 dd; 8.5, 3.4)	1	
	1	172.1 (C)			
	46	51.9 (CH ₃)	3.64 (s)	1	

Table IV.3. 1D and 2D NMR data for viridamide B (**2**) in CDCl₃ (¹H NMR at 500 MHz; ¹³C NMR at 75 MHz).

Residue	#	δ _C	δ _H (mult.)	gHMBC	gCOSY/TOCSY
Mdyna	43	68.4 (CH)			
	42	84.3 (C)			
	41	18.5 (CH ₂)	2.20 (dd; 6.0, 6.2)	43,40,38	40
	40	24.1 (CH ₂)	1.56 (m)	43	39,41
	39	32.2(CH ₂)	1.58 (m)		38,40
	38	79.3 (CH)	3.17 (m)		37,39
	37	32.8 (CH ₂)	1.48 (m)	35	36,38
	36	21.5 (CH ₂)	1.67 (m)		35,37
	35	36.8 (CH ₂)	2.22 (m)	36,34	36
	34	172.8 (C)			
	44	55.8 (CH ₃)	3.31 (s)	38	
N-Melle	33	31.5 (CH ₃)	3.1 (s)	34,28	
	28	60.4 (CH)	5.03 (d; 10.1)	27	29
	29	33.5 (CH)	2.03 (m)		28
	32	15.6 (CH ₃)	0.98 (d; 6.8)	28	
	30	24.8 (CH ₂)	1.0/1.34 (m)		
	31	10.31(CH ₃)	0.85 (dd; 6.6, 6.7)		
	27	172.85 (C)			
Val 2	NH		6.19 (d; 9.3)	27	
	23	53.4 (CH)	4.86 (d; 6.4)	27	24
	24	29.3 (CH)	2.2 (td; 6.4, 6.6)		23
	25	17.4 (CH ₃)	0.88 (d; 6.4)		
	26	19.6 (CH ₃)	0.96 (d; 6.4)		
	22	169.6 (C)			
Val 1	NH		6.33 (d; 9.1)	22	
	18	55.4 (CH)	4.59 (d; 6.7)	22	19
	19	30.8 (CH)	1.97 (td; 6.2, 6.7)		18
	20	19.6 (CH ₃)	0.96 (d; 6.2)		
	21	19.6 (CH ₃)	0.95 (d; 6.2)		
	17	172.1 (C)			
N-MeVal	16	29.5 (CH ₃)	2.99 (s)	17,12	
	12	61.4 (CH)	4.76 (d; 11.0)	11	13
	13	25.6 (CH)	2.27 (td; 6.4, 6.5)		11
	15	17.9 (CH ₃)	0.81 (d; 6.4)		
	14	17.4 (CH ₃)	0.88 (d; 6.4)		
	11	170.4 (C)			
Ahva	7	75.4 (CH)	4.96 (d; 6.8)	8	6
	8	33.4 (CH)	2.02 (m)	6	7
	10	19.6 (CH ₃)	0.95 (d; 6.8)		
	9	18.1 (CH ₃)	0.81 (d' 6.1)		
	6	170.0 (C)			
MePro	5	46.8 (CH ₂)	3.55/3.94 (m)		
	4	24.5 (CH ₂)	1.99/2.05 (m)		
	3	28.9 (CH ₂)	1.96/2.15 (m)	2	
	2	58.4 (CH)	4.38 (dd; 8.5, 2.5)	1	
	1	172.6 (C)			
	45	51.8 (CH ₃)	3.66 (s)	1	

References

- (1) http://www.who.int/neglected_diseases/en/
- (2) Trouiller, P.; Olliaro, P.; Torreele, E.; Orbinski, J.; Laing, R.; Ford, N. *Lancet* **2002**, *359*, 2188-2194.
- (3) Yamey, G. *Br. J. Med.* **2002**, *325*, 176-177.
- (4) Teixeira, A. R. L.; Nascimento, R. J.; Sturm, N. R. *Mem. Inst. Oswald Cruz, Rio de Janeiro.* **2006**, *101*, 463-491.
- (5) www.who.int/leishmaniasis/en/
- (6) Guerin, P.J.; Olliaro, P.; Sundar, S.; Boelaert, M.; Croft, S.L.; Desjeux, P.; Wasunna, M.K.; Bryceson, A.D.M. *Lancet Infect. Dis.* **2002**, *2*, 494-501.
- (7) World Health Organization, **2002**. Control of Chagas disease: second report of the WHO expert committee. Technical Report Series, Vol. 905, WHO, Geneva.
- (8) Sanderson, L.; Khan, A.; Thomas, S. *Antimicrob. Agents Chemother.* **2007**, *51*, 3136-3146.
- (9) (a) Lee J.; Michael, A. J.; Martynowski, D.; Goldsmith, E. J.; Phillips, M. A. *J. Biol. Chem.* **2007**, *282*, 27115-27125; (b) Priotto, G.; Kasparian, S.; Nqouama, D.; Ghorashian, S.; Arnold, U.; Ghabri, S.; Karunakara, U. *Clin. Infect. Dis.* **2007**, *45*, 1435-1442.
- (10) Carrillo, C.; González, N.S.; Algranati, I.D. *Biochimica et Biophysica Acta* **2007**, *1770*, 1605-1611.
- (11) Bouteille, B.; Oukem, O.; Bisser, S.; Dumas, M. *Fundam. Clin. Pharmacol.* **2003**, *17*, 171-181.

(12) Seifert, K.; Lemke, A.; Croft, S.L.; Kayser, O. *Antimicrob. Agents Chemother.* **2007**, *51*, 4525-4528.

(13) (a) Sanchez, L.A.; Capitan, Z.; Romero, L.I.; Ortega-Barria, E.; Gerwick, W.H.; Cubilla-Rios, L. *Nat. Prod. Commun.* **2007**, *2*, 1065-1069; (b) McPhail, K.L.; Correa, J.; Linington, R.G.; Gonzalez, J.; Ortega-Barria, E.; Capson, T.L.; Gerwick, W.H. *J. Nat. Prod.* **2007**, *70*, 984-988.

(14) Gerwick, W.H., Tan, L., Sitachitta, N. *The Alkaloids*; Academic Press: San Diego, 2001; Vol. 57, pp. 75-184.

(15) (a) Marquardt, J.; Palinska, K.A. *Archives of Microbiol.* **2007**, *187*, 5, 397-413; (b) Rajaniemi, P.; Hrouzek, P.; Kaštovská, K.; Willame, R.; Rantala, A.; Hoffmann, L.; Komárek, J.; Sivonen, K. *Int. J. Syst. Evol. Microbiol.* **2005**, *55*, 11-26; (c) Clark, B.R.; Engene, N.; Gerwick, W.H. *J. Nat. Prod.* **2008** [In review].

(16) Repetitive extraction with CH₂Cl₂/ CH₃OH (2:1) followed by normal phase vacuum liquid chromatography using organic mobile phase of increasing polarity generating nine fractions (A-I).

(17) These fractions were initially active in a cell toxicity screen, but the activity did not repeat.

(18) (a) FujIV, K.; Ikau, Y.; Oka, H.; Suzuki, M.; Harada, K. *Anal. Chem.* **1997**, *69*, 3346-3352. (b) FujIV, K.; Ikau, Y.; Oka, H.; Suzuki, M.; Harada, K. *Anal. Chem.* **1997**, *69*, 5146-5151. (c) Marfey, P. *Calsberg Res. Commun.* **1984**, *49*, 591-596.

(19) Mamer, O. A. *Meth. Enzymol.* **2000**, *324*, 3-10.

(20) Linington, R.G., Gonzalez, J., Ureña, L.D., Romero, L.I., Ortega-Barria, E., Gerwick, W.H. *J. Nat. Prod.* **2007**, *70* (3), 397-401.

(21) (a) Geitler, L. *Akademische Verlagsgesellschaft.* **1932**, 942-943; (b) Komárek, J. & Anagnostidis, K. *Süsswasserflora von Mitteleuropa.* **2005**, *19/2*, 576-579.

- (22) Castenholz, R.W., Rippka, R., Herdman, M. *Bergey's Manual of Systematic Bacteriology*. **2001** Vol. **1**, 492-553.
- (23) Abed, R.M., Palinska, K.A, Camoin, G., Gulobic, S. *FEMS Microbiol. Lett.* **2006**, *260*, 171-177.
- (24) Sudek, S., Haygood, M.G., Youssef, D.T.A., Schmidt, E.W. *Appl Environ Microbiol.* **2006**, *72*, 4382-4387.
- (25) Van Wagoner, R.; Drummond, A.K.; Wright, J.L.C. *Adv. Appl. Microbio.* **2007**, *61*, 89-217.
- (26) Katircioğlu, H., Akın, B.S., Tahir, A. *African Journal of Biotechnology* **2004**, *3* (12), 667-674.
- (27) Wilkinson, C.R. & Sammarco, P.W. *Mar. Ecol. Prog. Ser.* **1983**, *13*, 15-19.
- (28) (a) Mynderse, J.S.; Moore, R.E.; Kashiwagi, M.; Norton, T.R. *Science*. **1977**, *196*, 538-540; (b) Mynderse, J.S.; Moore, R.E. *J. Org. Chem.* **1978**, *43*, 11, 2301-2303.
- (29) Hooper, G.J.; Orjala, J.; Schatzman, R.C.; Gerwick, W.H. *J. Nat. Prod.* **1998**, *61*, 529-533.
- (30) Edwards, D.J.; Marquez, B.L.; Nogle, J.N.; McPhail, K.; Goeger, D.E.; Roberts, M.A.; Gerwick, W.H. *Chem. Biol.* **2004**, *11*, 817-833.
- (31) Leusch, H.; Yoshida, W.Y.; Moore, R.E.; Paul, V.J. *J. Nat. Prod.* **2000**, *63*, 1106-1112.
- (32) (a) Gerwick, W. H.; Roberts, M. A.; Proteau, P. J.; Chen, J-L. *J. Appl. Phycol.* **1994**, *6*, 143-149; Nubel, U.; Garcia-Pichel, F.; Muyzer, G. *Appl. Environ. Microbiol.* **1997**, *63*, 3327-3332.
- (33) Buckner, F.S.; Verlinde, C.L.; LaFlamme, A.C.; Van Boris, W.C. *Antimicrob. Agents. Chemother.* **1996**, *40*, 2592-2597.

(34) Gutierrez, M.; Capson, T.L.; Guzman, H.M.; Gonzalez, J.; Ortega-Barria, E.; Quinoa, E.; Riguera, R. *J. Nat. Prod.* **2006**, *69*, 1379-1383.

(35) Calderon, A.; Romero, L.; Oretga-Barria, E.; Brun, R.; Correa, M.; Gupta, M.P. *Panama Pharm. Biol.* **2006**, *44*, 1-16.

(36) Kumar, S.; Tamura, K.; Nei, M. *Brief. Bioinform.* **2004**, *5*, 150-163.

Acknowledgments

The text of IV, in full, is the manuscript draft to be submitted to an academic journal as it will appear: Simmons, T.L., Engene, N., Gerwick, L., Gerwick, W.H. Viridamides A and B, lipodepsipeptides with anti-protozoan activity from the marine cyanobacterium *Oscillatoria nigro-viridis*. The dissertation author was the primary author and directed and supervised the research which forms the basis for this chapter.

Kaviol A, a Halogenated Phenolic Inhibitor of Histone Deacetylase from the marine alga

Boodlea sp.

Abstract

Kaviol A (**1**) is a new secondary metabolite with an unusual halogenated structure isolated from the marine alga *Boodlea* sp. by histone deacetylase (HDAC) inhibitory activity guided fractionation. The structure of **1** is only the second example of a C₆-C₄-C₆ compound isolated from a marine alga and potentially identifies the mode of action for this unusual structural class. Kaviol A (**1**) displays potent inhibition of the Class I HDAC enzyme (isoforms 1-4, 6, 8) with an IC₅₀ = 1.6 μM. The structure of **1** was determined by detailed 1D and 2D NMR analysis. Compound **1** was shown to inhibit six isoforms of HDAC (1-4, 6, 8) with low micromolar IC₅₀ values without suppressing non-histone β-catenin or P53 activity.

Introduction

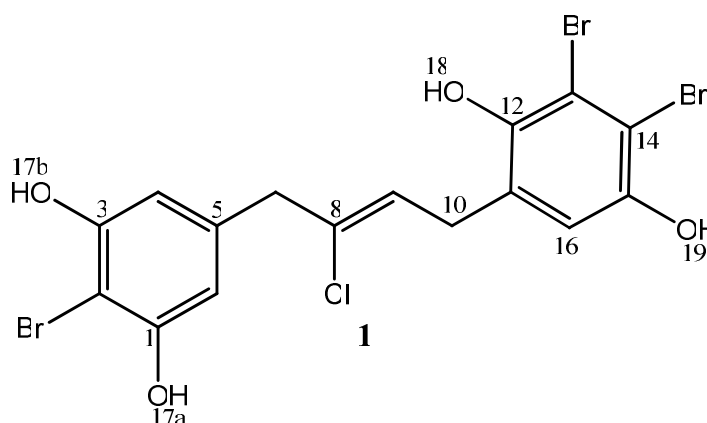
Cancer is characterized by aberrant cell growth and invasion into healthy tissues. Whether through an inherited predisposition or induced by environmental stimuli (or both), a hallmark of cancer is an alteration of expression or mutation of the genes controlling the growth and survival of tumor cells. Chromatin structure plays an important role in the regulation of eukaryotic gene expression and strict control of gene expression is required for normal cell cycling. This control is maintained by the opposing actions of histone acetyltransferases (HATs) and histone deacetylases (HDACs). An important mechanism in this is the reversible acetylation of lysine groups in nuclear histones, where competing activities of HAT and HDAC result in cell-specific patterns of gene expression. A higher degree of histone acetylation (HAT activity) or inhibition of HDACs (HDAC-1 & -6) leads to open chromatin structure and enables transcriptional activation.¹ Irregular transcription and expression of HATs and HDACs is fundamental to the onset and progression of cancer, such that inhibition of HDAC enzymes can reactivate suppressor gene expression and reduce the proliferation and survival of cancer cells.²

The National Cooperative Drug Discovery Groups (NCDDG) program was established to identify novel synthetic or naturally-derived anticancer agents working by new molecular mechanisms. Our program is focused on the discovery of new antitumor leads from marine algae and cyanobacterial.³ A systematic collection and evaluation program led us to investigate a field collected strain of the marine alga *Boodlea* sp.

Organic extracts of this green alga showed good activity in a fluorescent HDAC activity assay, and bioassay guided fractionation yielded a new halogenated diphenyl butenyl molecule, kaviol A (**1**), which exhibits low micromolar activity against Class I HDAC enzymes ($IC_{50} = 1.6 \mu\text{M}$ vs. HDAC isoforms 1-6).

Results and Discussion

Organic extraction of the marine alga *Boodlea* sp., collected near Kavieng, Papua New Guinea, yielded 2.1 grams of extract which was subjected to normal-phase vacuum liquid chromatography (VLC) resulting in nine fractions (A-I). Three contiguous fractions (E-G) displaying strong HDAC inhibition were profiled by HPLC MS and then fractionated by C_{18} RP HPLC to give kaviol A (**1**) (6.4 mg, 0.03% wet weight).



Negative ion HR ESI TOF MS for **1** gave an $[M-H]^-$ isotopic cluster with m/z 538.7876 (26.15%), 540.7857 (85.22%), 542.7838 (100%), 544.7818 (48.9%), and

546.7801 (7.86%), which corresponded to the molecular formula $C_{16}H_{12}Br_3ClO_4$ for **1** (calcd $[M-H]^-$ m/z 542.7933). The nine degrees of unsaturation inherent in this molecular formula was supported by the NMR data (Table V.1). Interpretation of the 1H and ^{13}C NMR spectra, combined with the phase sensitive multiplicity edited HSQC revealed the presence of one methine, two methylenes, and ten quaternary carbon atoms (H/C ratio = $12/16 = 0.75$). From chemical shift analysis (Table V.1) and the high degree of unsaturation, **1** was deduced to possess one olefin and two aromatic rings. Inspection of the 1H NMR spectrum revealed the presence of four hydroxyl protons appearing as three distinct broad hydroxyl singlets at δ_H 8.76 (1H), 9.89 (1H) and δ_H 9.92 (2H). Furthermore, the H/C ratio of 0.75 combined with the down field shifts of the protonated carbon atoms indicated a highly substituted system. Fortunately however, detailed interpretation of the 1H - 1H gCOSY and 1H - ^{13}C gHMBC data afforded two partial structures (**a** and **b**) that accounted for all atoms predicted by the molecular formula (Figure V.1).

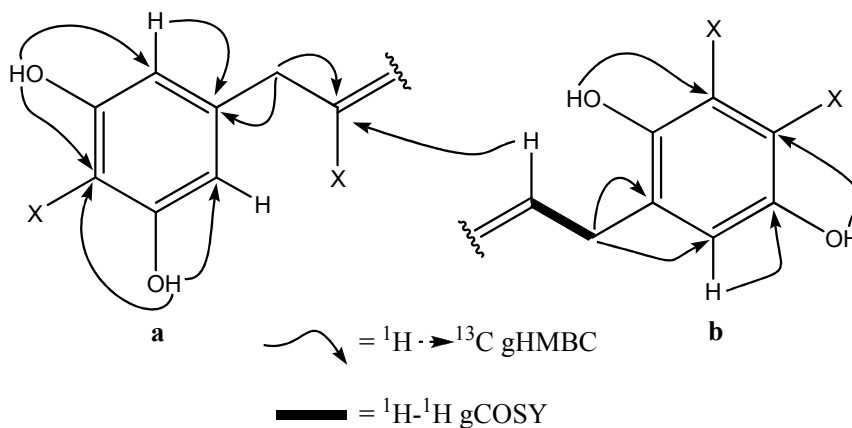


Figure V.1. Substructures **a** and **b** of kaviol A (**1**) showing HMBC and COSY derived partial structures.

Substructure **a** was deduced from ${}^1\text{H}$ - ${}^{13}\text{C}$ HMBC and chemical shift analysis, and was composed of five fully substituted olefinic carbon atoms (δ_{C} 155.1, 96.1, 155.1, 137.4, 133.7), two protonated olefinic carbons (δ_{C} 107.3, 107.3), and a methylene (δ_{C} 44.3). J^2 gHMBC from the broad exchangeable hydroxy protons (δ_{H} 9.92) to the subtending low field carbons at δ_{C} 155.1 ppm⁴ and three bond correlations to adjacent olefin carbons at δ_{C} 96.09 and 107.30 allowed assembly of the 5-allylbenzene-1,3-diol as subunit **a**. Fragment **b** similarly, was deduced from gHMBC and ${}^1\text{H}$ - ${}^1\text{H}$ gCOSY interpretation, and was comprised of five quaternary olefinic carbons (δ_{C} 128.5, 145.0, 115.8, 109.8, and 148.7), two methine carbons (δ_{C} 115.5, 124.8) and a methylene carbon (δ_{C} 29.8). J^2 and J^3 heteronuclear correlations from the down field hydroxyl protons (δ_{H} 8.76, 9.89), and the ${}^1\text{H}$ - ${}^1\text{H}$ COSY cross peak between the C-9 olefin (δ_{C} 124.8; δ_{H} 5.92) and C-10 methylene (δ_{C} 29.8; δ_{H} 3.41) positions as well as the methylene protons and olefin

carbons at C-11 and C-16 allowed assembly of the 5-allylbenzene-1,4-diol substructure (Figure 1).

Two quaternary olefinic carbon atoms seen in partial structure **a**, C-2 (δ_C 96.1) and C-8 (δ_C 133.7), were interpreted through HMBC and chemical shift models to have bromine and chlorine substitutions, respectively (Figure V.1).⁵ Bromine atom locations on fragment **b** were determined similarly, and were assigned to the tri-substituted aromatic sp^2 carbons C-13 (δ_C 115.8) and C-14 (δ_C 109.8). Union of subunits **a** and **b** across the tri-substituted olefin was apparent through the HMBC correlations from the two high field methylene positions H-10 (δ_H 3.41) and H-7 (δ_H 3.50) to the chlorine substituted C-8 (δ_C 133.7) and protonated C-9 (δ_C 124.8, δ_H 5.92), respectively.

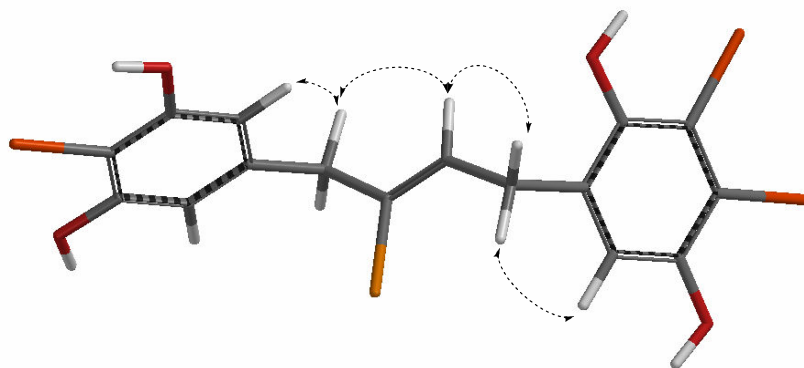


Figure V.2. Key ROESY correlations used for the assignment of *Z*-olefin geometry of **1**.

Due to the low solubility of **1** in most solvents, d_6 -DMSO was used for NMR analysis, and enabled clear long range heteronuclear correlations from the exchangeable hydroxyl protons to key carbon atoms in the structure. ROESY with a mixing time of 0.4

s and spin-lock power at 2500 Hz gave an Overhauser effect between H-9 (δ_{H} 5.92) and H-7 (δ_{H} 3.5), defining a Z-geometry for the olefin (Figure 2).

Table V.1. ^1H and ^{13}C NMR data for kaviol A (**1**).

#	$\delta_{\text{C}}^{\text{a}}$	$\delta_{\text{H}}^{\text{b}}$	COSY	HMBC	rOe
1	155.13				
2	96.09				
3	155.13				
4	107.30 CH	6.30 s		2,3,7	7
5	137.43				
6	107.30 CH	6.30 s		1,2,7	7
7	44.33 CH ₂	3.50 s		4,5,6,8	4,9
8	133.74				
9	124.82 CH	5.92 (t, 6.8)	10	7,8,10	7,10
10	29.82 CH ₂	3.417 (d, 6.8)	9	8,9,11,16	9,16
11	128.54				
12	145.07				
13	115.84				
14	109.86				
15	148.75				
16	115.55 d, CH	6.78 s		10,12,14,15	
18	-OH	8.76 bs		11,12,13	
17a	-OH	9.92 bs		1,2,6	
17b	-OH	9.92 bs		2,3,4	
19	-OH	9.89 bs		14,15,16	16

^a acquired at 75 MHz; ^b acquired at 500 MHz in *d*₆-DMSO (δ_{H} 2.51, δ_{C} 39.5 ppm)

Biosynthetically, these unusual C₆-C₄-C₆ molecules appear to originate from basic building blocks of primary metabolism (Figure V.3).

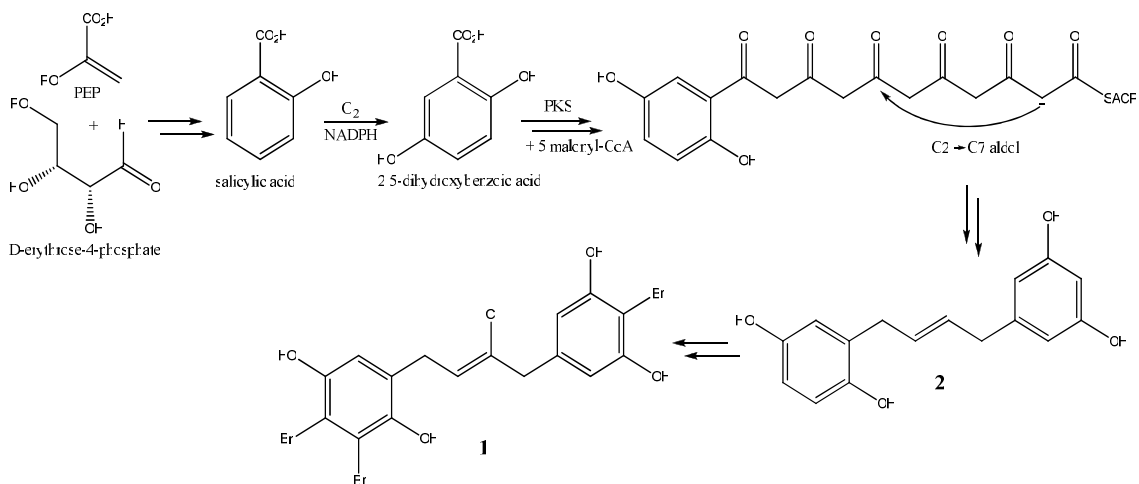


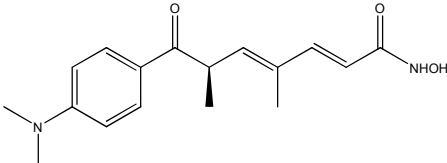
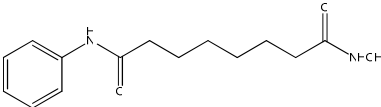
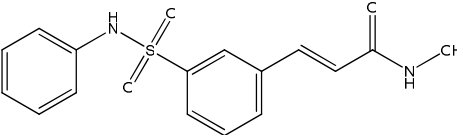
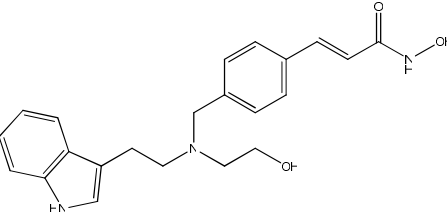
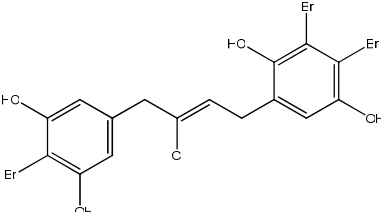
Figure V.3. A Plausible Biosynthesis of **1** and other C₆-C₄-C₆ compounds.

One hypothesis for the assembly of **1** combines elements of the shikimic acid biosynthetic pathway with those from polyketide biosynthesis. Shikimic acid (produced by the coupling of phosphoenolpyruvate (PEP) and D-erythrose-4-phosphate) is converted into chorismic acid by way of the 3-enolpyruvylshikimic acid 3-phosphate (EPSP) synthase. Chorismic acid then isomerizes and eliminates pyruvic acid to give salicylic acid. NADPH dependent oxygenation yields 2,5-dihydroxybenzoic acid, which is activated to the dihydroxybenzoic acid-CoA. Conversion to the acyl carrier protein (ACP) bound thioester prepares the substrate for PKS extension. Next, the ACP-bound

starter unit is extended by two carbon units (acetate equivalents) in five successive Claisen condensation reactions with malonyl-CoA. A proposed C2-C7 intramolecular aldol condensation liberates C1 as carbon dioxide and forms the second six membered carbocycle.^{6,7} Although the timing of the following steps is difficult to predict, the (*E*)-5-(4-(2,5-dihydroxyphenyl)but-2-enyl)benzene-1,3-diol (**2**) is formed by multiple ketoreductase, dehydratase and enoylreductase catalytic cycles. Subsequent addition of the chlorine and three bromine atoms is likely to occur via a vanadium-dependent haloperoxidase mechanism, as known to occur in other marine alga. In these reactions, the hypohalite species are delivered in a regiospecific manner by nucleophilic attack from the electron rich substrate.^{8,9}

Effect of kaviol A (1) on Histone Deacetylase. Kaviol A (**1**) displayed HDAC inhibitory activity (against isoforms 1-4, 6, 8) with an $IC_{50} = 1.6 \mu\text{M}$. Although **1** exhibited equivalent potency against all six HDAC enzyme isoforms tested, it had negligible effects on the non-histone proteins β -catenin and P53. Histone deacetylases can be inhibited by a structurally diverse group of small molecules and these HDAC inhibitors induce growth arrest, differentiation and/ or apoptosis of cancer cells in vitro and in vivo (Table 2).^{10,11,12}

Table V.2. Small-molecule pan inhibitors of HDAC and their respective IC₅₀ values (nM).

Selected Small-Molecule HDAC inhibitors	HDAC IC ₅₀ (nM)	
TSA ¹³		≥ 11
SAHA ¹⁴		≥ 50
PXD101 ¹⁵		≥ 200
NVP-LAQ824 ¹⁶		≥ 32
Kaviol A (1)		1.6x10 ³

The proposed mechanism for HDAC activity involves “a bound water molecule activated by a zinc cation and a histidine-aspartate charged relay system” which attacks

the amide bond of acetylated lysine.¹⁷ The four known small molecule HDAC inhibitors shown in Table V.2 all inhibit HDAC enzymes in a similar manner. The hydroxamic acid functional group chelates the zinc cation and creates hydrogen bonds with various amino acids in the active site. Each of these four compounds contains an aliphatic chain that mimics that of lysine and forms van der Waals interactions with residues lining the channel. Finally, each has a ‘cap group’ which interacts with residues around the rim of the HDAC channel. Combinatorial synthesis of small-molecule HDAC inhibitors has shown that an optimal chain length of the aliphatic chain is 5-6 carbons.¹⁷

It is possible that phenolic HDAC inhibitors such as kaviol A (**1**) utilize a similar mechanism of action as that discussed above. Conceptually, one of the phenolic groups in **1** could chelate the zinc cation and form hydrogen bonds with residues inside the HDAC active site; the four carbon aliphatic chain connecting the two bromo-phenolic groups could allow HDAC active site entry, creating the required van der Waals interactions, while the ‘unbound’ phenolic moiety would serve as the ‘cap group’. These features of **1** may explain its reduced potency relative to the known HDAC inhibitors in Table V.2, in that the ‘double-headed’ nature of kaviol A may result in steric conflict as it enters the active site tunnel of the HDAC enzyme. More work is needed to fully understand the binding orientation and kinetics of this new HDAC inhibitor structure class.

It remains unclear whether pan HDAC inhibition or the targeting of specific HDAC isoforms is the more effective strategy against cancer. It is known, however, that certain cancers exhibit aberrant expression of specific HDACs from both class I and II. A recent study has addressed this issue by testing various HDAC inhibitors against a panel of recombinant human HDAC isoforms, and showed that while both pan HDAC and

class I specific inhibitors increased the acetylation of histones, only the pan HDAC inhibitors also increased tubulin acetylation. Furthermore, data from recent clinical trials of belinostat, vorinostat and other pan HDAC inhibitors have shown associated toxicities are no more severe than those seen in patients treated with class I selective inhibitors. This suggests the possibility that, pan HDAC inhibitors are more desirable as cancer therapies due to their ability to inhibit both HDAC classes.¹⁸

There is one other compound of this C₆-C₄-C₆ structure class reported in the literature. Colpol, isolated from the brown alga *Colpomenia sinuosa* collected in the Red Sea, has a similar 1,3- and 1,4- oxygenation pattern, is brominated at C-2 and C-14 (equivalent positions) and exhibits toxicity against P388, A549, HT-29 and CV-1 tumor cells, with IC₅₀s at 10 µg/mL for each.¹⁹ In addition to providing a second example of this marine algal chemotype, the present work may offer insight to the mechanism of antitumor activity for this unique class of molecules.

Experimental Section

Algal Collection and Extraction. The marine green alga *Boodlea* sp. (voucher specimen available as collection number PNG-05/19/05-12) was collected by TLS, C.M. Sorrels, and R.V. Grindberg from an unnamed lagoon (GPS S 4°14.105 x E 152°25.605) in shallow water (1 m). The material was preserved in EtOH/sea water (1:1) and stored at reduced temperature until extracted. Approximately 1 L of preserved algal tissue was repetitively extracted with CH₂Cl₂:CH₃OH (2:1) at 40°C. A saturated aq NaCl solution

was added, the organic phase collected and the resultant organic oil was then concentrated by rotary evaporation under reduced pressure.

General Experimental Procedures. The optical rotation was measured on a Perkin-Elmer 243 polarimeter, UV was recorded on a Waters model 996 LC photodiode array detector and the IR spectrum was recorded on a Nicolet 510 Fourier transform IR spectrophotometer. ^1H and 2D NMR spectral data were obtained on a Varian Inova 500 MHz spectrometer, and ^{13}C NMR spectra were acquired on a Varian Inova 75 MHz spectrometer. Low resolution LC MS data were acquired on a Thermo Finnigan LCQ Advantage Max spectrometer with ESI source and Surveyor Series LC. High resolution mass spectra were collected on a high accuracy Agilent HR ESI TOF MS at The Scripps Research Institute, La Jolla, CA. Molecular geometry optimization models were formed *ab initio* under 6.31G basis sets using Spartan '04 for Windows (www.wavefun.com).

Isolation of kaviol A (1). The crude $\text{CH}_2\text{Cl}_2:\text{CH}_3\text{OH}$ extract (1.29 g) was fractionated by normal phase vacuum liquid chromatography (VLC) on Si gel in a step gradient scheme resulting in nine fractions of increasing polarity (A, 100% hexanes; B, 10% EtOAc in hexanes; C, 20% EtOAc in hexanes; D, 40% EtOAc in hexanes; E, 60% EtOAc in hexanes; F, 80% EtOAc in hexanes; G, 100% EtOAc; H, 25% CH_3OH in EtOAc; I, 100% CH_3OH). These nine fractions and the crude extract were submitted for bioassay against various cancer and tropical disease assays. Based on the assay results fractions E was subjected to RP HPLC (Phenomenex Jupiter 250 x 10 mm) with 45 min gradient using 45% aq CH_3CN to 100% CH_3CN at 3.0 mL/min. Kaviol A (6.4 mg) was

subsequently purified by isocratic HPLC (Phenomenex Jupiter 250 x 10 mm) using 40% CH₃CN in H₂O at 3.0 mL/min.

Kaviol A (1): yellow oil; $[\alpha]_D^{23} = 0$ (*c* 0.1, CH₃OH); UV (CH₃OH) λ_{\max} 280; IR (neat) ν_{\max} 3450, 3300, 2962, 1640, 1450, 1135, 700 cm⁻¹; ¹H NMR (500 MHz, *d*₆-DMSO) and ¹³C NMR (75 MHz, *d*₆-DMSO), see table 1.; HR ESI TOF MS [M-H]⁻ at *m/z* 542.7838 (100%); 540.7857 (78 %); 544.7818 (48.5 %); 538.7876 (26.5 %); 543.7866 (17.7 %); 541.7866 (15.1 %).

References and Notes

- (1) Gallinari, P.; Di Marco, S.; Jones, P.; Pallaoro, M.; Steinkühler, C. *Cell Res.* **2007**, *17*, 1-17.
- (2) Johnstone, R.W. *Nat. Rev. Drug Dis.* **2002**, *1*, 287-299.
- (3) Gerwick, W.H.; Tan, L.; Sitachitta, N. *The Alkaloids*; Academic Press: San Diego, 2001; Vol. 57, pp. 75-184.
- (4) Integration of the proton signal at 6.30 ppm indicates 2H and a doubling of relative intensity was observed for the ^{13}C NMR resonance at 107.3 ppm.
- (5) Chemical shift model and resonance estimation protocols provided in supporting information. ^{13}C NMR chemical shift predictions were modeled for various halogen substitutions about the two phenol systems and butenyl linker. ChemNMR ^{13}C Estimation; ChemBioDraw Ultra 11.0, www.CambridgeSoft.com.
- (6) Austin, M.B.; Noel, J.P. *Nat. Prod. Rep.* **2003**, *20*, 79-110.
- (7) Reinecke, T.; Kindl, H. *Phytochemistry* **1994**, *35*, 63-66.
- (8) Butler, A.; Carter-Franklin, J. *Nat. Prod. Rep.* **2004**, *21*, 180-188.
- (9) Vaillancourt, F.H.; Yeh, E.; Vosburg, D.A.; Garneau-Tsodikova, S.; Walsh, C.T. *Chem. Rev.* **2006**, *106*, 3364-3378.
- (10) (a) Remiszewski, S.W. Recent advances in the discovery of small molecule histone deacetylase inhibitors. *Curr. Opin. Drug Discov. Devel.* **2002**, *5*, 487-499; (b) Remiszewski, S.W.; Sambucetti, L.C.; Bair, K.W.; Bontempo, J.; Cesarz, D.; Chandramouli, N.; Chen, R.; Cheung, M.; Cornell-Kennon, S.; Dean, K.; Diamantidis, G.; France, D.; Green, M. A.; Howell, K. L.; Kashi, R.; Kwon, P.; Lassota, P.; Martin, M. S.; Mou, Y.; Perez, L. B.; Sharma, S.; Smith, T.; Sorensen, E.; Taplin, F.; Trogani, N.; Versace, R.; Walker, H.; Weltchek-Engler, S.; Wood, A.; Wu, A.; Atadja, P. *J. Med. Chem.* **2003**, *46*, 4609-4624.

(11) Rodriguez, M.; Aquino, M.; Bruno, I.; De Martino, G.; Taddei, M.; Gomez-Paloma, L. *Curr. Med. Chem.* **2006**, *13*, 1119-1139.

(12) Minucci, S.; Pelicci, P.G. *Nat. Cancer Rev.* **2006**, *6*, 38-51.

(13) Elaut, G.; Laus, G.; Alexandre, E.; Richert, L.; Bachellier, P.; Tourwé, D.; Rogiers, V.; Vanhaecke, T. *J. Pharmacol. Exp. Ther.* **2007**, *321*, 400-408.

(14) Hanessian, S.; Auzzas, L.; Giannini, G.; Marzi, M.; Cabri, W.; Barbino, M.; Vesci, L.; Pisano, C. *Bioorg. Med. Chem. Lett.* **2007**, *17*, 6261-6265.

(15) Glaser, K.B. *Biochem. Pharmacol.* **2007**, *74*, 659-671.

(16) Remiszewski, S.W. *Curr. Med. Chem.* **2003**, *10*, 2393-2402.

(17) Grozinger, C.M.; Schreiber, S.L. *Chem. & Biol.* **2002**, *9*, 3-16.

(18) Khan, N.; Jeffers, M.; Kumar, S.; Hackett, C.; Boldog, F.; Khramtsov, N.; Qian, X.; Mills, E.; Berghs, S.C.; Carey, N.; Finn, P.W.; Collins, L.S.; Tumber, A.; Ritchie, J.W.; Jensen, P.B.; Lichenstein, H.S.; Sehested, M. *Biochem. J.* **2007**, doi:10.1042/BJ20070779

(19) Green, D.; Kashman, Y. *J. Nat. Prod.* **1993**, *56*, 1201-1202.

Acknowledgments

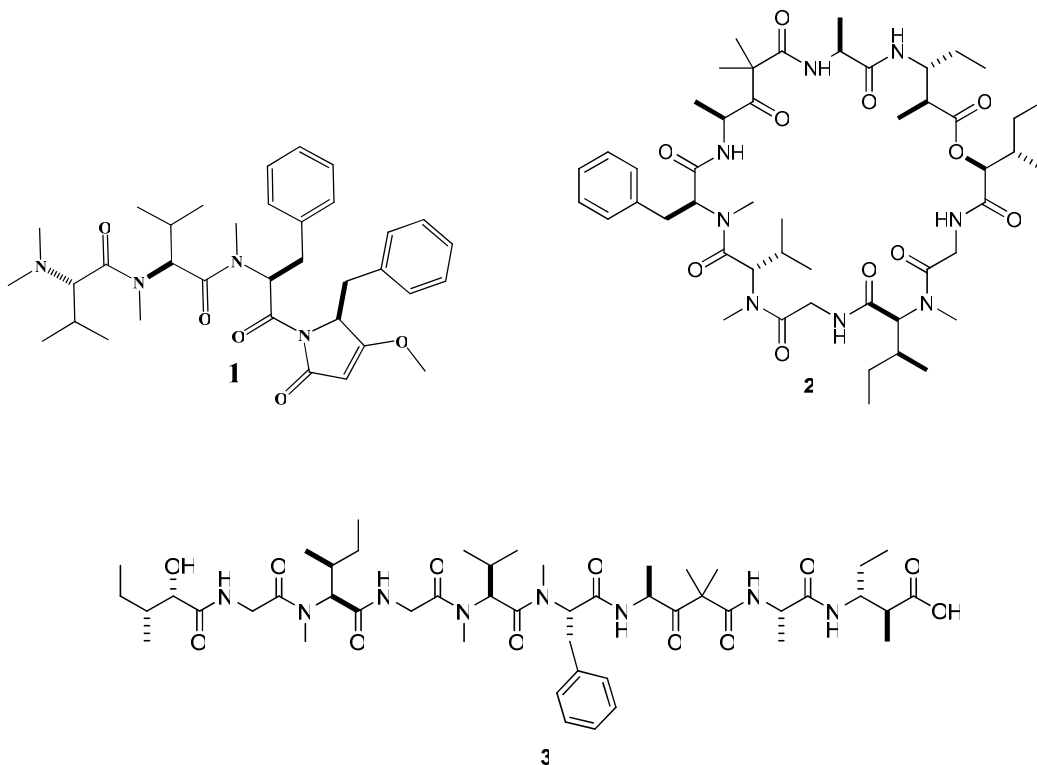
The text of V, in full, is the manuscript draft to be submitted to an academic journal as it will appear: Simmons, T.L., Wood, A., Fiorilla, C., Gerwick, W.H. Kaviol A, a Halogenated Phenolic Inhibitor of Histone Deacetylase from the marine alga *Boodlea* sp. The dissertation author was the primary author and directed and supervised the research which forms the basis for this chapter.

VI

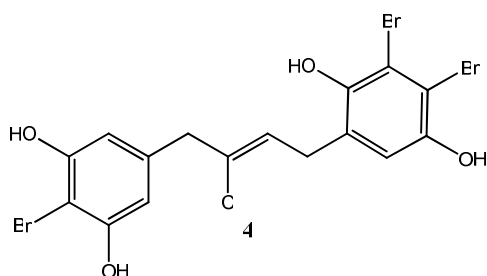
Conclusions

VI. Conclusions

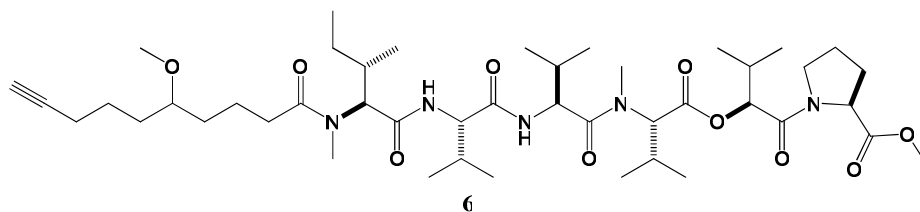
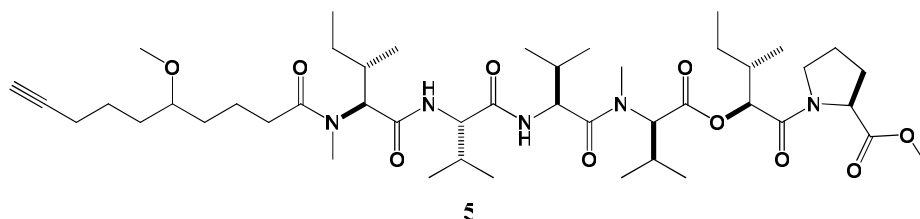
This thesis described the successful chemical investigation of marine prokaryotes and eukaryotic organisms for the presence of novel molecules with medically relevant biological activities. Here I report the finding of six new marine secondary metabolites that show efficacy against cancer (**1-4**) and infections disease (**5-6**). Belamide A (**1**) and DMMC (**2**) were directly isolated from the marine cyanobacteria *Lyngbya majuscula* and *Symploca* sp., respectively. The third, a linear analog of DMMC (**3**), was generated by the base hydrolysis of **2**.



A fourth compound with anticancer properties is the metabolic product of the eukaryotic marine green alga *Boodlea* sp., kaviol A (**4**).



The viridamides A and B (**5** and **6**) were isolated from the marine cyanobacterium *Oscillatoria nigro-viridis*. These new linear depsipeptides were shown to have cytotoxic activities against the protozoan pathogens *Trypanosoma cruzi* and *Leishmania mexicana*.



The planar molecular structures of **1-6** were solved by the utility of advanced 1D and 2D NMR and mass spectrometry. The absolute configurations of **1-3**, **5**, **6** were determined by chemical degradation and derivatization followed by chiral chromatography, while the three dimensional structure of **4** was determined by nOe NMR

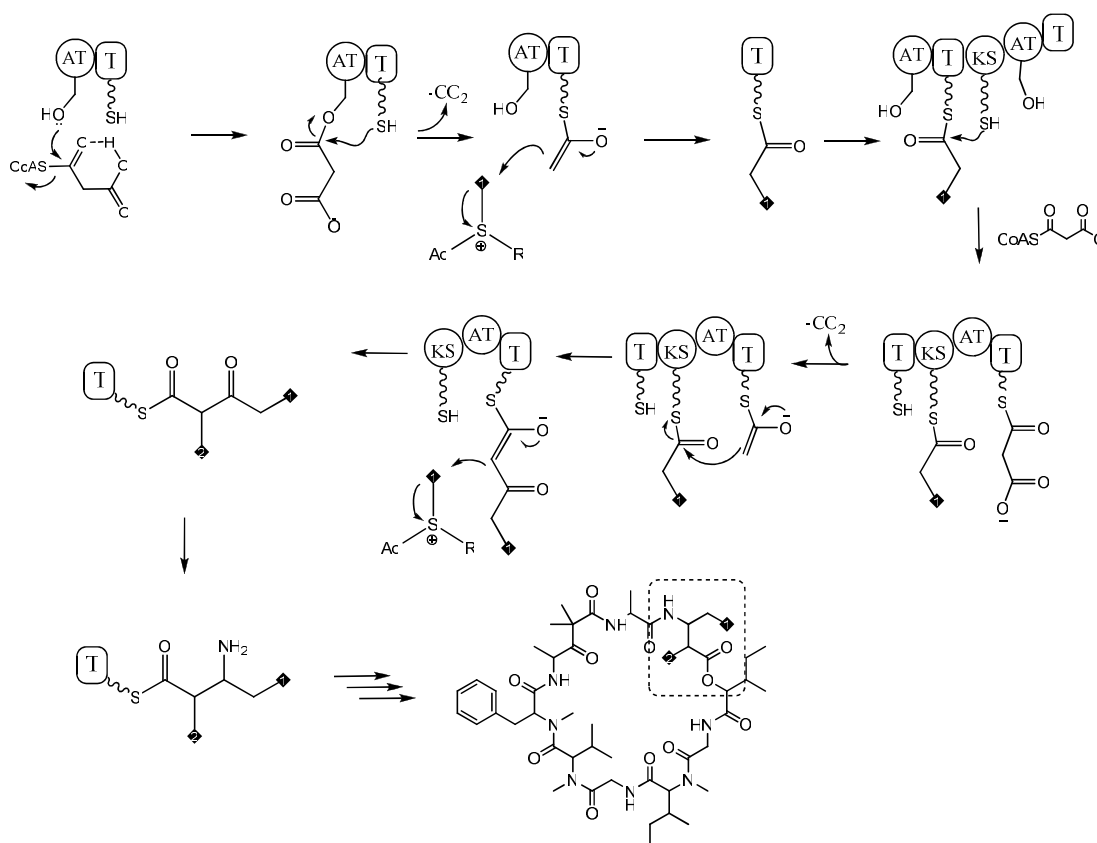
spectroscopy. These molecules each have interesting structural features and biological activities worthy of further discussion.

Belamide A (**1**) is the result of NRPS biosynthesis. The level of *N*- and *O*-methylation found in this compound suggests very high expression of *N*- and *O*-methyltransferase genes inherent in the enzymatic construction of **1**. Further, the presence of the C-terminal benzyl-methoxypyrrolinone (presumably generated by the acetate extension of phenylalanine followed by an intramolecular condensation) suggests that one PKS domain is also active at the C-terminus of the biosynthetic gene cluster for **1**. As genome sequences become more readily available it should be interesting to look for the presence of adjacent inactive PKS domains. Future advances in epigenetics should allow variable regulation of these respective genes, thus allowing the engineering of novel ‘tertiary’ metabolites.

The isolation of belamide A (**1**) was guided by MCF7 human breast cancer cytotoxicity assay. Although the initial extreme potency ($IC_{50} < 8$ ng/mL) of the crude extract was not reproducible, pure **1** gave a very respectable $IC_{50} = 0.74$ μ M against this cell line. Mechanism of action studies were done using (rapidly dividing) A10 cells and revealed belamide A to act through the binding to and depolymerization of cellular microtubules with ‘classic’ antimetabolic characteristics. Molecular modeling studies were undertaken to compare the lowest energy solution conformation of **1** to those of the dolastatins 10 and 15 (structural analogs with extremely potent antimetabolic activity). These data helped rationalize the reduced bioactive of **1** as compared to the dolastatin 10 and 15. As of the writing of this chapter at least one total synthesis of belamide A has been completed (personal communication), and although it is not known whether

structural analogs were generated, an SAR study of such a library will certainly be interesting.

DMMC (**2**) is also an NRPS product with a high degree of methylation, but has only minimal PKS character in its biosynthesis. Members of this cyclic depsipeptide structure family all possess the interesting 3-amino-2-methylpentenoate (Map) unit. This residue is likely generated by C2 methylation of the enzyme bound diketide, followed by transamination of the β -keto group which prepares this β -amino acid for incorporation (as shown below).



Another exciting aspect of this project was the bioactivity of the linear hydrolysis product of DMMC (**3**). This linear analog **3** exhibited equivalent solid tumor selective cytotoxicity and to function by the same actin microfilament depolymerization mechanism as **2**. Considering the number of bioactive structural analogs reported (to date) for these compounds, this finding raises some important questions regarding the active form of these depsipeptides. Molecular optimization models were generated to understand the predicted structures of these compounds in solution and lowest energy conformations were predicted for conditions representing cellular cytosol and cell wall. Under both models the cyclic **2** held a fairly consistent shape while the linear **3** had strikingly different conformations under these two conditions. Both **2** and **3** display 'mild' selectivity for solid tumor cell lines (this may seem obvious considering their MOA) with neither affecting neuro-2A cells yet displaying low nano-molar IC₅₀ values against colon cancer cells. These encouraging results certainly warrant further SAR development through solid-phase peptide synthesis (these efforts are underway in the laboratory of our collaborator F. Valeriote).

Kaviol A (**4**) is a new member of the unique C₆-C₄-C₆ structure class of small molecules. The isolation of **4** was guided by an enzyme based HDAC inhibition assay and yielded the novel halogenated phenolic compound **4** with low micromolar IC₅₀ values against six HDAC isoforms. Unlike the other compounds discovered during this thesis research kaviol A (**4**) was not isolated (directly) from a microbe, rather from *Boodlea* sp. (*Kingdom* Plantae; *Phylum* Chlorophyta), a eukaryotic genus that is poorly defined at the species level. The unique diphenyl butenyl carbon skeleton appears to be constructed through the combined efforts of PKS and shikimic acid biosynthetic pathways. While a

rationalization of molecular assembly is important for the assignment of the producing organism, in this case it does not immediately indicate the biosynthetic origin of this structure class (i.e. microbes and higher plants are both known to utilize the shikimic acid and acetate pathways). There is one feature, however, that may shed light which organism is making this compound. The C2-C7 aldol condensation which forms the second phenyl ring has only been observed in higher plants. A type III PKS, bibenzyl synthase (BBS) extends dihydro-*m*-coumaryl-CoA by three malonyl-CoA units, and performs the C2-C7 aldol cyclization, has been characterized from the orchid *Blerilla striata*. The resultant dibenzyl molecule has an oxygenation pattern similar to **4**, and thus the possibility of a similar enzyme (accepting a hexaketo-substrate) functioning in *Boodlea* seems reasonable. Interestingly, expression of BBS is up-regulated dramatically following inoculation of the orchid with *Rhizoctonia* species and subsequent physical injury.¹ This requirement may suggest that the plant is responding to infection by increased biosynthesis of a defensive agent or that the fungus or even an unknown bacterial member of the rhizo-sphere is producing this molecule as an ecological response. It is unknown whether production of **4** by *Boodlea* is influenced by, or involves an associated microorganism.

The viridamides A and B (**5** and **6**) were isolated by an ‘interesting NMR spectrum and data base search’ guided fractionation of a cyanobacterial extract. Through extensive NMR and MS analysis these mixed NRPS/PKS molecules were determined to contain the novel 5-methoxydec-9-ynoic acid (Mdyna) in addition to six more common amino- and hydroxy-acid residues.

Subsequent evaluation of **5** and **6** against the protozoa *Trypanosoma cruzi* and *Leishmania mexicana* indicated efficacy with $IC_{50} = 1.1$ and $1.6 \mu M$, respectively, against these pathogens. This is important because these parasites are responsible for the Neglected Tropical Diseases, Chagas and leishmaniasis; these two diseases combined affect over 100 million people world wide. Unfortunately, due to the pan-tropical distribution of these organisms (and NTDs in general) the majority of those afflicted are poverty-stricken, and therefore, not able to afford any of the current medical treatments. Hence, few new agents have entered the global market. The viridamides are currently undergoing further biological evaluation to gain a deeper understanding regarding their potential as anti-protozoan agents.

The search for new and useful pharmaceutical agents is centered on the chemical diversity of small molecules and the genetic diversity inherent in their biosynthesis. This thesis has successfully demonstrated that the chemical investigation of diverse marine cyanobacterial and algal taxa is a valid approach to the discovery of new secondary metabolites with pharmaceutical potential.

Reference

- (1) Reinecke, T.; Kindl, H. *Phytochemistry* **1994**, *35*, 63-66

Appendix

Supporting information for chapter II



Available online at www.sciencedirect.com



Tetrahedron Letters 47 (2006) 3387–3390

Tetrahedron
Letters

Belamide A, a new antimitotic tetrapeptide from a Panamanian marine cyanobacterium

T. Luke Simmons,^{a,b} Kerry L. McPhail,^b Eduardo Ortega-Barría,^c
Susan L. Mooberry^d and William H. Gerwick^{a,b,*}

^aCenter for Marine Biotechnology and Biomedicine, Scripps Institution of Oceanography, University of California-San Diego, La Jolla, CA 92093-0212, USA

^bCollege of Pharmacy, Oregon State University, Corvallis, OR 97331-4003, USA

^cInstituto de Investigaciones Científicas Avanzadas y Servicios de Alta Tecnología, Centro de Estudios Biomédicos, Clayton, Bldg. 175, PO Box 7250, Panama 5, Panama

^dSouthwest Center for Biomedical Research, San Antonio, TX 78245, USA

Received 9 December 2005; revised 10 March 2006; accepted 14 March 2006

Abstract—The isolation and structure elucidation of belamide A from the marine cyanobacterium *Symploca* sp. is described. Belamide A is a highly methylated linear tetrapeptide with structural analogy to the important linear peptides dolastatins 10 and 15. Disruption of the microtubule network in A-10 cells was observed at 20 μ M and displayed classic tubulin destabilizing antimitotic characteristics. The moderate cytotoxicity of belamide A (IC₅₀ 0.74 μ M vs HCT-116 colon cancer line) provides new insights into structure–activity relationships for this drug class.

© 2006 Elsevier Ltd. All rights reserved.

Marine cyanobacteria synthesize a myriad of structurally complex and biologically active secondary metabolites.¹ Of specific importance to human health is a diverse family of peptides and depsipeptides known as the dolastatins. Originally isolated from the sea hare *Dolabella auricularia*, dolastatins 10 and 15 display extraordinary cytotoxicity to cancer cells (IC₅₀ values 0.059 and 2.9 nM, respectively).² Although neither of these two compounds is still undergoing clinical evaluation, they have stimulated extensive synthetic efforts resulting in several drug leads currently in clinical trials.³ These synthetic efforts have generated considerable structure–activity knowledge in this compound family.³ Here we report a novel structural analog of dolastatins 10 and 15, belamide A (**1**), as a major metabolite of the marine cyanobacterium *Symploca* sp. Belamide A, a highly methylated tetrapeptide, contains two characteristic residues of dolastatin 15 (Fig. 1), the N-terminal *N,N*-dimethylvaline and C-terminal benzyl-methoxy-pyrrolinone moieties. This letter expands on the reper-

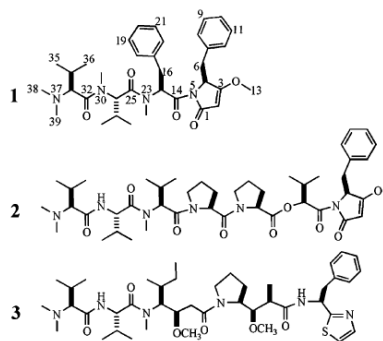


Figure 1. Belamide A (**1**), dolastatin 15 (**2**), and dolastatin 10 (**3**).

toire of linear peptides from marine cyanobacteria and contributes to our knowledge of SAR features for this important class of lead anticancer compounds.

The organic oil (CH₂Cl₂–MeOH, 360 mg) of a Panamanian cyanobacterium *Symploca* sp.⁴ was initially found

Keywords: *Symploca* sp.; Linear peptide; Dolastatins; Marine natural products.

* Corresponding author. Tel.: +1 858 534 0578; e-mail: wgerwick@ucsd.edu

0040-4039/\$ - see front matter © 2006 Elsevier Ltd. All rights reserved.
doi:10.1016/j.tetlet.2006.03.082

to be highly cytotoxic to the MCF-7 breast cancer cell line (IC₅₀ 8 ng/mL), and was thus fractionated using a silica gel solid phase extraction column and elution solvents of increasing polarity. The resultant four fractions (A–D)⁵ were profiled by ¹H NMR, and fraction D exhibited interesting signals typical for a modified peptide. Thus, it was subjected to exhaustive RPHPLC⁶ to yield 3.6 mg of pure belamide A (**1**) (Fig. 1).⁷

HRTOF-MS (ES⁺) measurement indicated a molecular formula of C₃₅H₄₈N₄O₅ (M+H obs. *m/z* 605.3643; calcd 605.3624), and was in agreement with the observed physical data.⁷ Although **1** readily dissolved in CDCl₃, some isochronous proton chemical shifts were observed; these were resolved in C₆D₆ which was used in the remainder of this study (Table 1).

1D NMR spectra were well dispersed in C₆D₆, and indicated the presence of *N*- and *O*-methyl functionalities. Three *N*-methylated amino acid substructures were deduced from 2D NMR data (¹H–¹H COSY, multiplicity edited ¹H–¹³C HSQC, and ¹H–¹³C HMBC) as well as tandem MS data (Fig. 3), including *N*-Me-Phe (C-14

to C-23); *N*-Me-Val (C-25 to C-32) and *N,N*-diMe-Val (C-33 to C-39; see Table 1).

The interesting chemical shifts recorded for a methine carbon (C-2, δ_C 95.0; δ_H 4.28) adjacent to the quaternary carbon at δ_C 177.7 (C-3) suggested oxygenation at the latter position. Additionally, HMBC correlations between H-2 (δ 4.28) and C-1 (δ 169) and C-4 (δ 59.9); H-4 (δ 4.57) and C-2 (δ 95.0); H-5 (δ 2.91) and C-3 (δ 177.7) were observed, and defined a substituted pyrrolinone ring (see Fig. 2). By additional HMBC correlations from the C-6 methylene protons to C-7 and C-8/12, one substituent was revealed as a benzyl moiety. A second substituent was a methoxy group (3H at δ 3.38) located at C-3 by a long range ¹H–¹³C correlation between the methoxy proton resonance (H₃-12) and C-3. These data were reinforced by MS/MS fragments (see Fig. 3), which further supported a benzyl-methoxypyrrolinone moiety present at the C-terminus of **1**.

It was readily apparent that the *N,N*-diMe-Val residue formed the N-terminus and the benzyl-methoxypyrrolinone moiety formed the C-terminus of belamide A.

Table 1. NMR data for belamide A (600 MHz for ¹H; 75 MHz for ¹³C)^a

Unit	C/H No.	δ _H , mult. (<i>J</i> in hertz)	δ _C (75 MHz, mult.)	¹ H– ¹ H COSY	¹ H– ¹³ C HMBC ^b	
Bn- <i>O</i> -Me-pyrrolinone	1		169.0 (C)			
	2	4.28 (s)	95.0 (CH)		C1, C4	
	3		177.7 (C)			
	4	4.57 (dd, 3.3, 3.6)	59.9 (CH)	H-6	C2	
	N-5					
	6	2.91 (dd, 3.0, 2.8) 3.68 (dd, 4.4, 4.5)	35.10 (CH ₂)	H-4	C3, C7, C8/12	
	7		138.1 (C)			
	8/12	7.27 (m)	130.1 (CH)	H-9/11		
	9/11	7.28 (m)	128.6 (CH)	H-8/12		
	10	7.00 (m)	126.8 (CH)			
	13	3.38 (s, 3H)	58.9 (CH ₃)		C3	
	<i>N</i> -Me-Phe	14		172.6 (C)		
		15	2.77 (m)	57.3 (CH)	H-16	C14, C17, C24, C25
16		2.82 (dd, 3.7, 2.6) 3.52 (dd, 3.4, 3.2)	34.1 (CH ₂)	H-15	C18/22	
17			134.9 (C)			
18/22		7.43 (m)	129.2 (CH)	H-19/21		
19/21		7.09 (m)	128.7 (CH)	H-18/22		
20		7.08 (m)	127.4 (CH)			
N-23						
<i>N</i> -Me-Val	24	2.75 (s)	32.8 (CH ₃)			
	25		173.0 (C)			
	26	5.65 (d, 10.4)	58.3 (CH)	H-27	C25, C31	
	27	2.53 (m)	27.7 (CH)	H-26,28,29		
	28	0.90 (d, 6.7)	19.2 (CH ₃)	H-27	C26, C27, C29	
	29	1.11 (d, 6.4)	20.1 (CH ₃)	H-27	C26, C27, C28	
<i>N,N</i> -diMe-Val	N-30					
	31	2.57 (s)	30.3 (CH ₃)		C32	
	32		171.7 (C)			
	33	2.85 (d, 10.3)	68.9 (CH)	H-34	C32, C38, C39	
	34	2.33 (m)	28.8 (CH)	H-33,35,36		
	35	1.03 (d, 6.6)	20.3 (CH ₃)	H-34	C33	
	36	0.57 (d, 6.7)	20.5 (CH ₃)	H-34	C33	
	N-37					
	38	2.36 (s)	41.4 (CH ₃)		C33	
39	2.36 (s)	41.4 (CH ₃)		C33		

^aNMR chemical shifts were assigned by ¹H–¹H COSY, ¹H–¹³C HSQC, and modified 1D ¹H–¹³C HMBC experiments (C₆D₆; 128.02/7.16 ppm).

^bIncludes data from 1D ¹H–¹³C HMBC with a delay time for the evolution of long-range heteronuclear coupling optimized for 4 Hz (125 ms).

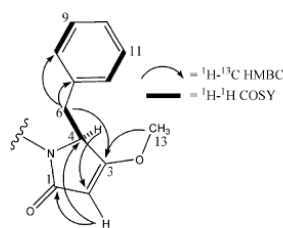


Figure 2. HMBC and COSY correlations for the benzyl-methoxy-pyrrolinone ('dolapyrrolidone') residue in belamide A (**1**).

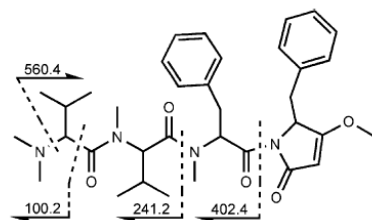


Figure 3. Tandem MS fragments of belamide A (**1**).

Sequencing of the remaining residues was accomplished by HMBC (Table 1) and Tandem MS (Fig. 3). Correlations between H-26 (δ 5.65) and C-31 (δ 30.3) as well as H₃-31 (δ 2.57) and C-32 (δ 171.7) linked the *N*-Me-Val and *N,N*-diMe-Val residues. Finally, correlations between H-15 (δ 2.77) and C-25 (δ 173.0) and H-26 (δ 5.65) and C-25 linked the *N*-Me-Val and *N*-Me-Phe residues. Tandem electrospray ionization (ESI) mass spectral fragmentation patterns were straightforward and allowed facile residue sequencing for the planar structure of belamide A (**1**).

The absolute configuration of **1** was based on chiral HPLC analysis.⁸ Retention times of the 6 N HCl hydrolysate components of **1** were compared to commercially available amino acid standards, and indicated *L*-configurations for the *N*-Me-Phe and *N*-Me-Val units. In the case of *N,N*-diMe-Val, analytical standards were synthesized from *S*- and *R*-valine using literature methods,⁹ and compared with the hydrolysate of **1** by chiral HPLC; this residue was also of *L*-configuration. Determination of C-4 required ozonolysis of **1** followed by acid hydrolysis which yielded free phenylalanine; this was also determined to be *L* by chiral HPLC.⁸

Pure belamide A (**1**) assayed against the MCF7 breast cancer cell line displayed an IC_{50} = 1.6 μ M, while to the HCT-116 colon cancer cell line it was somewhat more potent giving an IC_{50} = 0.74 μ M.

Bai et al. have shown that β -tubulin binding for this class of linear peptides (there now exist many synthetic analogs) is mainly influenced by the N-terminal residue sequence and configuration at key stereogenic centers.¹⁰ Mitra and Sept have developed an alternative model based on the *in silico* binding behavior of known tubulin binding compounds (viz. dolastatin 10, cryptophycin 52,

and others), in conjunction with multiple X-ray crystal structures of bovine β -tubulin.¹¹ These models support a single high affinity binding pocket at the 'plus' end of the β -tubulin monomer adjacent to the exchangeable GTP site; however, there is some discussion regarding which residues of dolastatins 10 and 15 are critical for this interaction.^{10–13} Interestingly, structural features of both of these two drugs are found in belamide A, and appear to be consistent with the SAR developed from extensive analog work evaluated both *in vitro*¹² and *in vivo*.¹³

The N-terminus of belamide A is formed by an *N,N*-dimethylvaline residue, a feature found in both dolastatins 10 and 15, and which is reported to be one of the more critical residues for potent biological activity. However, the naturally occurring analog symprostatin 1 possesses an *N,N*-dimethylisoleucine residue and is nearly as potent as dolastatin 10,¹⁴ and synthetic analogs possessing a *N,N*-dimethylglycine terminus were only modestly diminished in potency.¹⁵ The second residue is also a valyl derivative (as in both **2** and **3**); however, in belamide A this residue is *N*-methylated. No reported analogs in the dolastatin 10 or 15 series possess *N*-methylation at this position, and this may explain the lower potency of compound **1**. In the dolastatin 15 series, the third residue is *N*-methylvaline; synthetic studies have shown that slight variations in side chain structure result in analogs with only modest variations in potency. In fact, in the dolastatin 10 series, residues with a bulkier side chain at residue-3 (i.e. isoleucyl derivative) have greater *in vivo* potency versus the smaller valine analog.¹³ Therefore, the larger *N*-methyl Phe residue of belamide A should not necessarily diminish the activity of **1**. Residue-3 of both dolastatins 10 and 15 is *N*-methylated, as it is in belamide A; this is a required feature for high potency as demonstrated by synthetic analogs.¹⁵

The final residue of belamide A is precisely as that found for the C-terminal residue of dolastatin 15, benzyl-methoxypyrrolinone. Numerous analogs of the carboxy terminus in both the dolastatins 10 and 15 series have been examined, and in general, this residue is highly tolerant of change, although the required structural feature appears to be a benzyl group. In the case of a terminating benzyl-methoxypyrrolinone residue, the *S*-stereoconfiguration as that found in belamide A has been shown to be critical.¹⁶ Truncated tri- and tetra-peptides have been synthesized and examined for their properties as well. Analogs composed of the N-terminal first three residues or C-terminal four residues of dolastatin 10 were active in inhibiting tubulin assembly, but only weakly cytotoxic.¹⁷

Given the structural similarity of belamide A to the dolastatins 10 and 15, we were interested to further understand the reduced bioactivity of belamide A. From molecular mechanics calculations of the energy minimized structures of belamide A (**1**) and dolastatin 15 (**2**) and aligning of their C-termini, only a weak overlap correlation was observed.¹⁸ However, alignment of the N-terminal regions of these two linear peptides resulted in a reasonably good fit for the first three residues of both compounds. However, the two adjacent proline residues in **2** result in back-to-back β -turns, thereby

'swinging' the C-terminal pyrrolinone moiety out of conformational overlap with belamide A. Similar analysis was performed with dolastatin 10 (**3**); in this case, alignment of the N-termini of **1** and **3** resulted in a very poor conformational overlap. The dolaproine unit of dolastatin 10 causes the peptide to adopt an overall 'sickle' shape, whereas belamide A retains a more linear conformation.

In the absence of definitive crystal structures of **2** or **3** bound to tubulin, there remains a debate regarding the critical pharmacophore for this family of anticancer agents. Our results for belamide A are intermediate between the pharmacophore hypotheses put forth by Bai et al.¹⁰ (dolavaline-valine-dolaisoleuine) and that of Mitra and Sept¹¹ (valine-dolaisoleuine-dolaproine). Belamide A displays classic microtubule depolymerizing effects in A-10 cells, including concentration dependent interphase microtubule loss, micronucleation and abnormal mitotic spindle formation at 20 μ M, and is a moderately potent cytotoxin to HCT-116 cells (IC₅₀ 0.74 μ M). These biological effects may be attributed to the N-terminal residue sequence and its hydrophobic binding interaction within the peptide-groove of β -tubulin. However, if belamide A does bind to this peptide-groove, it does so with relatively low affinity, possibly due to one or a combination of missing structural features or steric hindrance, as discussed above. Further biological evaluation of belamide A is needed to fully appreciate the biomedical potential of this new modified peptide natural product.

Acknowledgments

We thank H. Gross, for helpful suggestions with this investigation, particularly the NMR studies. Financial support was provided by the Fogarty International Center's International Cooperative Biodiversity Groups (ICBG) program in Panama (ICBG TW006634). High resolution and tandem MS data provided by J. Moore at the Environmental Health Sciences Mass Spectroscopy Facility (NIEHS grant P30 ES00210) and 600 MHz NMR data were acquired at the Biochemistry and Biophysics NMR facility, both at OSU.

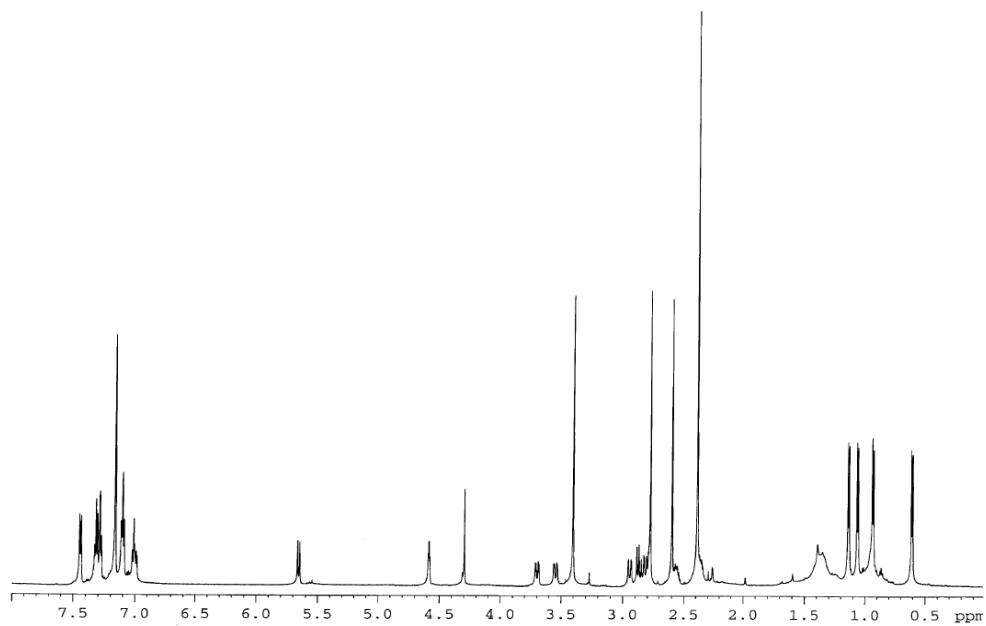
Supplementary data

Supplementary data associated with this article can be found, in the online version, at doi:10.1016/j.tetlet.2006.03.082.

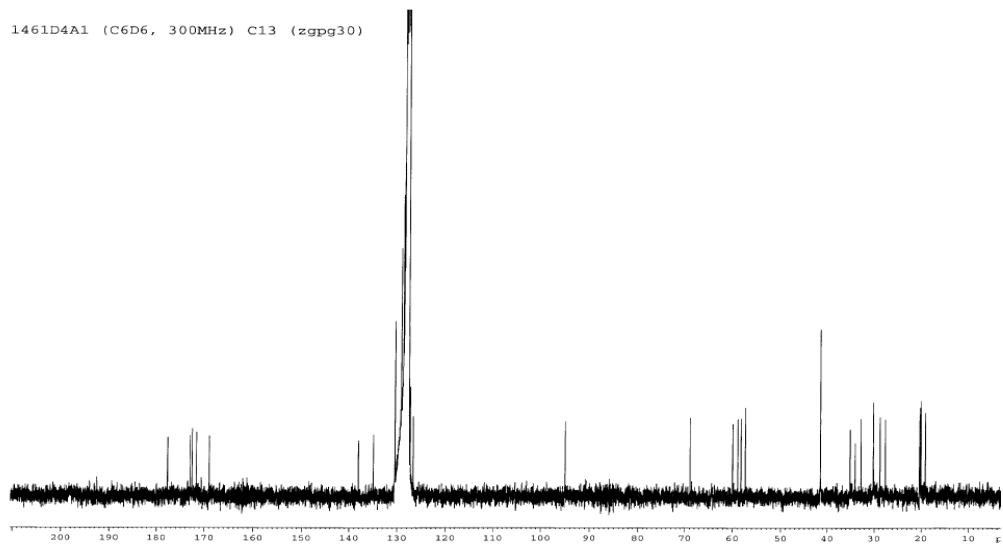
References and notes

- Gerwick, W. H.; Tan, L. T.; Sitachitta, N. Nitrogen-containing metabolites from marine cyanobacteria. In *The Alkaloids*; Cordell, G., Ed.; Academic Press: San Diego, 2001; Vol. 57, pp 75–184.
- (a) Pettit, G. R.; Kamano, Y.; Herald, C. L.; Tuinman, A. A.; Boettner, F. E.; Kizu, H.; Schmidt, J. M.; Baczynskij, L.; Tomer, K. B.; Bontems, R. J. *J. Am. Chem. Soc.* **1987**, *109*, 6883–6885; (b) Pettit, G. R.; Kamano, Y.; Dufresne, C.; Cerny, R. L.; Herald, C. L.; Schmidt, J. M. *J. Org. Chem.* **1989**, *54*, 6005–6006.
- (a) Newman, D. J.; Cragg, G. M. *J. Nat. Prod.* **2004**, *67*, 1216–1238; (b) Simmons, T. L.; Andrianasolo, E.; McPhail, K.; Flatt, P.; Gerwick, W. H. *Mol. Cancer Ther.* **2005**, *4*, 333–342.
- Live algal sample collected on 11/3/03 at Salmedina Reef, Portobelo, Panama; N 09°33.799' \times W 79°41.642'; in shallow water by Drs. Kerry L. McPhail and William H. Gerwick.
- Phenomenex Strata (Si-1; 55 μ m particle) NP solid phase extraction column eluted with 100 mL of each the following solvent compositions, fraction: (A) [8:2] hexanes–EtOAc; (B) [1:1] hexanes–EtOAc; (C) 100% EtOAc; (D) 100% MeOH.
- Phenomenex Synergi 4 μ m Fusion-RP 250 \times 10 mm column; isocratic [8:2] MeOH–H₂O, then [7:3] MeOH–H₂O.
- Belamide A (**1**) was isolated as a yellow glassy oil, $[\alpha]_D^{25} +16$ (*c* 0.002, CDCl₃); UV (CHCl₃) λ_{max} 240 nm; IR ν_{max} (KBr) 2960, 2926, 2853, 2790, 1997, 1722, 1697, 1630 cm⁻¹.
- All chiral HPLC analysis was performed using a Phenomenex Chirex 3126 D column with a 2 mM CuSO₄/CH₃CN mobile phase except the *N,N*-diMe-Val which required 100% 2 mM CuSO₄ buffer.
- Pettit, G. R. Inventor; Arizona Board of Regents, assignee. Synthesis of Dolastatin 10. United States Patent U.S. 4,978,744, 1990.
- Bai, R.; Roach, M. C.; Jayaram, S. K.; Barkoczy, J.; Pettit, G. R.; Luduena, R. F.; Hamel, E. *Biochem. Pharmacol.* **1993**, *45*, 1503–1515.
- Mitra, A.; Sept, D. *Biochemistry* **2004**, *43*, 13955–13962.
- Pettit, G. R.; Srirangam, J. K.; Barkoczy, J., et al. *Anti-Cancer Drug Design* **1998**, *13*, 243–277.
- Miyakaki, K.; Kobayashi, M.; Natsume, T.; Gondo, M.; Mikami, T.; Sakakibara, K.; Tsukagoshi, S. *Chem. Pharm. Bull.* **1995**, *43*, 1706–1718.
- Luesch, H.; Moore, R. E.; Paul, V. J.; Mooberry, S. L.; Corbett, T. H. *J. Nat. Prod.* **2001**, *64*, 907–910.
- Bai, R.; Pettit, G. R.; Hamel, E. *Biochem. Pharmacol.* **1990**, *40*, 1859–1864.
- Poncet, J.; Busquet, M.; Roux, F.; Pierré, A.; Atassi, G.; Jouin, P. *J. Med. Chem.* **1998**, *41*, 1524–1530.
- (a) Hamel, E. *Biopolymers (Pept. Sci.)* **2002**, *66*, 142–160; (b) Hamel, E.; Covell, D. G. *Curr. Med. Chem.: Anti-Cancer Agents* **2002**, *2*, 19–53.
- Spartan'04, Wavefunction, Inc., Irvine, CA.

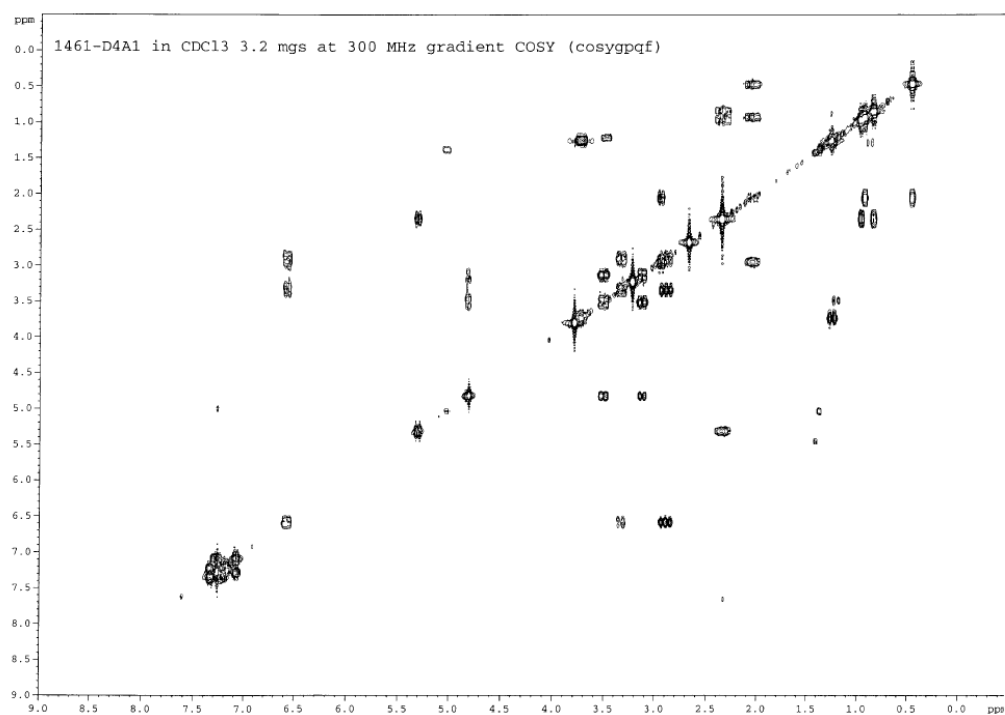
^1H NMR spectrum of belamide A (600 MHz; C_6D_6)

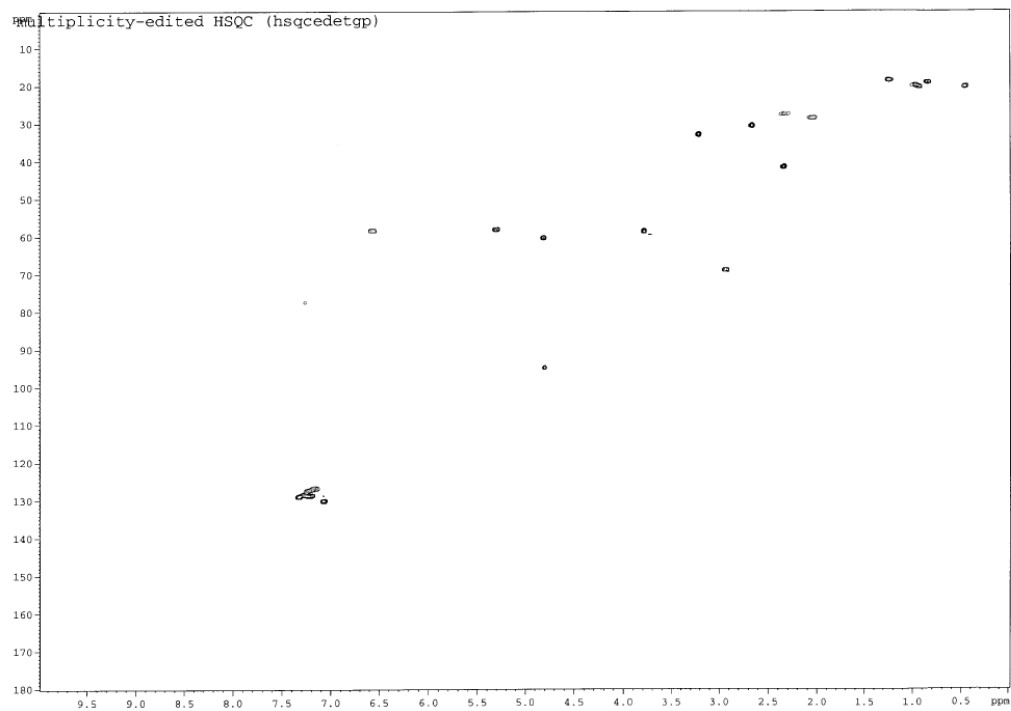


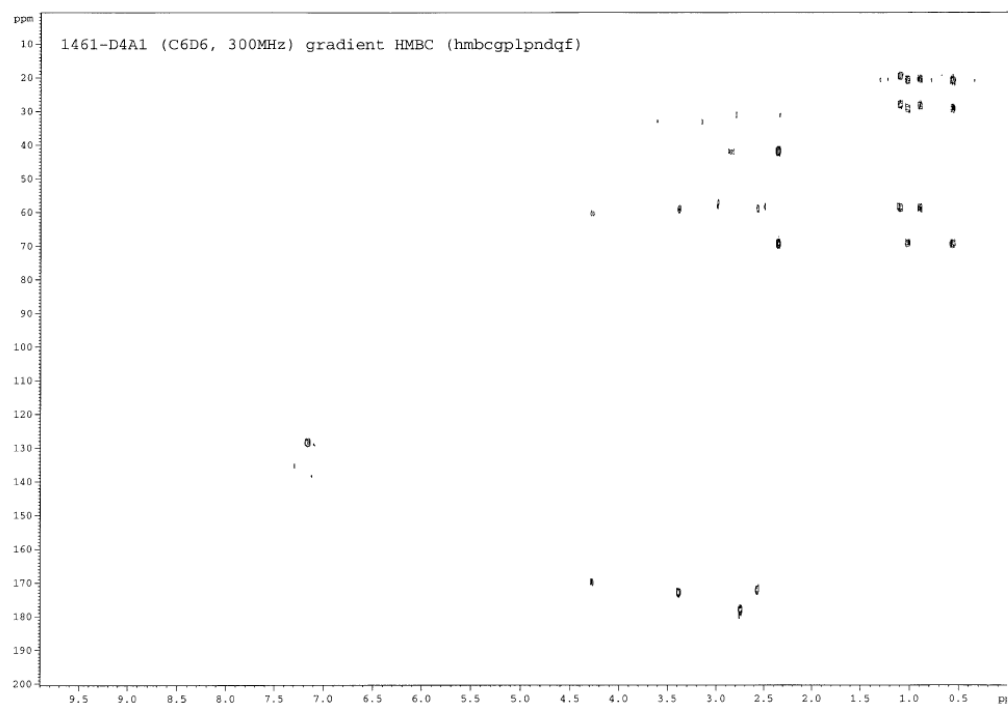
^{13}C NMR spectrum of belamide A (75 MHz; C_6D_6)



^1H - ^1H COSY NMR spectrum of belamide A (300 MHz; CDCl_3)



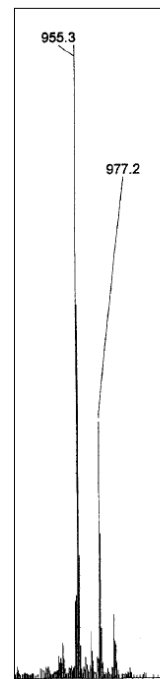
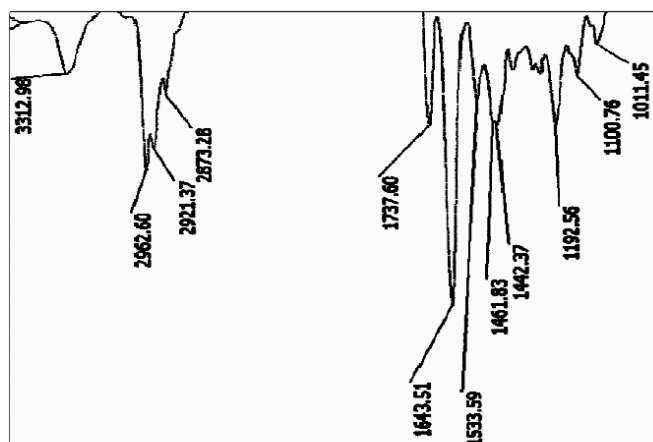
^1H - ^{13}C HSQC NMR spectrum of belamide A (CDCl_3)

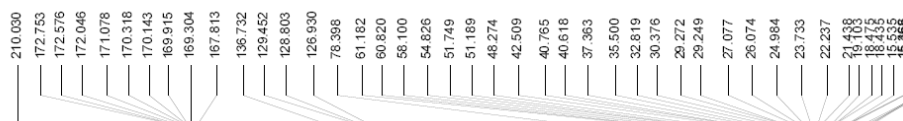
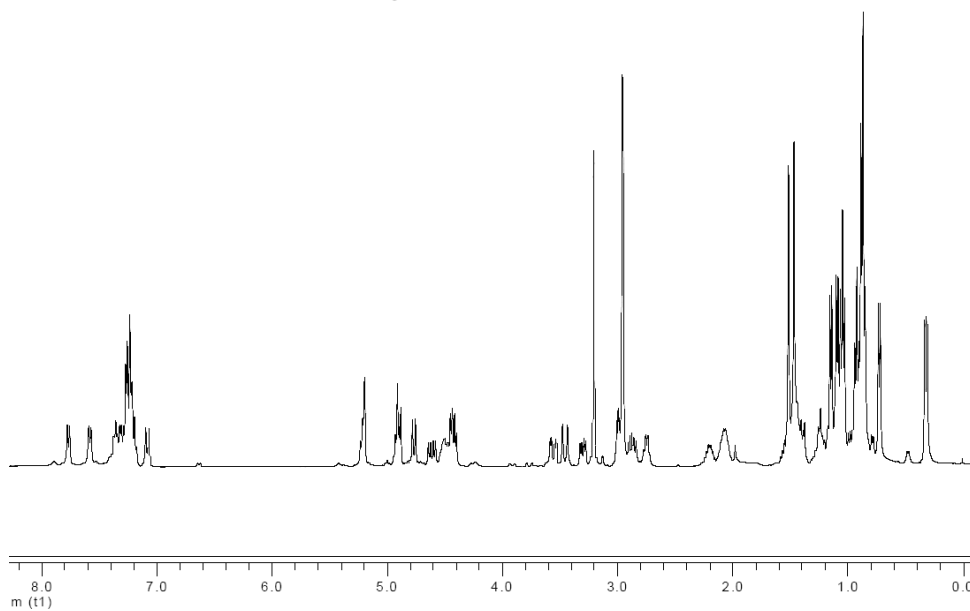
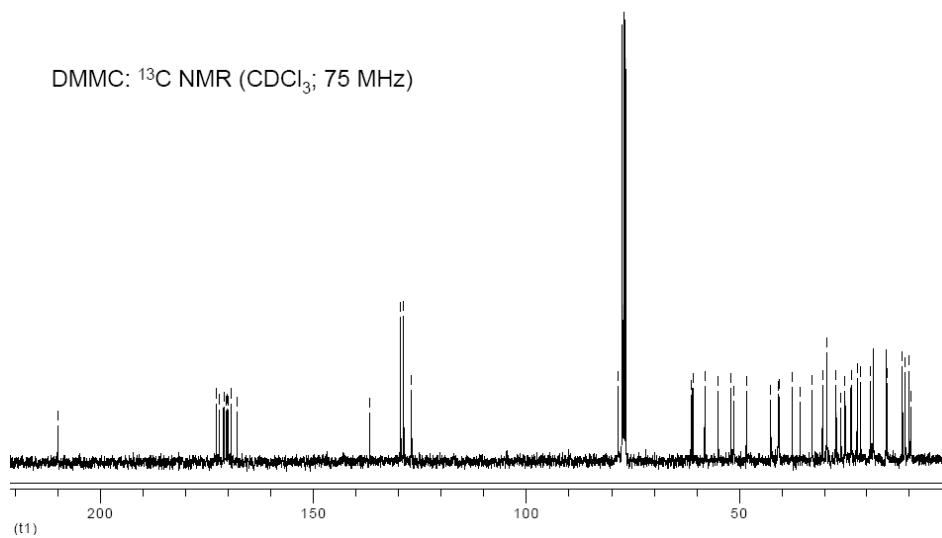
^1H - ^{13}C gHMBC NMR spectrum of belamide A (C_6D_6)

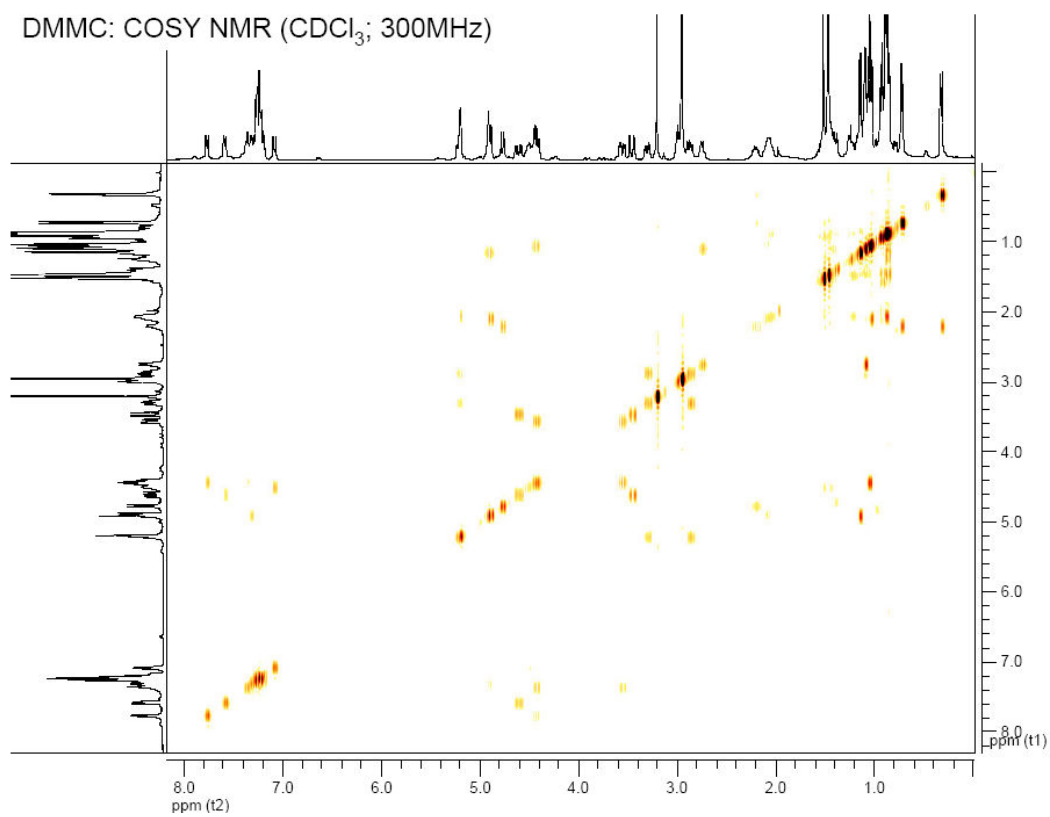
Supporting information for Chapter III

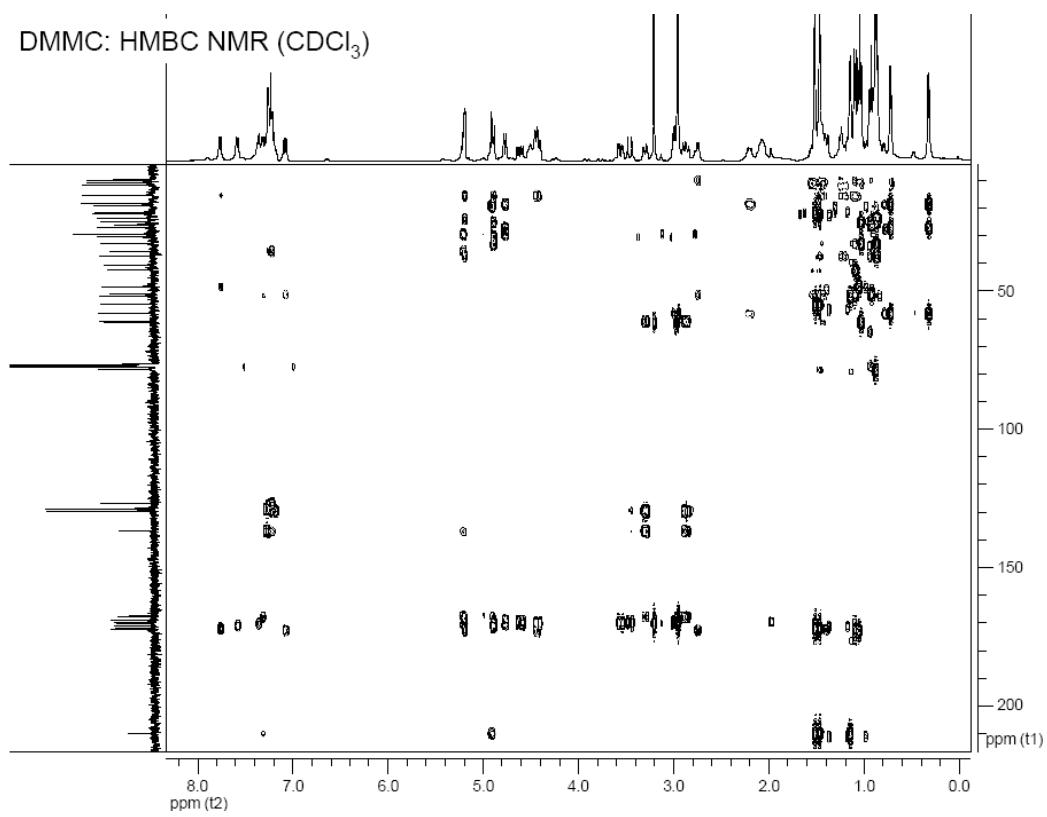
DMMC FT-IR and MS

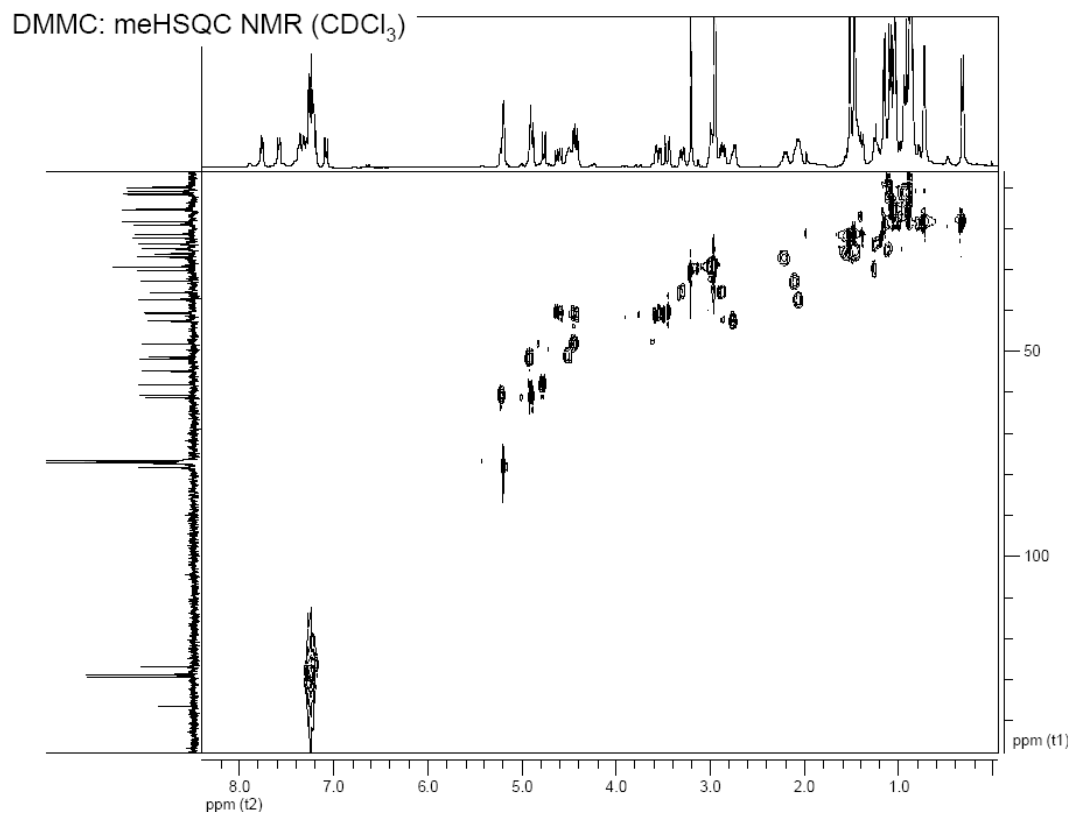
- glassy oil with optical rotation $[\alpha]_D^{22} -104.1^\circ$
- MALDI-TOF-MS: gave m/z 955.5867 $[M+H]^+$
- deduced MF: $C_{49}H_{78}N_8O_{10}$



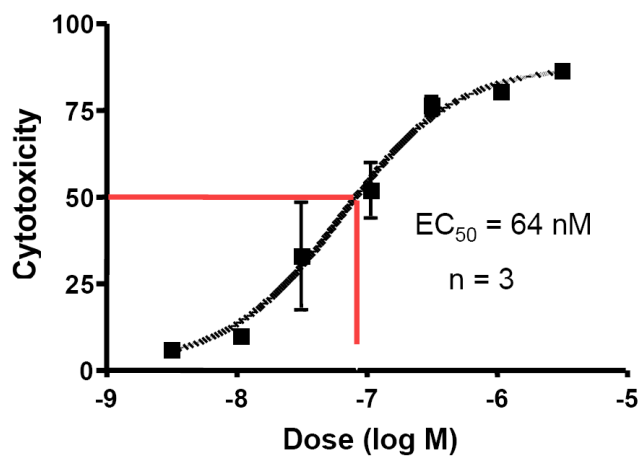
DMMC: ^1H NMR (CDCl_3 ; 300 MHz)DMMC: ^{13}C NMR (CDCl_3 ; 75 MHz)



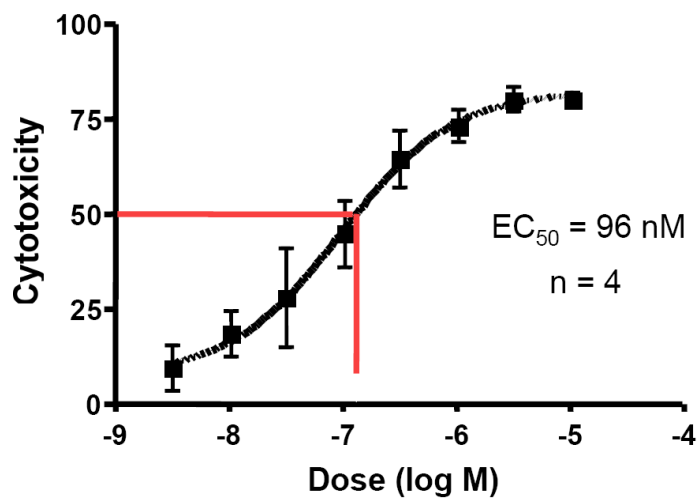


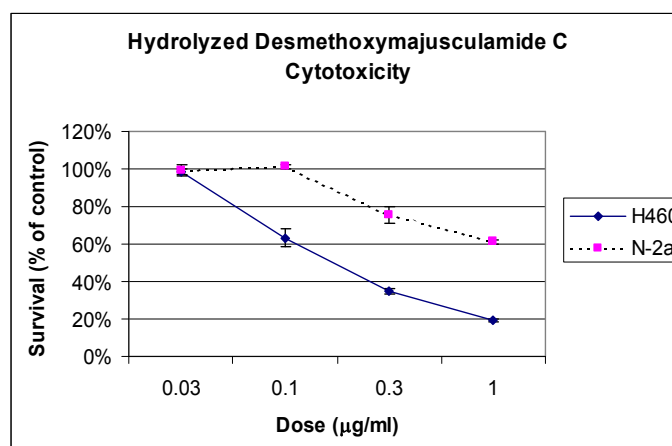
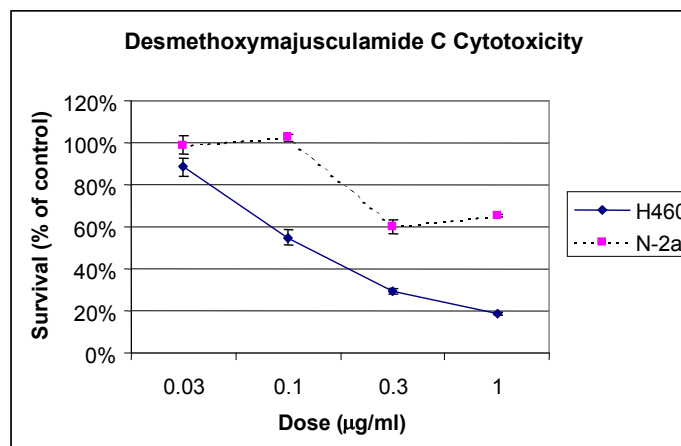
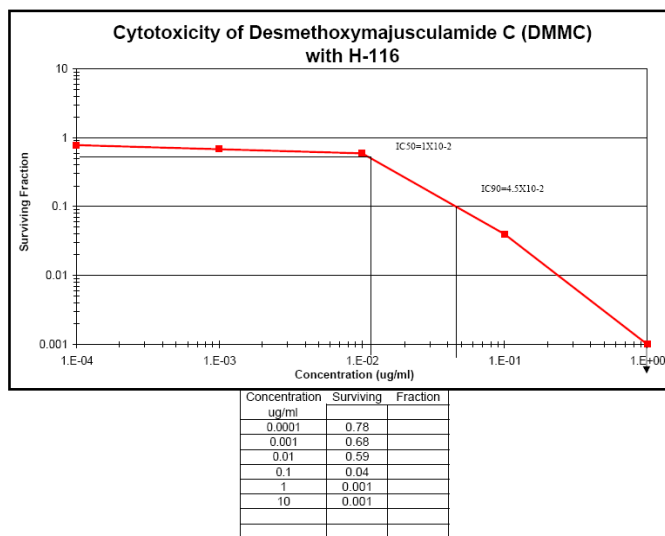


Desmethoxymajusculamide C Cytotoxicity in H460 Cells



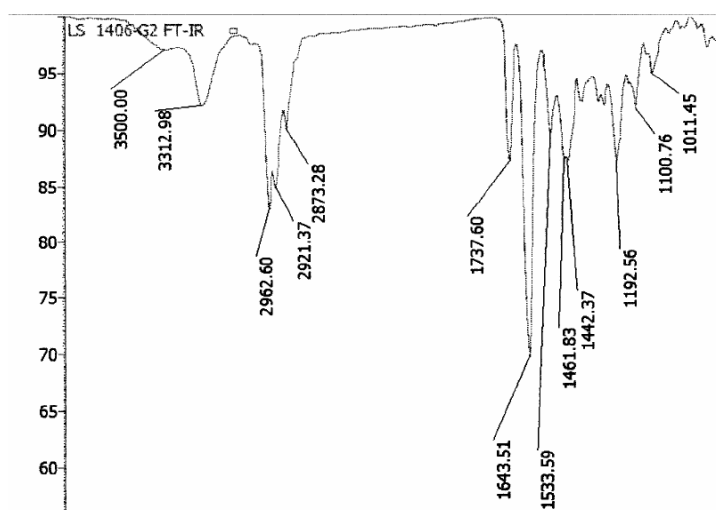
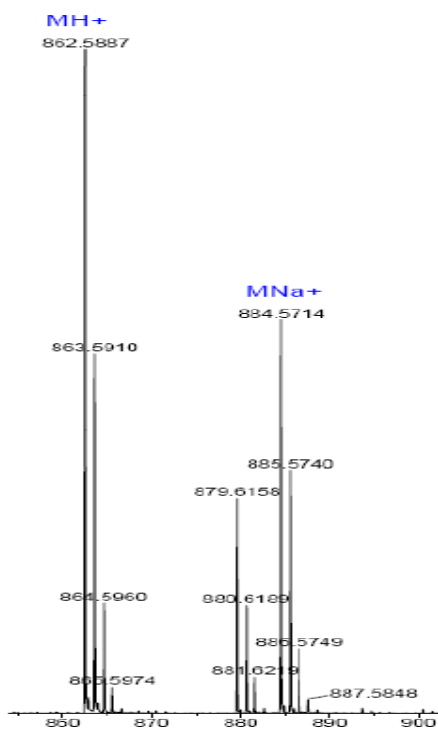
Linear Desmethoxymajusculamide C Cytotoxicity in H460 Cells



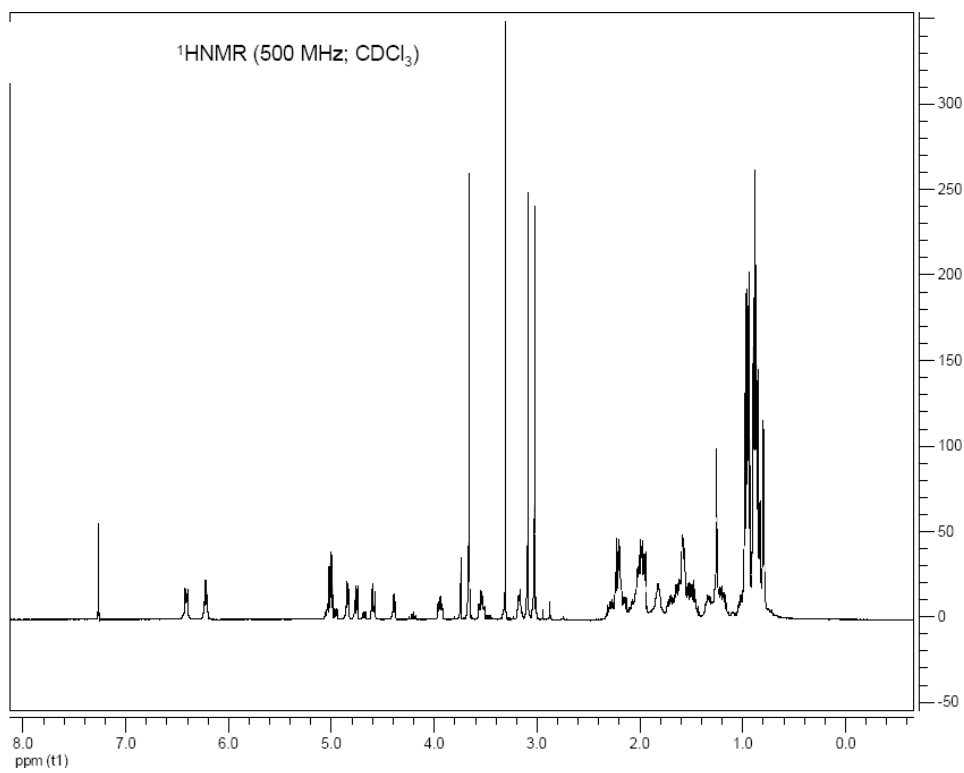


Supporting information for Chapter IV

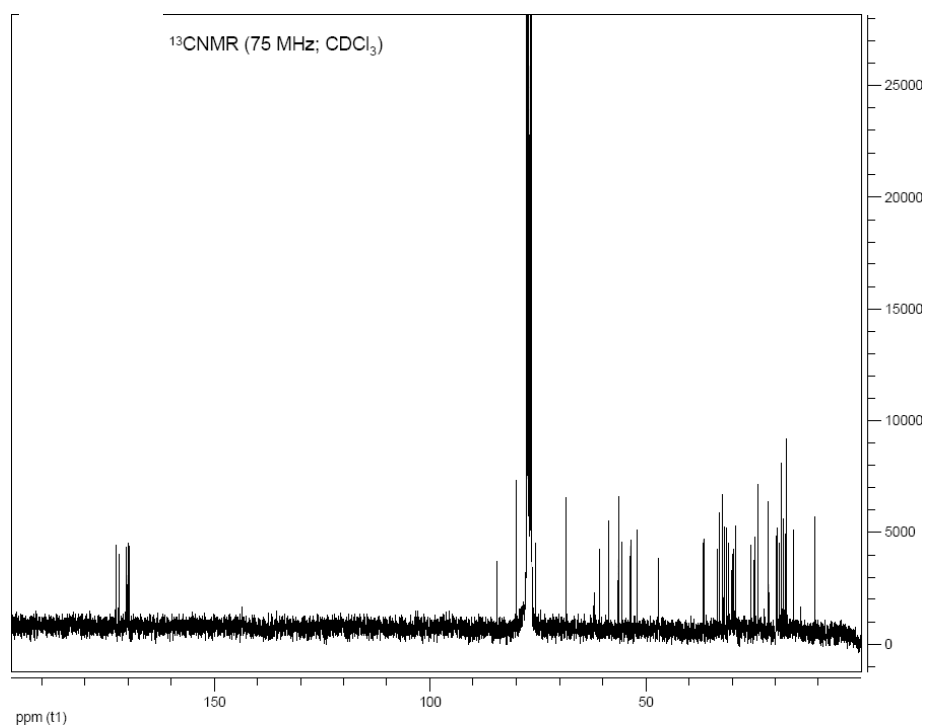
HR ESI TOF MS for viridamide A.



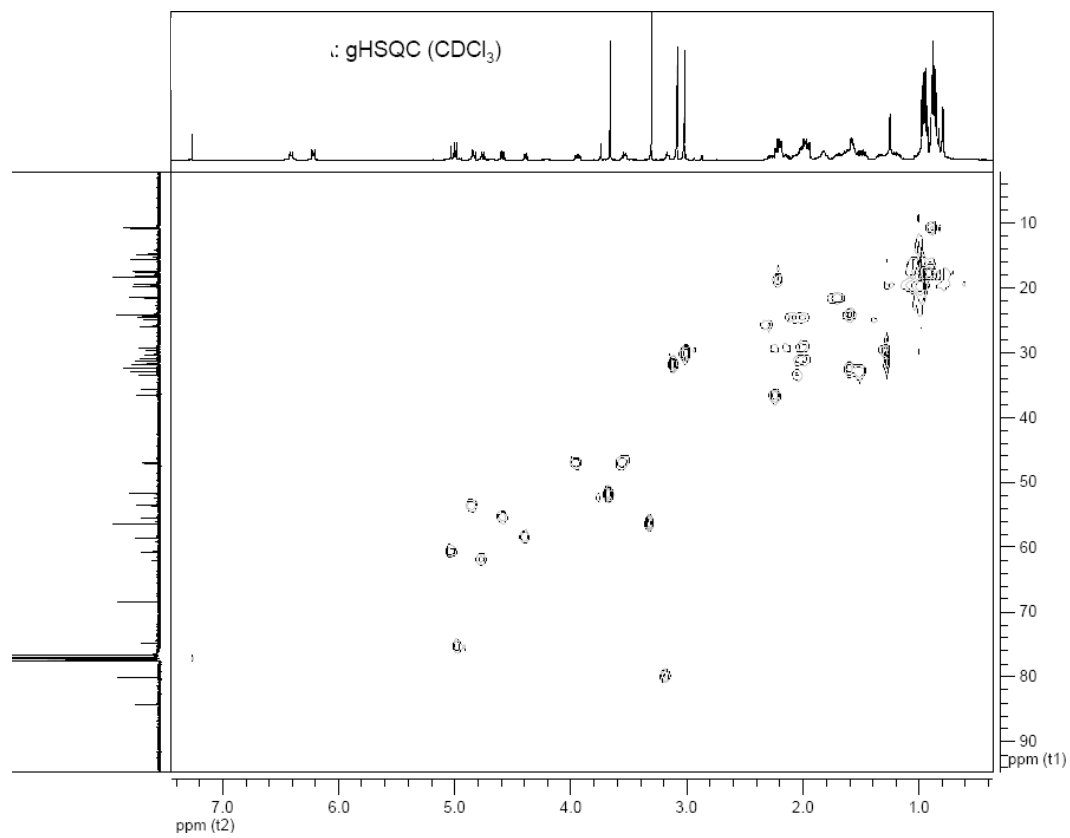
^1H NMR spectrum for viridamide A (500 MHz; CDCl_3)



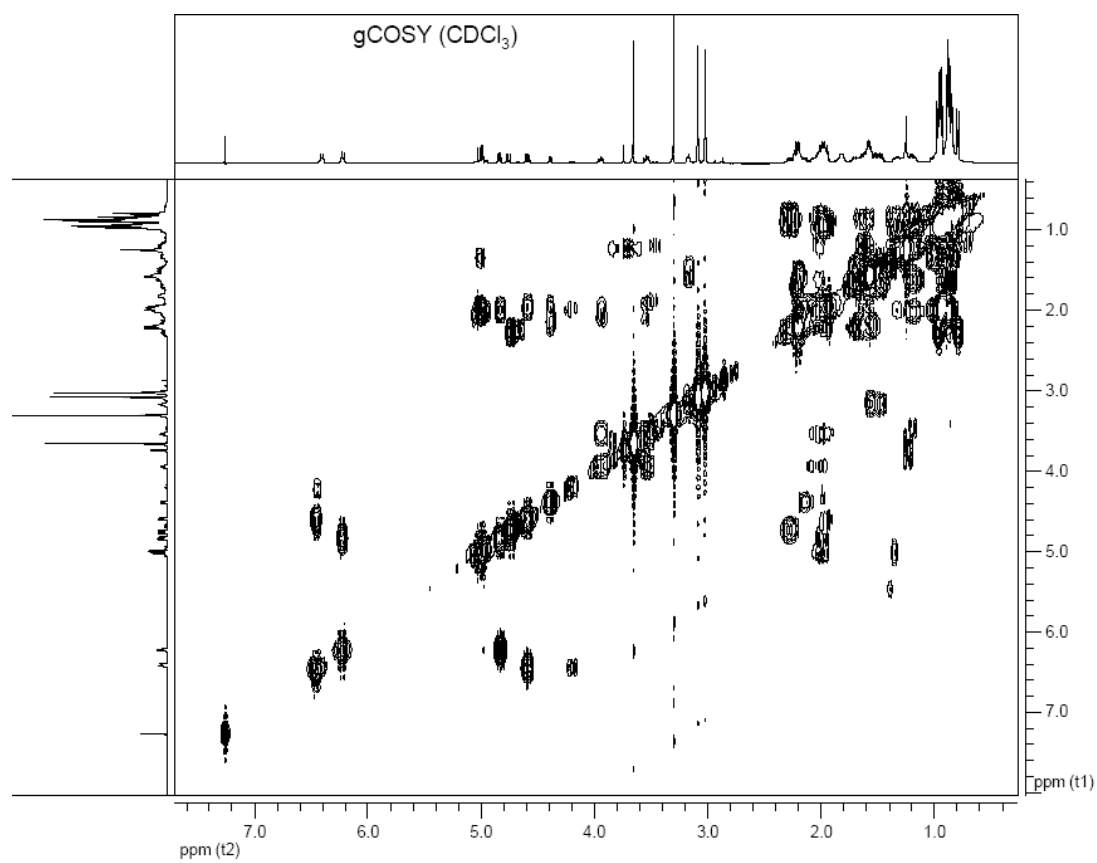
^{13}C NMR spectrum of viridamide A



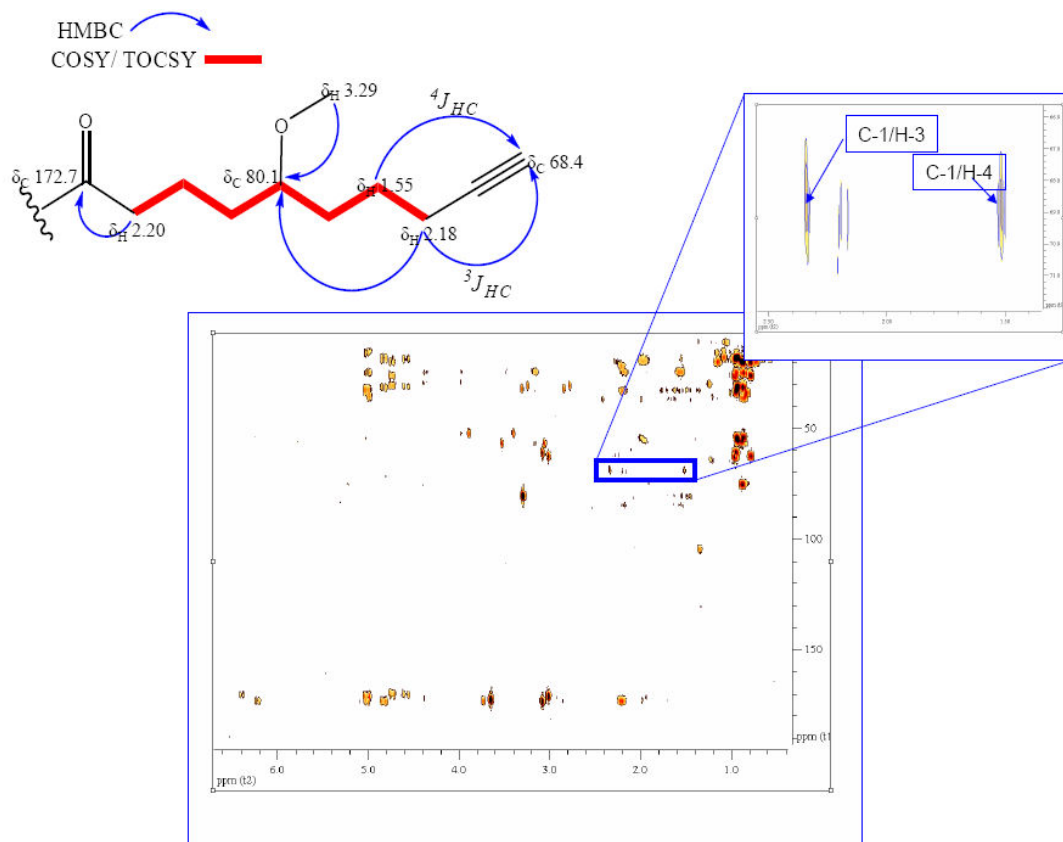
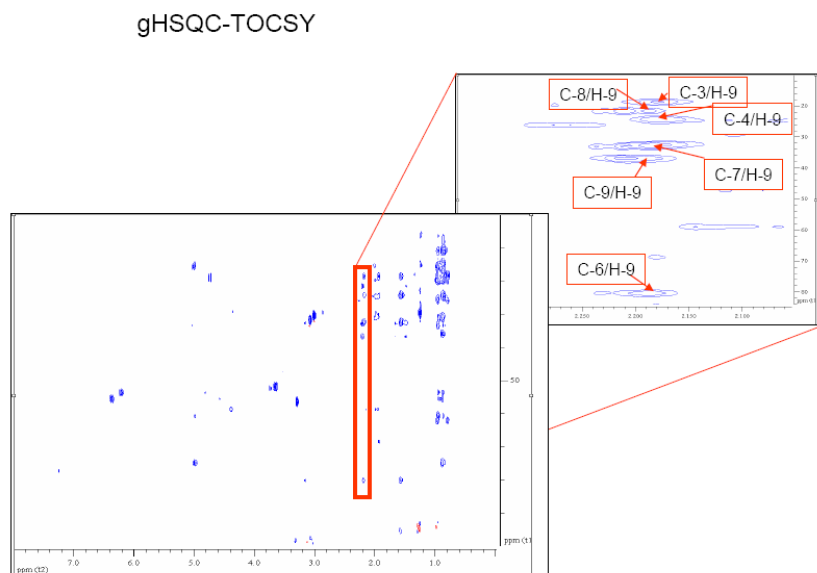
HSQC NMR spectrum of viridamide A.

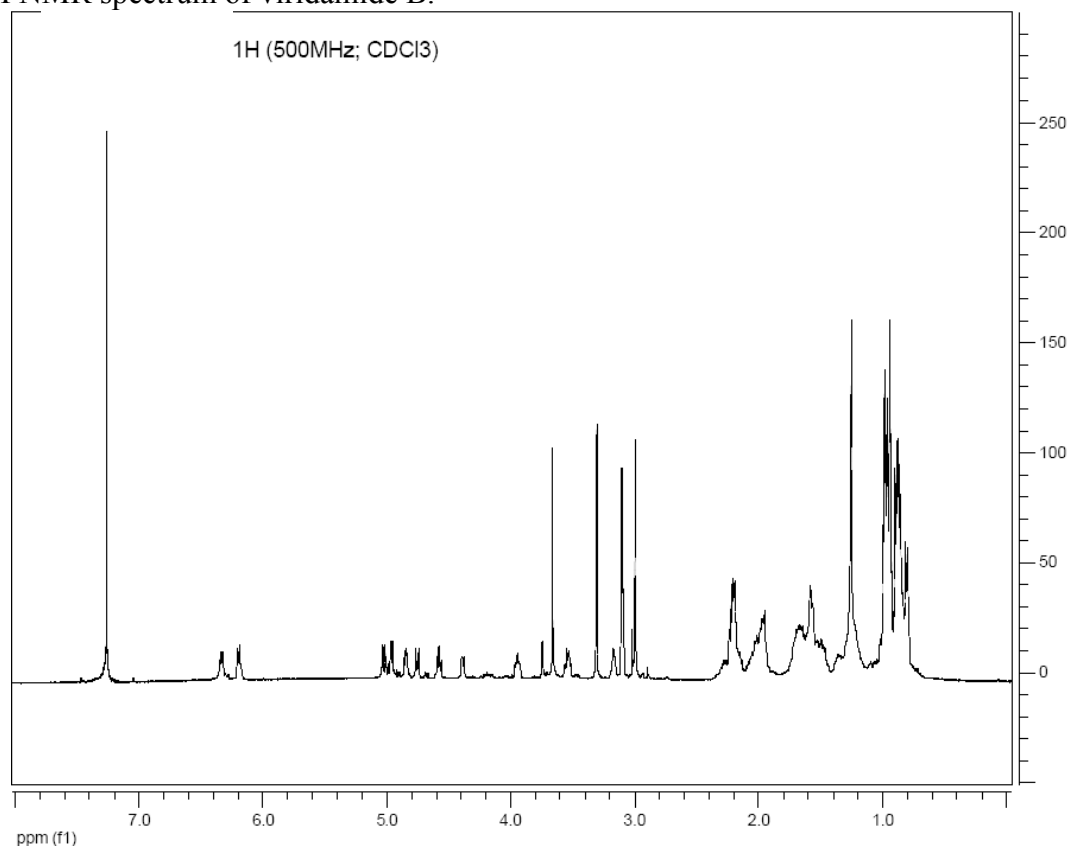


gCOSY NMR spectrum of viridamide A.

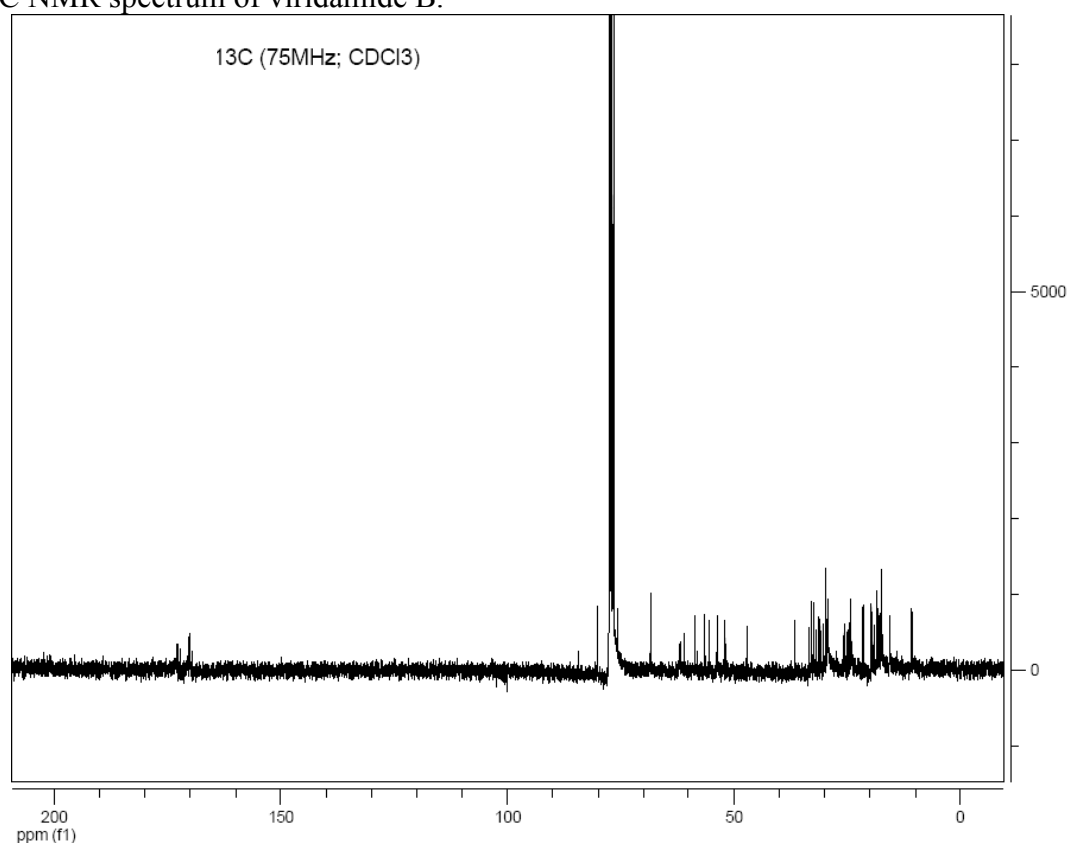


HSQC-TOCSY NMR spectrum of viridamide A.



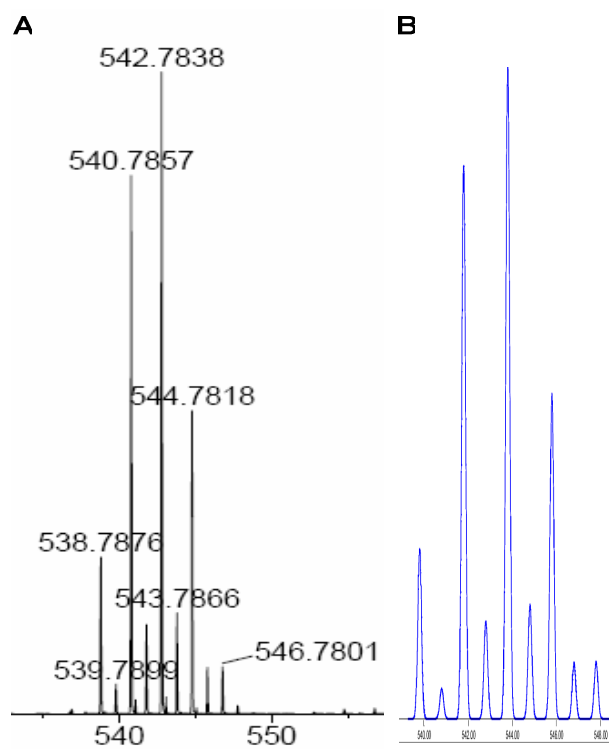
¹H NMR spectrum of viridamide B.

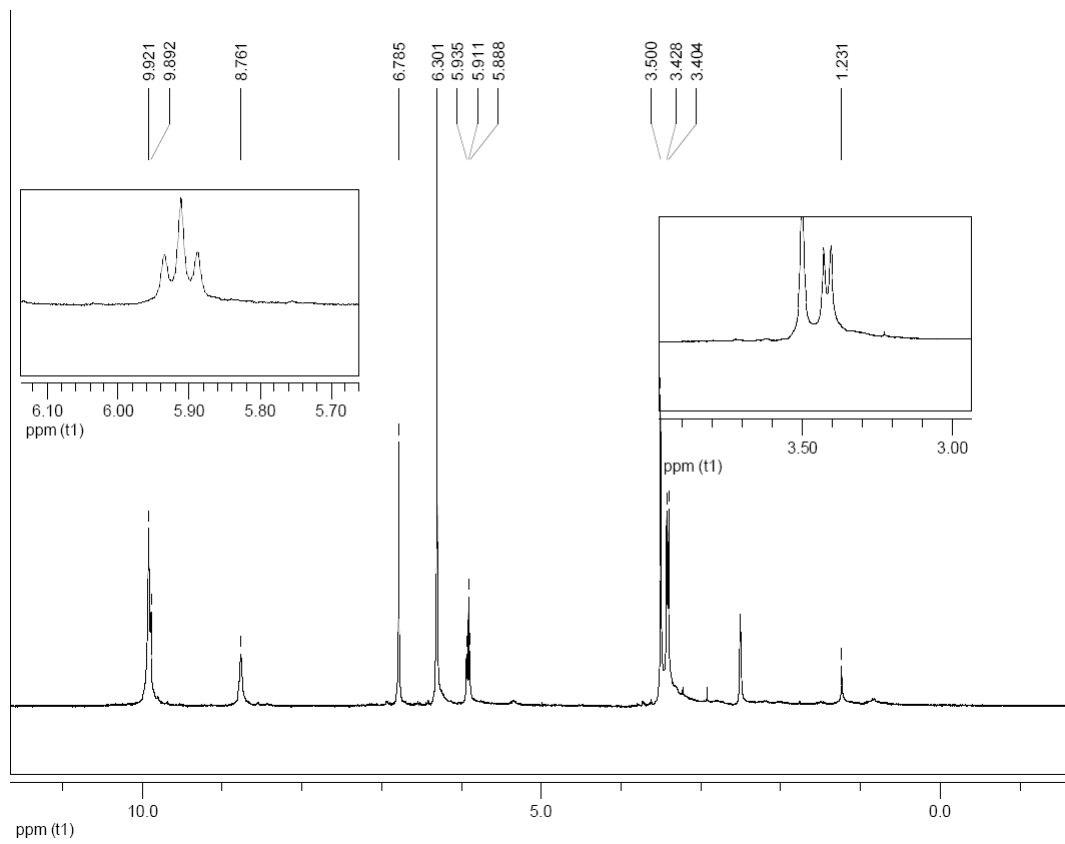
^{13}C NMR spectrum of viridamide B.

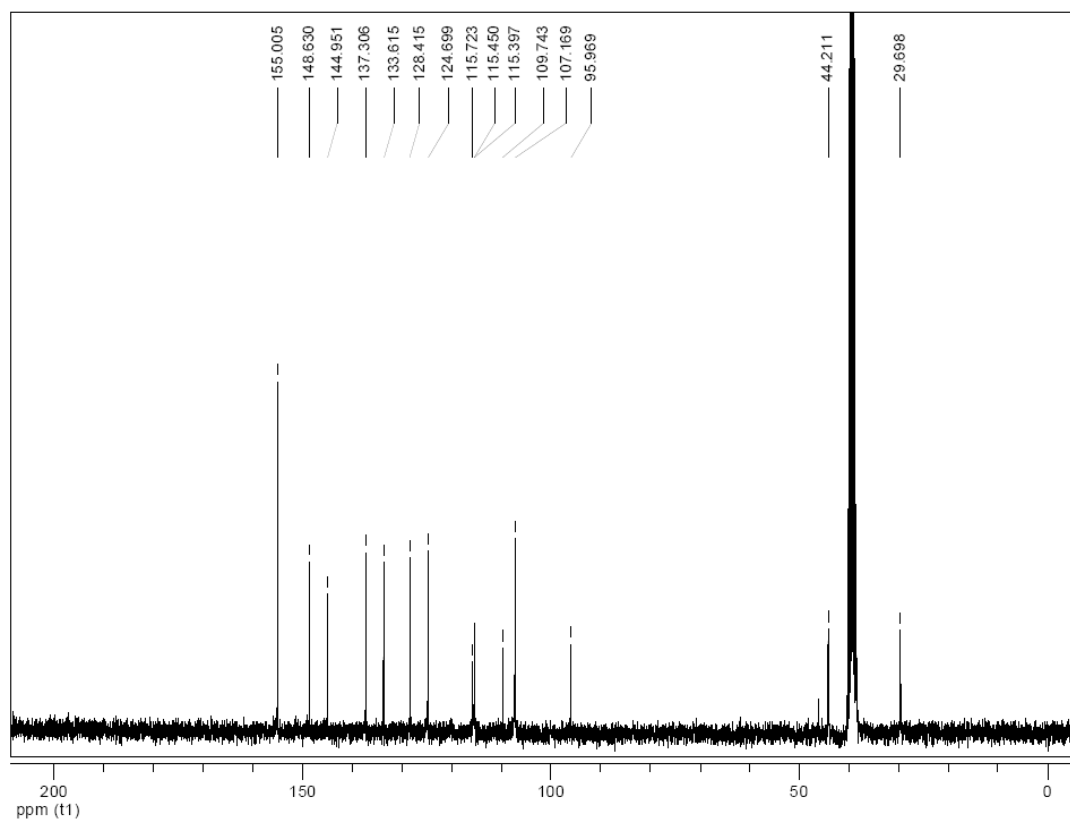


Supporting information for Chapter V

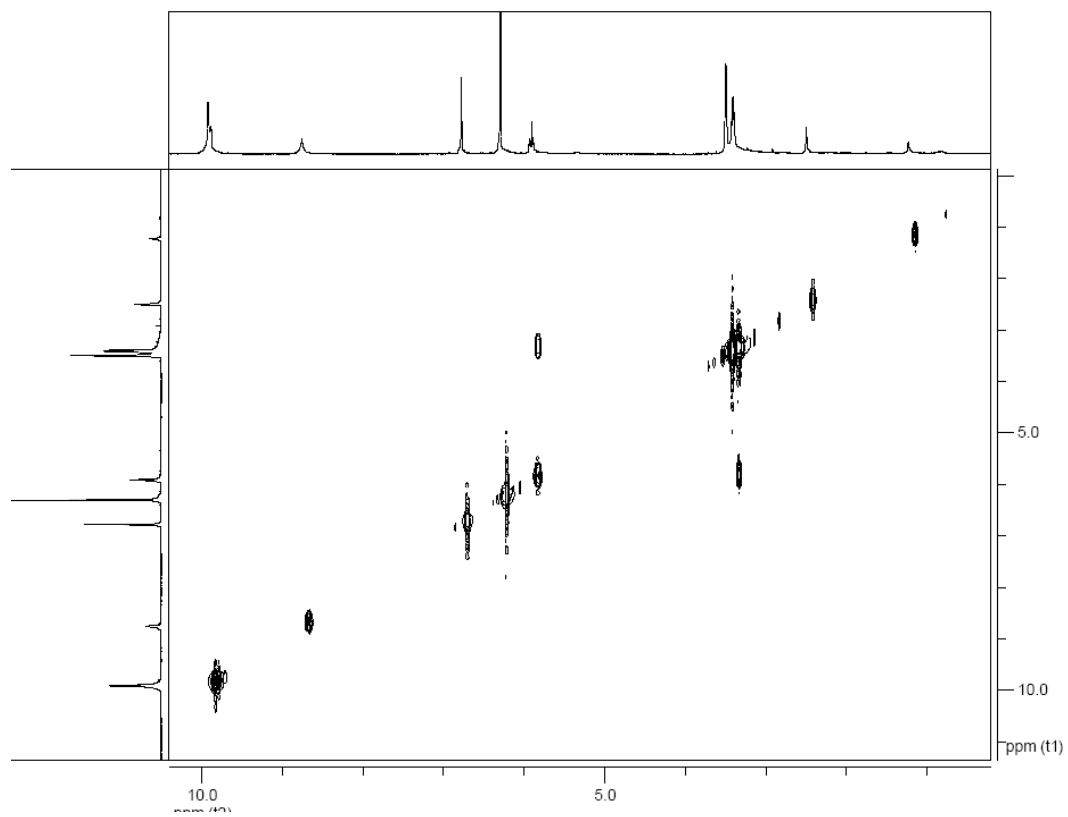
HR ESI TOF MS of kaviol A and predicted isotopic ratio pattern for the proposed MF.



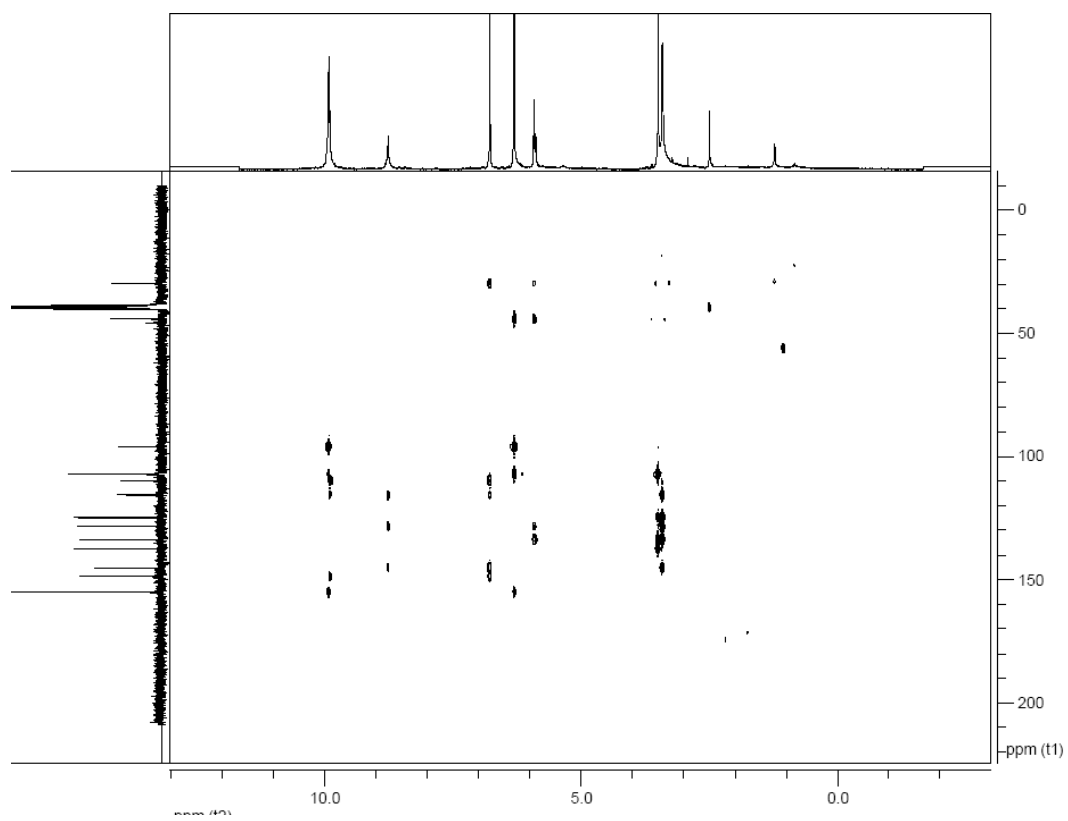
¹H NMR spectrum of 1549E4 (500 MHz; *d*₆-DMSO)

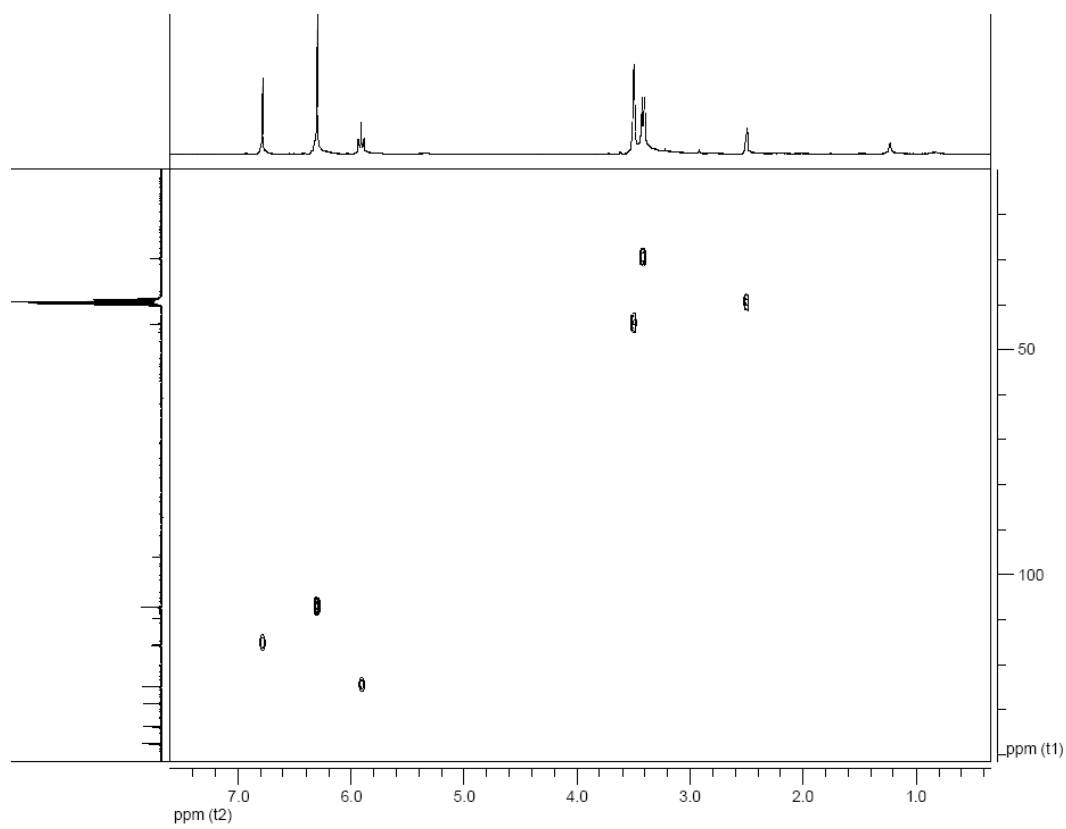
^{13}C NMR spectrum of 1549E4 (125 MHz; d_6 -DMSO)

^1H - ^1H COSY NMR spectrum of 1549E4 (500 MHz; d_6 -DMSO)

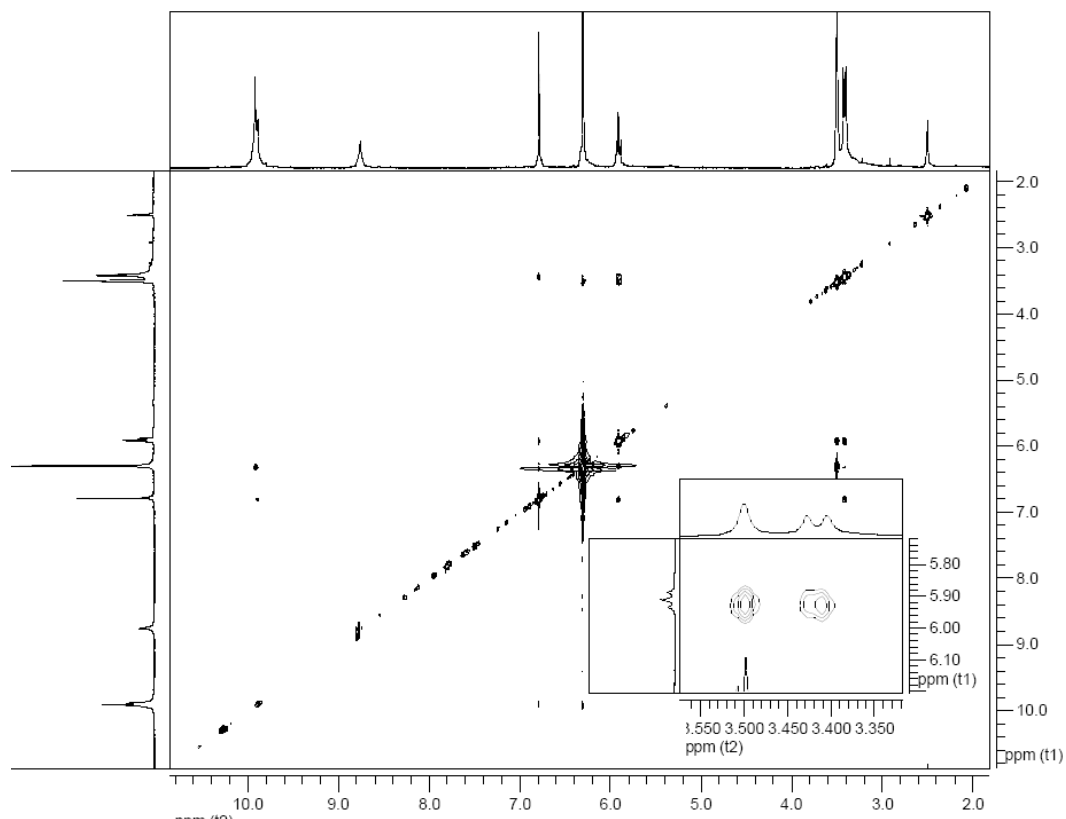


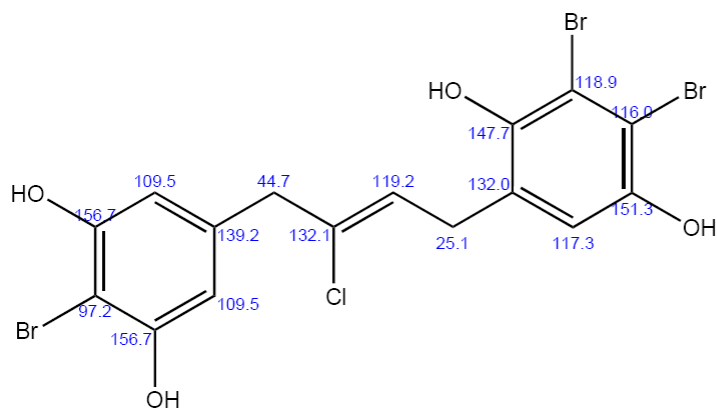
^1H - ^{13}C gHMBC NMR spectrum of 1549E4 (d_6 -DMSO)



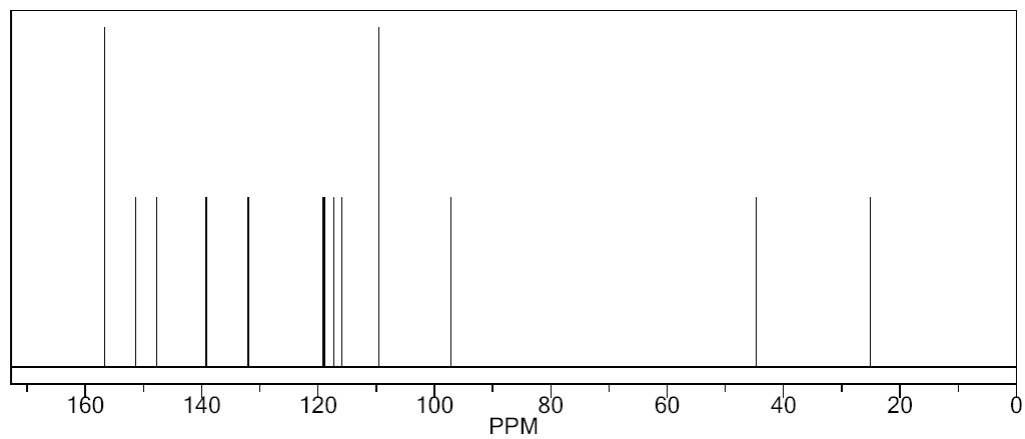
^1H - ^{13}C gHSQC NMR spectrum of 1549E4 (d_6 -DMSO)

^1H - ^1H ROESY NMR spectrum of 1549E4 (500 MHz; d_6 -DMSO)



ChemNMR ^{13}C Estimation

Estimation quality is indicated by color: good, medium, rough



Protocol of the C-13 NMR Prediction:

Node	Shift	Base + Inc.	Comment (ppm rel. to TMS)
C	118.9	128.5	1-benzene
		-5.4	1 -Br
		3.3	1 -Br
		-12.8	1 -O
		1.4	1 -O
		-0.1	1 -C
C	116.0	4.0	general corrections
		128.5	1-benzene
		3.3	1 -Br
		-5.4	1 -Br
		1.4	1 -O
C	97.2	-12.8	1 -O
		-3.0	1 -C
		4.0	general corrections
		128.5	1-benzene
		-5.4	1 -Br
		-12.8	1 -O

WG-EXT-1549-E4 from UCSD2 was tested against 6 isoforms of HDAC:

Target	IC50 (ug/mL)
HDAC1	3
HDAC2	2
HDAC3	4
HDAC4	3
HDAC6	3.5
HDAC8	4.5

1549-E4 vs. HDAC

